

Hydraulic Design of an Overland Flow Distribution System Using Lateral Weirs

by

Victor M. Vargas Lugo

A report submitted in partial fulfillment of the requirements for the degree of

MASTER OF ENGINEERING
in
CIVIL ENGINEERING

UNIVERSITY OF PUERTO RICO
MAYAGÜEZ CAMPUS
2014

Approved by:

Walter F. Silva Araya Ph.D.
President, Graduate Committee

Date

Raúl E. Zapata López, Ph. D.
Member, Graduate Committee

Date

Jorge Rivera Santos, Ph. D.
Member, Graduate Committee

Date

Francisco Monroig Salter, Ph. D.
Representative Graduate Studies

Date

Ismael Pagán Trinidad, M.S.C.E.
Chairperson of the Department

Date

ABSTRACT

Jobos Bay Estuary Research Reserve (JBNERR) is located Salinas in Puerto Rico. Mar Negro wetland is the biggest mangrove forest in the area located at the south boundary of JBNERR. The north side of the Reserve has been used for agricultural activities since the Spanish Colonial times. Since 1993 the mangrove started to diminish and its mortality was promoted by antropogenic activities.

This project consisted of: 1) Study of the hydrologic and hydraulic conditions existing at the north side of JBNERR; 2) Hydraulic design of channels with a system of weirs to re-direct irrigation and rain runoff to a parcel of land before discharging into Mar Negro. This water distribution will control surface runoff, reduce surface erosion, and improve the quality of runoff waters discharging into the mangrove. The project analysis was prepared using SWMM software, field work, and historical rainfall data to get the details features of the study area.

Keywords: Jobos Bay, JBNEER, Hydrology, Hydraulics, Side Wiers, Wiers, SWMM, Watershed, Channel, Riprap, ArcGIS, AutoCAD, Mangroves, Rainfall, Transitions

RESUMEN

La Reserva de Investigación Estuarina Bahía de Jobos (JBNERR) se encuentra Salinas, Puerto Rico. Mar Negro es el mayor bosque de manglar ubicado al sur de JBNERR. El área norte de la Reserva se ha utilizado para actividades agrícolas desde los tiempos coloniales españoles. Desde 1993, el manglar comenzó a disminuir y su mortandad ha sido promovida por actividades antropogénicas.

Este proyecto consistió en: 1) Estudio de las condiciones hidrológicas e hidráulicas existentes al norte de JBNERR; 2) Diseño hidráulico de canales con un sistema de vertedores para redirigir las escorrentías por riego y de lluvia a una parcela antes de alcanzar al mar Negro. Esta distribución de agua controlará la escorrentía superficial, reducirá la erosión, y mejorará la calidad del agua de escorrentía que alcance el manglar. El análisis del proyecto se preparó utilizando SWMM, trabajo de campo, y datos históricos de precipitación para obtener los detalles del área de estudio.

Palabras claves: Bahía de Jobos, JBNEER, Hidrología, Hidráulicas, Vertedores Laterales, Vertedor, SWMM, Cuenca, Canal, Riprap, ArcGIS, AutoCAD, Manglar, Precipitación, Transición.

Copyright © 2014 by Victor M. Vargas Lugo All rights reserved. Printed in the United States of America. Except as permitted under the United States Copyright Act of 1976, no part of this publication may be reproduced or distributed in any form or by any means, or stored in a data base or retrieved system, without the prior written permission of the publisher.

Dedicado a:

A Dios sobre todas las cosas.

Mi madre Lucia Lugo por su apoyo incondicional.

La novia eterna, Lizbeth por su apoyo, ayuda y comprensión.

A mi mentor, el Dr. Walter Silva por su paciencia, enseñanza y guiarme en este proyecto.

Dedicated to:

God above all things.

My mother Lucia for their unconditional support.

The eternal girlfriend, Lizbeth for their support, help and understanding.

To my mentor, Dr. Walter Silva for his patience, teaching and guiding me in this project.

ACKNOWLEDGMENTS

The author would like to express sincere thanks to Dr. Walter F Silva Araya, for his support, patience, and encouragement throughout the graduate studies. Also, I want to appreciate the opportunity to work for the Puerto Rico Water Resources and Environmental Research Institute.

I want acknowledge the people who contributed substantially to this project: Roy Ruiz Velez, Assistant Researcher Water Resources; Jesenia Carrero Lorenzo, Administrative Assistant from Puerto Rico Water Resources and Environmental Research Institute; Rubén C. Soto Maisonet, Surveying and Civil Engineering Student at UPRM; Angel Dieppa, Puerto Rico Department of Natural and Environmental Resources-Jobos Bay National Estuarine Research Reserve who assisted with data collection at the site.

Finally I would like to thanks Mrs. Carmen González Sifonte, Jobos Bay National Estuarine Research Reserve Manager, for her cooperation and assistance in Jobos area. Also, for being the person on whose concern for Jobos Bay protection, this project could be performed.

TABLE OF CONTENT

	Page
List of Tables	x
List of Figures.....	xii
Figures in Appendix.....	xv
List of Acronyms	xvi
CHAPTER 1 INTRODUCTION.....	1
1.1 PROBLEM STATEMENT	2
1.2 SCOPE AND OBJECTIVE OF THE STUDY	6
CHAPTER 2 STUDY AREA DESCRIPTION	7
2.1 LOCATION AND PHYSIOGRAPHIC REGION.....	7
2.2 EXISTING TOPOGRAPHY	9
2.3 CLIMATE	10
2.4 GEOLOGY.....	10
1.1 AGRICULTURAL ACTIVITIES.....	13
CHAPTER 3 MODEL DESCRIPTION	14
3.1 RUNOFF AND HYDRAULIC SIMULATION.....	14
3.2 CONCEPTUAL MODEL.	15
3.2.1 HYDROLOGICAL COMPUTATIONS	16
3.2.2 INFILTRATION	17
3.2.3 HYDRAULICS COMPUTATIONS	18
3.2.4 FLOW ROUTING METHODS	19
CHAPTER 4 HYDROLOGY	22
4.1 STORM RAINFALL EVENTS.....	22
4.2 WATERSHED	22
4.3 OVERLAND FLOW ROUGHNESS	25
4.4 HYDROLOGIC ABSTRACTION.....	26
4.5 HISTORICAL RAINFALL	31
4.6 AGRICULTURAL IRRIGATION	32
4.7 SWMM HYDROLOGY SETTING AND MODELING.....	33

4.8 HYDROLOGIC ANALYSIS	34
4.8.1 RUNOFF BY CN METHOD	35
4.8.2 IRRIGATION DATA.....	35
CHAPTER 5 HYDRAULICS	37
5.1 GENERAL HYDRAULIC PROCEDURES	38
5.2 CHANNELS CHARACTERISTICS AND SIDE WEIRS DESIGN.....	39
5.3 CHANNEL LINING.....	41
5.4 RIPRAP – LINING CHANNEL DESIGN PROCEDURES.....	43
5.4.1 RIPRAP DESIGN CRITERIA	43
5.4.2 RESULTS AND DISCUSSION	48
5.5 CHANNEL BEND.....	50
5.6 CHANNEL TRANSITION.....	54
5.7 SIDE WEIRS DESIGN.....	71
5.7.1 SPILLFLOW CALCULATIONS	78
5.7.2 RESULTS.....	79
5.7.3 SIDE WEIR PROFILE.....	85
5.7.4 VERIFICATION OF WATER SURFACE PROFILE.....	86
5.8 RECOMMENDED CHANNEL DIMENSIONS	91
CHAPTER 6 PROJECT REPRESENTATION IN SWMM.....	94
6.1 MODELING DESIGN	95
6.2 SENSITIVITY ANALYSIS	96
CHAPTER 7 DESIGN ALTERNATIVES.....	110
CHAPTER 8 ANALYSIS AND DISCUSION.....	114
CHAPTER 9 DESIGN RECOMENDATIONS.....	121
9.1 LAND SURVEY	121
9.2 CUT AND FILL	125
9.3 COST ESTIMATE	133
BIBLIOGRAPHY.....	138
APPENDIX.....	144

APPENDIX A	CURVE NUMBER TABLES.....	144
APPENDIX B	MAXIMUM 24-HR RAINFALL FOR EACH YEAR OF ANALYSIS PERIOD.	145
APPENDIX C	COMPLETE STORM EVENTS HYETOGRAPHS.....	148
APPENDIX D	DEPTH-DURATION–FREQUENCY CURVES FOR GUAYAMA, PUERTO RICO	150
APPENDIX E	RIPRAP FREEBOARD CHART.....	151
APPENDIX F	SPILLFLOW COEFFICIENT CHARTS FOR SIDE WEIRS	152
APPENDIX G	EULER IMPROVED METHOD FOR SIDE WEIR WATER PROFILE – EXCEL VBA.....	153
APPENDIX H	SYNTETIC RAIN 1YR-24HR.....	156
APPENDIX I	SINTHETIC RAINS	157
APPENDIX J	MISCELLANEOUS	162
APPENDIX K	CONVERSION FACTORS	164

LIST OF TABLES

	Page
Table 4.1 Precipitation partial duration series–based precipitation frequency estimates (in millimeters) at Salinas, P.R. Lat. 17.9702; Long.-66.2061– Guayama-Salinas, P.R.....	23
Table 4.2 Areas per subcatchment	24
Table 4.3. Roughness Coefficient for flood plains (NRCS, 1986).	25
Table 4.4. Hydrologic group percentages of the watershed.....	27
Table 4.5. Hydrologic group percentages by subcatchment.	27
Table 4.6 Hydrologic Unit.	29
Table 4.7. Curve number distribution percentages of the watershed	30
Table 4.8. Complete Storms; 10 Years Historical Events.....	36
Table 4.9. Storms; 10 Years Historical Events and 24 hours duration	36
Table 5.1. West Channel and East Channe general geometric data.	40
Table 5.2. Channel riprap lining design configuration data.....	49
Table 5.3. Channel bend design data.	54
Table 5.4. Inlet loss coefficient (Chow, 1959).....	56
Table 5.5. Design computations for Transition T1, length of 7 m. $Q_{design} = 0.35 \text{ m}^3/\text{s}$	61
Table 5.6. Design computation for T2, length of 4 m. $Q_{design} = 0.23 \text{ m}^3/\text{s}$	61
Table 5.7. Design computations for T3, length of 3 m. $Q_{design} = 0.12 \text{ m}^3/\text{s}$	62
Table 5.8. Design computation for T4, length of 6 m. $Q = 1.09 \text{ m}^3/\text{s}$	66
Table 5.9. Design computation for T5, length of 4 m.....	66
Table 5.10. Design computation for T6, length of 3 m.....	67
Table 5.11. Transition length and flare angle.	67
Table 5.12. Discharge coefficient equations for rectangular sharp crest side weirs reported by Emiroglu, et. al, 2011.....	76
Table 5.13. Discharge coefficient (C_d) and effective discharge coefficient (C_e) for West Channel side weirs (3 rd weir belongs to downstream weir).....	81
Table 5.14. Discharge coefficient (C_d) and effective discharge coefficient (C_e) for East Channel side weirs (3 rd weir belongs to downstream).....	82
Table 5.15. West side weirs design data.	83
Table 5.16. East side weirs design data.	84
Table 5.17. West Channel length and depth by section.	92
Table 5.18. East Channel length and depth by section.	93
Table 6.1. Synthetic rains and historical rains for Sensitivity Analysis.....	100
Table 8.1. Comparison between steady state computation and values obtained in PCSWMM.....	120
Table 9.1. Cut and Fill for Area Between Cross Section A-A` and B-B`	128
Table 9.2. Cut and Fill for Area Between Cross Section B-B` and C-C`	129
Table 9.3. Cut and Fill for Area Between Cross Section C-C` and D-D`	130
Table 9.4. Cut and Fill for Area Between Cross Section D-D` and E-E`	131
Table 9.5. Balance cut and fill material volumes.....	132

Table 9.6. Grouted Riprap Lining Estimate Cost.....	135
Table 9.7. Reinforced Concrete Lining Cost Estimate. Channel wall and bed width is 0.15 m.	135
Table 9.8. Cost Estimate for Grouted Riprap Lining.	136
Table 9.9. Cost Estimate adding the clearing, cut and fill of the A.O.I (optional).	137
Table A.1. Curve Number For hydrologic soil groups (NRCS, 1986).	144

LIST OF FIGURES

	Page
Figure 1.1. Location of Jobos Bay National Estuarine Research Reserve, JBNERRS delineated areas shapefile from NERRS.	3
Figure 1.2. Location of the drainage channels. (Aerial image by 3001, Inc. 2007)	3
Figure 1.3. Sequence of aerial photos showing the evolution of the project area during the last decade. Project area shown in the orange box. Aerial Images by 3001 Inc., 2007	5
Figure 2.1. Jobos Bay National Estuarine Research Reserve (Zitello, Whitall, Dieppa, Christensen, Monaco, and Rohman, 2008).	8
Figure 2.2. Land use distribution in Central Aguirre watershed and percentage coverage (Zitello, Whitall, Dieppa, Christensen, Monaco, & Rohman, 2008).	8
Figure 2.3. A: Topographic measure points of the study area. B: Contour lines and elevation modeling of the study area (msl).....	9
Figure 2.4. Hydrogeology of the Jobos Bay watershed (Rodríguez, 2006).	11
Figure 2.5. Hydrogeology cross section A-A' from south to north bound of the Jobos Bay Watershed (Rodríguez, 2006).	12
Figure 3.1. Illustration of the water balance variables and surface runoff computation.	16
Figure 3.2. Weir schematics: A: lateral view of the weir; B: Top view of the wier.	19
Figure 4.1. Deliniated watershed of AOI	24
Figure 4.2. Representation of the hydrologic group.	27
Figure 4.3. SCS map units.	29
Figure 4.4 Weighted curve number by watershed	30
Figure 4.5. Hyetograph of historical storm of September 22, 2008 showing the distribution of the rain along 24 hours.....	31
Figure 4.6. Irrigation subareas for the pivot area at north of Jobos Bay (William C. O. et al., 2012).	32
Figure 4.7. PCSWMM maximum surface runoff by subcatchment.....	34
Figure 5.1. General flowchart of the hydraulic Design.....	38
Figure 5.2. Channel Design Setup.	40
Figure 5.3. Flow chart of the riprap design procedure (Anderson et al., 1970).	44
Figure 5.4. Chart to determine the angle of repose of riprap in terms of the stone diameter chosen and the shape (Anderson et al., 1970).	46
Figure 5.5. Trapezoidal channel diagram.....	47
Figure 5.6. Riprap channel design, not at scale. For dimension of b and B please see the Table 5.2.....	49
Figure 5.7. Superelevation profile.....	50
Figure 5.8. Cross section sketch of secondary flow characteristics in a channel bend (Blanckaert et al., 2004).	51
Figure 5.9. A: Channel diagram. B: Dimensionless coefficient for shear stress caused by channel bends calculation (Akan, 2006).....	53
Figure 5.10. Transition types (Federal Highway Administration, 2012).	54

Figure 5.11. Energy diagram in gradually varied flow in open channel. A: Transition top view; B: Channel Cross section; C: Channel lateral cross section.....	58
Figure 5.12. Channel Transition design flow chart.....	60
Figure 5.13. Water depth and channel width variation along the T1 length.....	63
Figure 5.14. Water depth and channel width variation along the T2 length.....	64
Figure 5.15. Water depth and channel width variation along the T3 length.....	65
Figure 5.16. Water depth and channel width variation along the T4 length.....	68
Figure 5.17. Water depth and channel width variation along the T5 length.....	69
Figure 5.18. Water depth and channel width variation along the T6 length.....	70
Figure 5.19. Proposed Channel and Location of the Side Weirs.....	72
Figure 5.20. Typical operation of side weir: A: Water depth across the side weir. B: Top view of the side weir (May et al., 2003).....	73
Figure 5.21. Flow conditions on a side weir: A: Subcritical flow profile. B: Supercritical flow profile. C: Mixed flow. (May et al., 2003; Henderson F. M., 1966).....	74
Figure 5.22. Side weir design flowchart.....	80
Figure 5.23. Side Weir Channel sketch (No to scale).....	85
Figure 5.24. Side weir –wall transition details. (No to scale, exaggerate vertical axis).....	85
Figure 5.25. Gradually varied flow profiles (NDL = normal depth line; CDL = critical depth line) (Sturm, 2011).....	87
Figure 5.26. Mild slope profile (Chow, 1959).....	87
Figure 5.27. West channel side weir water profile: A: SW3, B: SW2 and C: SW1.....	89
Figure 5.28. East channel side weir water profile. A: SW6, B: SW5 and C: SW4.....	90
Figure 6.1. SWWM Modeling setup and features identification.....	94
Figure 6.2. West Channel flow distributions of the side weir during the design rainfall event.....	97
Figure 6.3. East Channel flow distributions of the side weir during the design rainfall event.....	98
Figure 6.4. Channel profile of the maximum water depth during August 22, 2011 rainfall event. A) West Channel profile. B) East Channel Profile.....	99
Figure 6.5. A: Historic rainfall from November 22, 2011. B: Amount of runoff that reaches the beginning of both channels C: East Channel. Side weirs operation with the maximum historical rainfall analyzed. D: West Channel. side weirs operation with the maximum historical rainfall analyzed. For localtion of side weirs (SW) refers to Figure 6.1.....	102
Figure 6.6. Channel profile of the maximum water depth during September 22, 2008 rainfall event. A) West Channel profile. B) East Channel Profile.....	103
Figure 6.7. A: Historic rainfall fromSeptember 22-27, 2008. B: Amount of runoff that reaches the beginning of both channels C: East Channel. side weirs operation with the maximum historical rainfall analyzed. D: West Channel. side weirs operation with the maximum historical rainfall analyzed. For location of side weirs (SW) refers to Figure 6.1.....	104
Figure 6.8. A:Synthetic rainfall (2yr-3hr). B: Amount of runoff that reaches the beginning of both channels. C: West Channel. Side Weirs operation with the maximum syntetic rain. D: East Channel. Side Weirs operation with the maximum syntetic rain. For location of side weirs (SW) refers to Figure 6.1.....	107

Figure 6.9. A: Syntetic rainfall (2yrs – 6hr) B: Amount of runoff that reaches the beginning of both channels. C: West Channel. Side Weirs operation with the maximum syntetic rain. D: East Channel. Side Weirs operation with the maximum syntetic rain. For location of side weirs (SW) refers to Figure 6.1.	108
Figure 6.10. A: Amount of runoff that reaches the beginning of both channels (sorghum irrigation data) B: East Channel. Side Weirs operation during irrigation process. C: East Channel. Side Weirs operation during irrigation process. For location of side weirs (SW) refers to Figure 6.1.	109
Figure 6.11. West Channel. Side Weirs operation during irrigation process.....	109
Figure 7.1. A: Single channel with six side weirs and a central culvert. This channel has a positive slope from the inlet to the center; The crest, length of the side weir and width of the channel varies from the inlet in both sides to the center. B: Channel top view geometry, not at scale.....	111
Figure 7.2. A: Two separates channels with 3 side weirs each. Slope is positive and short crest length, side weir length and the channel width. B: Channel top view geometry, not at scale. C= crest elevation.....	113
Figure 9.1. Location of the cross sections in the study area. Red dots represent the location of piezometers.	122
Figure 9.2. Cross Section A – A` with a vertical exaggeration of 10 times. Current Conditions.	122
Figure 9.3. Cross Section B – B` with a vertical exaggeration of 10 times. Current Conditions. This profile shows the location of the piezometers along the cross section line.....	123
Figure 9.4. Cross Section C – C` with a vertical exaggeration of 10 times. Current Conditions.	123
Figure 9.5. Cross Section D – D` with a vertical exaggeration of 10 times. Current Conditions. This profile shows the location of the piezometers along the cross section line.....	124
Figure 9.6. Cross Section E – E` with a vertical exaggeration of 10 times. Current Conditions.....	124
Figure 9.7. Cross Section I – I` with a vertical exaggeration of 10 times. Current Conditions. This cross section represents the area to build the hydraulic design.....	125
Figure 9.8. Cut and Fill calculation method. Location of stations and the cross sections lines presented in Figure 9.1.....	126
Figure 9.9. Cut and fill Section A-A`.....	127
Figure 9.10. Cut and fill Section B-B`.....	128
Figure 9.11. Cut and fill Section C-C`.....	129
Figure 9.12. Cut and fill Section D-D`.....	130
Figure 9.13. Cut and fill Section E-E`.....	131
Figure 9.14. Cut and fill Section I-I`.....	132

FIGURES IN APPENDIX

	Page
Figure B.1. Historical Rainfall Events (Hyetographs) from 2002 to 2005.	145
Figure B.2. Historical Rainfall Events (Hyetographs) from 2006 to 2009.	146
Figure B.3. Historical Rainfall Events (Hyetographs) from 2006 to 2009.	147
Figure C.1. Complete Storm Events (Hyetographs) from 2002 to 2004 and 2007 to 2008.	148
Figure C.2. Complete Storm Events (Hyetographs) from 20010 to 2011.	149
Figure D.1. Depth-duration-frequencys for Guayama’s Area (NOAA, Atlas 14, 2012).	150
Figure D.2. Precipitation depth - Recurrence Curve (NOAA, Atlas 14, 2012).	150
Figure E.1. Freeboard chart. Height of bank above water surface (Anderson, Paintal, & Davenport, 1970).	151
Figure F.1. Chart of J coefficient. Source (May, Bromwich, Gasowski and Rickard, 2003)	152
Figure F.2. Chart of K coefficient. Source (May, Bromwich, Gasowski and Rickard, 2003).....	152
Figure H.1. A: Synthetic rainfall. 1yr-24hr. B: Amount of runoff that reaches the beginning of both channels C: East Channel. side weirs operation. D: West Channel side weirs operation.....	156
Figure I.1. Synthetic Storms (Hyetographs).	157
Figure I.2. Synthetic Storms (Hyetographs).	158
Figure I.3. Synthetic Storm (Hyetographs).	159
Figure I.4. Synthetic Storm (Hyetographs).	160
Figure I.5. Synthetic Storm (Hyetographs).	161

LIST OF ACRONYMS

AOI	Area of Interest
ASCE	America Society of Civil Engineers
CDL	Critical Depth Line
cm	Centimeter
CN	Runoff Curve Number
CSS	Critical Shear Stress
CY	Cubic Yard
DDF	Depth-Duration Frecuency Curve
DEM	Digital Elevation Model
EGL	Energy Grade Line
EPA	Environmental Protection Agency
ESRI	Economic and Socila Research Institute
FHWA	Federal Highway highway Administration
GIS	Geographic Information System
HGL	Hidraulic Grade Line
hr	Hours
JBNERR	Jobos Bay National Estuarine Research Reserve
MGD	Million Gallons Per day
msl	Mean sea level
MSS	Maximum Shear Stress
NCDC	National Climatic Data Center
NCHRP	National Cooperative Highway Research Program
NDL	Normal Depth Line
NERRS	National Estuarine Research Reserve System
NOAA	National Oceanic and Atmospheric Admin
NRCS	Natural Resources Conservation Service
PCSWMM	PC Storm Water Management Model (SWMM)
PRASA	P.R. Aqueduct and Sewer. Authority
PRLA	Puerto Rico Land Authority
SCS	Soil Conservation Service
SI	International System (Metric System)
USCS	United States Customary System
USDA	U.S. Department of Agriculture
USGS	U.S. Geological Survey
VBA	Visual Basics for Aplications
WEF	Water Environmental Federation
WSS	NRCS - Web Soil Survey

CHAPTER 1 INTRODUCTION

The Jobos Bay National Estuarine Research Reserve (JBNERR) is one of 26 estuarine areas under the National Estuarine Research System designated by the National Oceanographic and Atmospheric Administration (NOAA). JBNERR (see Figure 1.1) is located between Salinas and Guayama at the south of Puerto Rico. Jobos Bay covers an area of 2,833 acres of mangrove forest and diverse habitats from the landward transition zone of coastal fan-delta and alluvial deposits to offshore cays in the Caribbean Sea (Kuniasky et al, 2010).

Since Spanish colonial time until 1970's, the principal land use in the Jobos Bay Reserve watershed was agriculture. From coconuts plantation bordering the shoreline to sugarcane on the coastal plain, agriculture was predominant. In the 1960's, the industrialization started in Puerto Rico and the sugarcane cultivation went down until the Central Aguirre closed on 1990. After the sugar cane era, these lands continued with the agricultural activity but changed to the production of vegetables and fruits (Whitall et al., 2011; Kuniasky et al., 2010).

Changes in water management in the Jobos area evolved parallel to agricultural activities. The drainage hydraulics and hydrology of the JBNERR area has been frequently modified by the construction of canals and ditches to capture water from the streams for irrigation purposes. From 1910 to 1935, sugarcane industry increased irrigation and a reservoir network was constructed to supply water to those uncultivated areas (Kuniasky et al., 2010). The sugar cane industry builds a series of canals to drain the water pumped from the wells. Excessive pumping started to lower the water table and the demand of water supply for agriculture increased.

In 1993, the Puerto Rico Land Authority (PRLA) selected Hacienda Aguirre (see Figure 1.2) to install a demonstration project on corn planting using an irrigation pivot system. The site was plowed and the top soil was placed near the northern boundary of Mar Negro, creating a dike

which was used as roadway. This dike altered of the flow pattern in the zone. Due to this action, six of seven abandoned ditches were cleaned and excavated. These ditches (two of them are in the area of interest of this project) drains from north to south, directly into the mangrove forest (Gregory L. Morris and Associates, 2000).

1.1 PROBLEM STATEMENT

It is believed that intensive agricultural activities north of the reserve caused a negative impact on mangroves. In 1993, as part of the demonstration project, PRLA cleaned a series of drainage channels to drain irrigation water excess direct to the mangrove forest (Gregory L. Morris and Associates, 2000). Figure 1.2 shows two of the channels that belong to the area of interest. The east channel starts at the center of the irrigation pivot and extends to the south toward the mangrove forest. This channel used to discharge fresh water from pumps, however, nowadays fresh water comes from leakage through the pumps. The west channel collects the water excess from the west side of the center pivot irrigation.

Preliminary studies reported that pesticides, fertilizers and chicken manure applied in agricultural fields were being transported and impacted the near-shore water and air in the estuary (Dieppa et al., 2008; Whitall et al., 2011). Both channels in Figure 1.2 were used to transport runoff and irrigation water directly into the mangrove area.

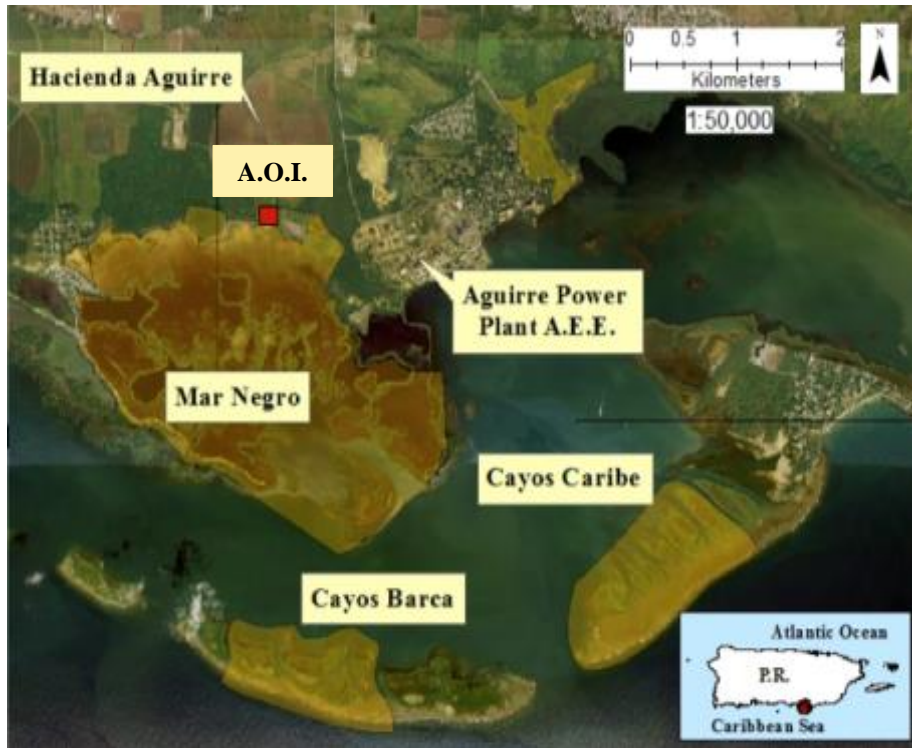


Figure 1.1. Location of Jobos Bay National Estuarine Research Reserve, JBNERRS delineated areas shapefile from NERRS.

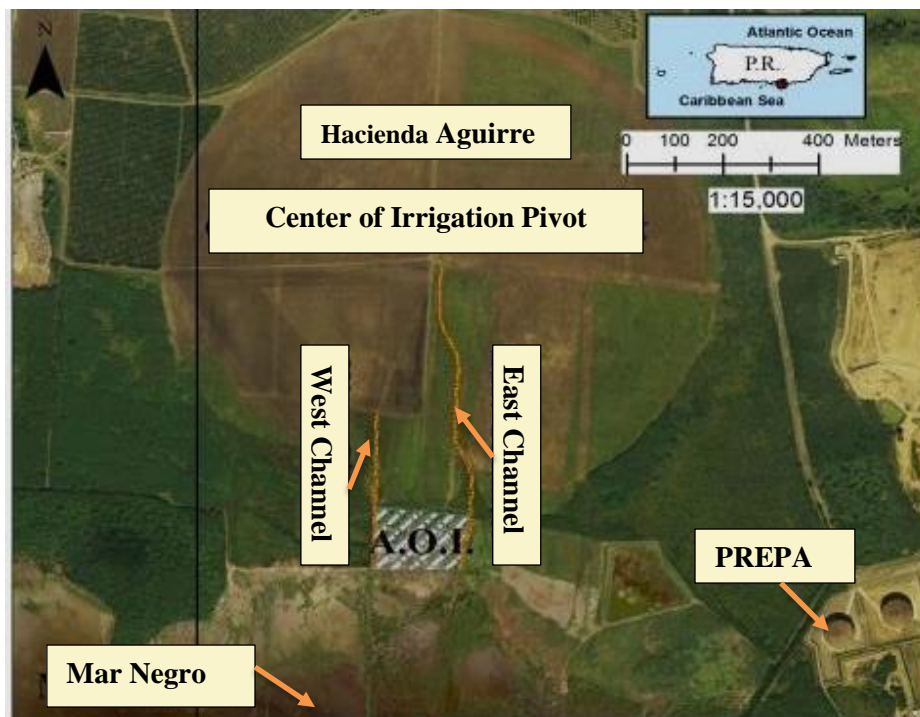


Figure 1.2. Location of the drainage channels. (Aerial image by 3001, Inc. 2007)

Nevertheless, the northern area of the Jobos Bay Reserve has been used for agricultural activities since the Spanish colonial times. Figure 1.3.A shows the study area in 1987. At this time agriculture was present under the sugar mill Central Aguirre until 1990 when this industry closed operations. In 1993, the center pivot irrigator system was introduced near the mangrove forest. Figure 1.3.B demonstrates that by 1997 the mangrove cover was residing. This irrigation method was operational until late 2009 when the PRLA decided to stop operations to upgrade the system. However, at current time, it remains non-operational.

In 1998, the Hurricane Georges affected the area causing great damage to the mangrove forest. The overall impact of hurricane Georges on Jobos Bay mangroves is not known with precision; however, hurricanes generally set back succession and reduce mangrove areas (Demopoulos, 2004). Figure 1.3.C shows the situation of the mangroves forest in 2007 which is similar to current conditions.

The mangrove mortality can be induced by anthropogenic activities such as deforestation, domestic sewage inputs to mangrove lagoons, change of hydrology by the constructions and agricultural practices at nearby locations (Román Guzmán, 2010). The mortality may be increased by natural factors such as hurricanes, storms, tsunamis, droughts, hydrologic changes, erosion and subsidence, hypersalinity, and pollution. Any of these factors can contribute to the mangrove mortality on the Jobos area, especially those which involve agricultural activities, change of hydrology and the natural factors such as the ones already observed in that area. However, the affected mangrove stand is over 30 years old and its proximity to farms bordering the JBNERR may indicate that the hydrology has changed as a result of changes in irrigation practices, water use, and rainfall (Kuniasky et al., 2010).

In 1995 JBNERR implemented a mangrove and wetland restoration program involving the monitoring of mangrove communities (Demopoulo, 2004). Drainage control system and water quality control have to be applied to restore the mangrove area and promote a healthy growth.

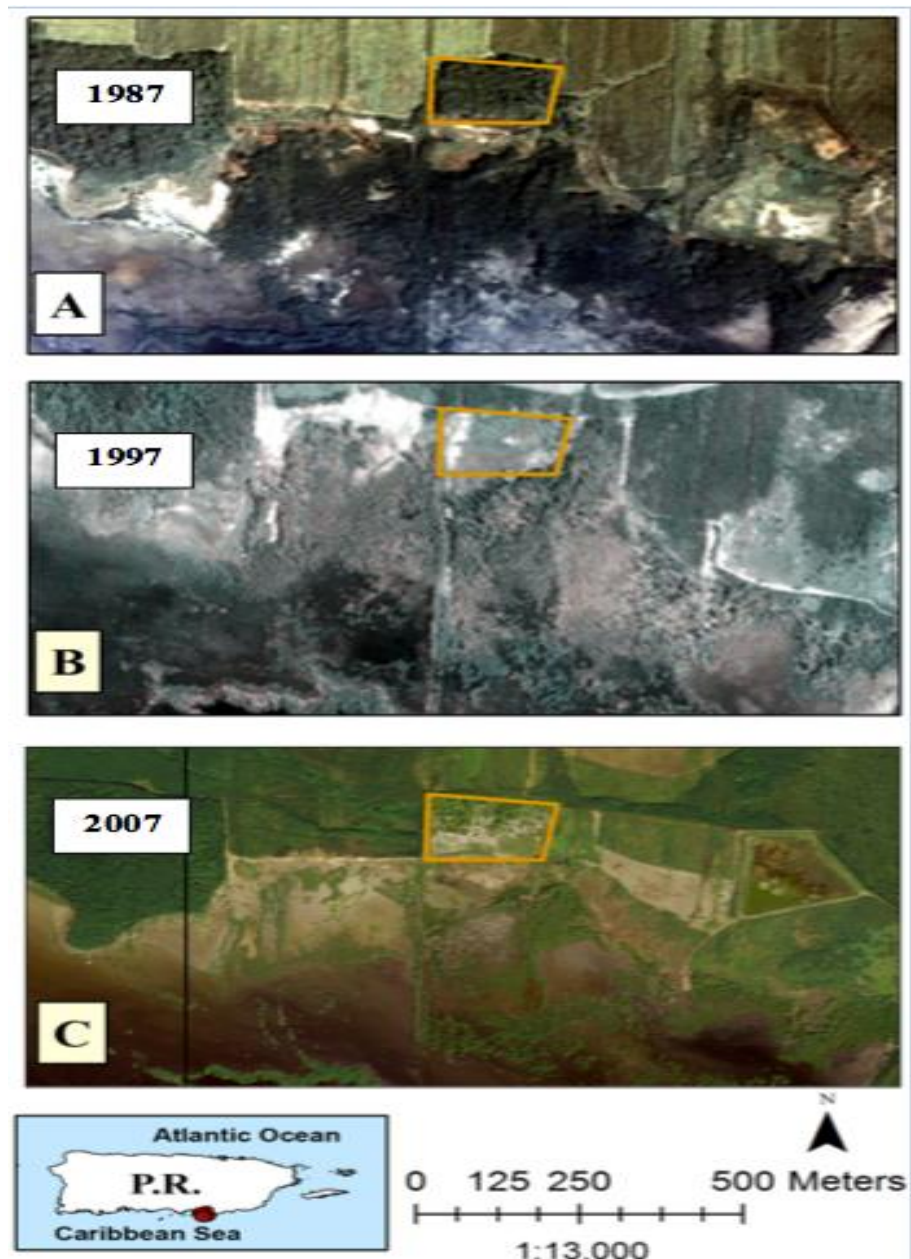


Figure 1.3. Sequence of aerial photos showing the evolution of the project area during the last decade. Project area shown in the orange box. Aerial Images by 3001 Inc., 2007

1.2 SCOPE AND OBJECTIVE OF THE STUDY

The purpose of this project is the design of an innovative overland flow water distribution system using lateral weirs to control surface runoff, reduce surface erosion and improve the quality of runoff waters discharging into the Jobos Bay mangrove area. The project will be focused on hydrologic and hydraulic design conditions according to the runoff and to the irrigation flow discharging into the project area. A cost analysis of the channels system, land movement, labor, materials and equipment is provided to complete the design.

CHAPTER 2 STUDY AREA DESCRIPTION

2.1 Location and Physiographic Region

The JBNERR is the second largest estuary in Puerto Rico and it is part of the National Estuarine Research Reserve System (NERRS) of NOAA. Jobos bay is located on the southeast coast of the island between the municipalities of Salinas and Guayama. The contributing watershed of this bay has an area of about 137 km² with a population of about 32,000 persons and a variety of land uses, predominantly agriculture (Whitall et. al, 2011). The Jobos Bay Reserve has a total surface area of 25 km² (Dieppa et al., 2008) and it is composed by areas knows as: Mar Negro, Hacienda Aguirre, Cayos Barca, and Cayos Caribe (see orange shaded areas in Figure 1.1). The area of interest (A.O.I.) for this project is a parcel located at the boundary between Mar Negro and Hacienda Aguirre (see Figure 1.2). Hacienda Aguirre shows a circular area with the pivot irrigation system.

The JBNERR watershed could be subdivided into nine subwatersheds (Figure 2.1.A) and the project area belongs to SW3 (Figure 2.1.B) with an area of 16.5 km² which extends from highway PR-52 to Jobos Bay coastline (Mar Negro wetland system). Similar to other Jobos Bay subwatersheds, the SW3 does not have a defined stream channel and the surface runoff discharges in several places of the bay depending on the topography.

This watershed has a diversity of land uses (see Figure 2.2) including industrial; residential development (which includes a population of about 2,652 residents, Census 2000), agriculture, wetlands areas, and forest areas. The dominant feature in the watershed is Mar Negro's mangrove forests and associated tidal waterways and mud flats (Zitello et al., 2008).

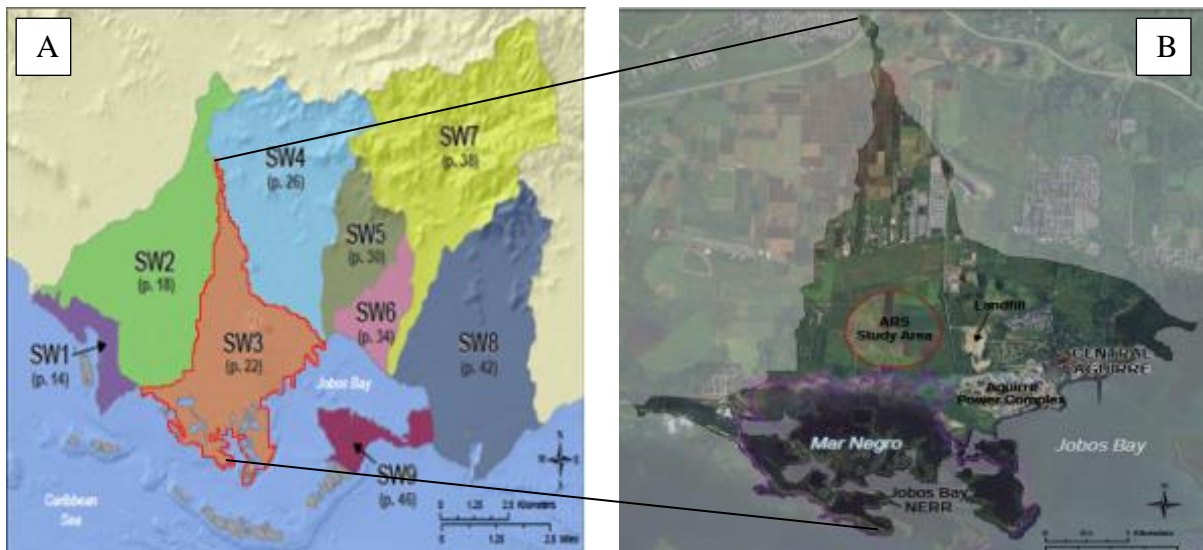


Figure 2.1. Jobs Bay National Estuarine Research Reserve (Zitello, Whitall, Dieppa, Christensen, Monaco, and Rohman, 2008).

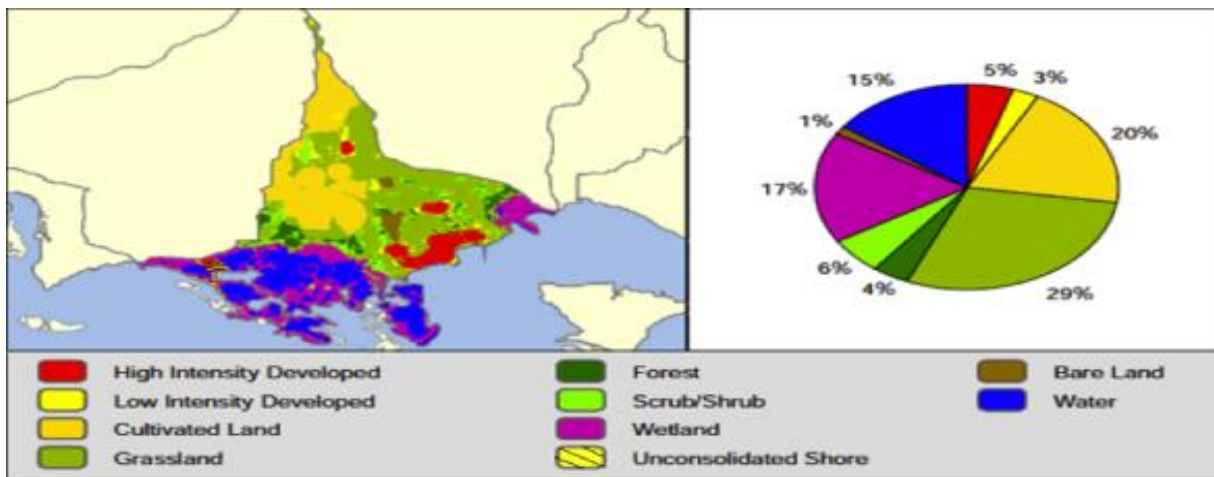


Figure 2.2. Land use distribution in Central Aguirre watershed and percentage coverage (Zitello, Whitall, Dieppa, Christensen, Monaco, & Rohman, 2008).

2.2 EXISTING TOPOGRAPHY

Field survey information was collected at the study area for general knowledge of the land elevation and for design purpose. Figure 2.3.A shows the distribution of the measured points and Figure 2.3.B is a topographic map prepared in ArcGIS for design purposes. The elevation of the areas varies from 2.5 meters at northern boundary region to approximately 0.6 meters at southern boundary region.

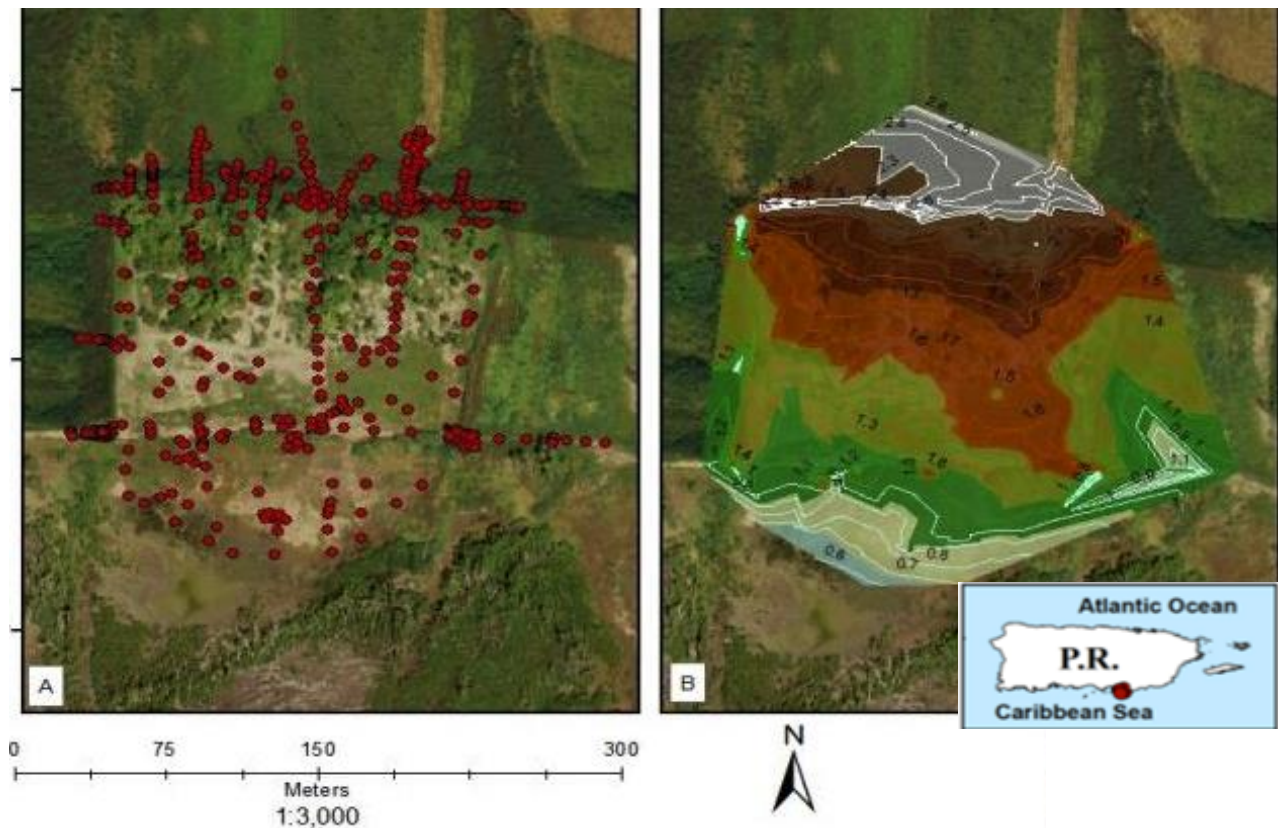


Figure 2.3. A: Topographic measure points of the study area. B: Contour lines and elevation modeling of the study area (msl).

2.3 CLIMATE

The watershed of Central Aguirre, as part of Jobos Bay, it is primarily comprised of the low relief South Coastal Plain of Puerto Rico. A natural mountain range (La Cordillera Central and La Sierra de Cayey) at the north of Jobos Bay watershed, protects the zone from moisture-laden northeast trade winds, causing a zone of low precipitation in the study area (Whitall, et al., 2011). Jobos Bay receives a mean precipitation of approximately 15.4 cm/yr (National Weather Service, Weather Forecast Office, 2009). During the period between 1999 to 2008 the mean precipitation was 99.6 cm at the Aguirre Gauge station, within the watershed boundaries. The wettest months are September and October with 167 mm and the driest month with 20 mm of rain is January (National Climatic Data Center (NCDC), 2010). The mean annual temperature between 1999 and 2008 was 26° C with a maximum of 27.5° C in August and a minimum of 24.3° C in January (NCDC, 2010).

The evapotranspiration of the area is around 25.59 cm/yr and it usually decreases as the water table level reaches a depth of approximately 2 meters from the surface (Rodríguez, 2006). This aquifer does not have great importance in the area but most of the domestic wells in the zone take their supply from the upper zone of this aquifer. The Puerto Rico Aqueduct and Sewer Authority (PRASA) and the water used for agriculture are collected from the unconfined aquifer that can be found at the bottom of the alluvial formation.

2.4 GEOLOGY

The watershed of Jobos Bay is composed of two principal hydrogeologic units; an upper zone typically composed of varying proportions of sand, gravel, and clay with the fraction of finer sediments increasing coastward; the second unit is composed of fan deltas and alluvial

deposits (Rodríguez, 2006). The alluvial deposits involve the coastal plain of the area and swamp deposits (unconsolidated clay, silt and organic matter) on the southern boundary of the coastal plain (see Figure 2.4) (Glover, 1961; Rodríguez, 2006). In general, the watershed area is mostly composed of alluvial fan deposits covering layers of volcanic rocks at the north; volcanoclastics rocks combined with minor limestone at the central region from cretaceous and at south sedimentary rock of tertiary (see Figure 2.5).

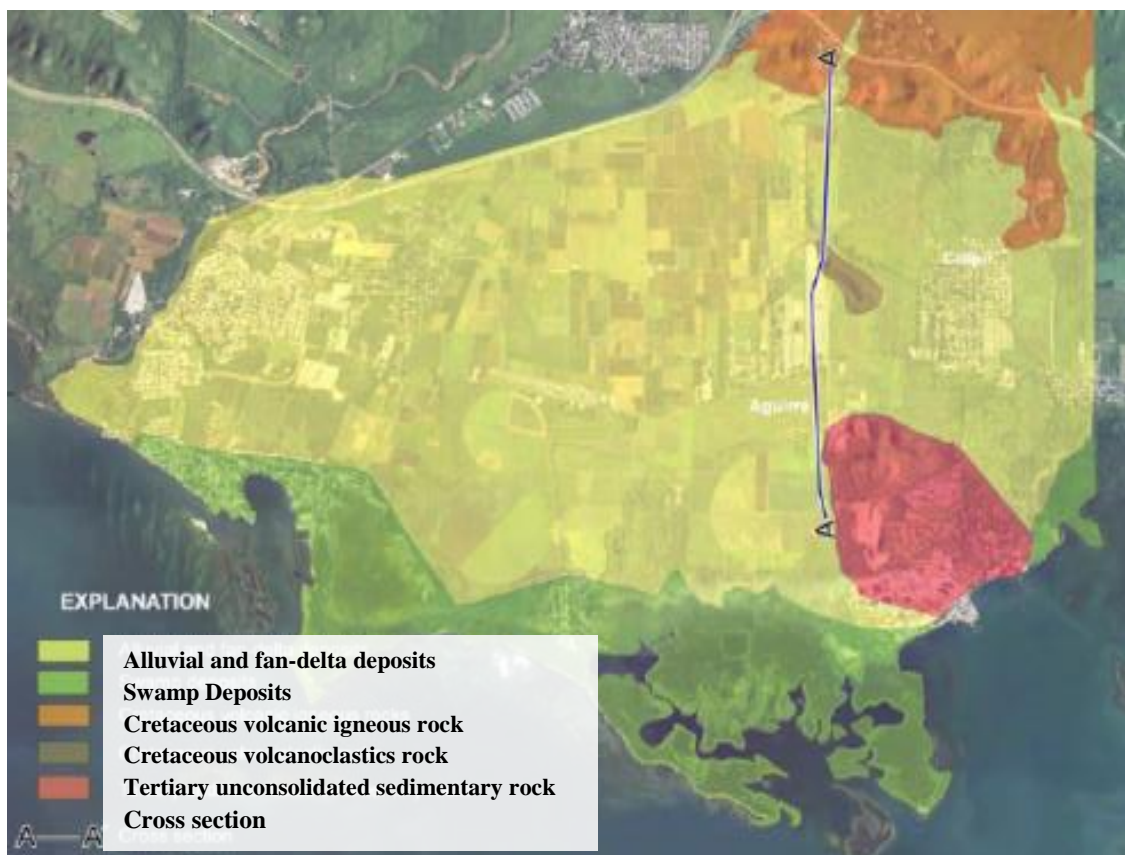


Figure 2.4. Hydrogeology of the Jobos Bay watershed (Rodríguez, 2006).

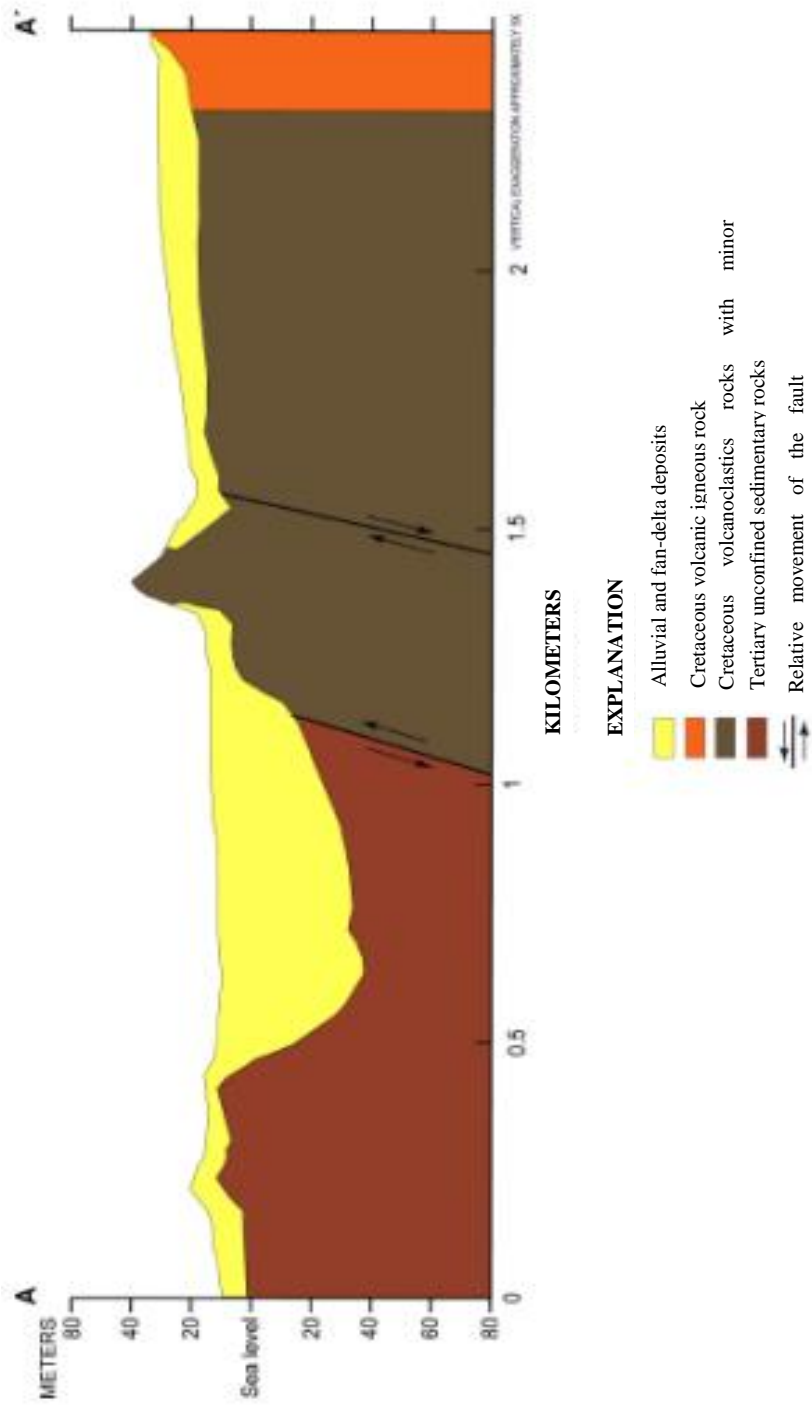


Figure 2.5. Hydrogeology cross section A-A' from south to north bound of the Jobos Bay Watershed (Rodríguez, 2006).

These alluvial deposits constitute the Salinas Alluvial Fan Aquifer, which extends from Nigua river in Salinas to Guamani river in Guayama. This aquifer forms part of the Santa Isabel – Patillas Region aquifer system. This aquifer unit covers the coastline area extending from one (1) mile (at Bahía de Jobos) to four (4) mile (in the Salinas fan delta) inland (Quiñones-Aponte, et al., 1996). One of the hydrogeological characteristics of this aquifer is the specific yield, is of approximately 25 % (Quiñones-Aponte et al., 1996). That specific yield is a representation of the unconfined conditions in the aquifer's upper zone. The unconfined conditions varies as it approaches to the coast by a fine-grains formation that acts as semiconfined condition (Rodríguez, 2006). The storage coefficient of this aquifer was found to be around 0.0003 and the hydraulic conductivity of the alluvial deposits were in a range from 8 m/d near to the Cordillera Central and 30 m/d close to the Salinas town and the coast.

1.1 AGRICULTURAL ACTIVITIES

Since late 1800's until 1990 when the sugar cane era ended, the Hacienda Aguirre used furrow irrigation. In 1994, a pivot drip systems and center-pivot sprinkler irrigation were installed using groundwater wells. This new technology replaced the traditional flooding irrigation practices (Dieppa et al., 2008). Changes in irrigation methods and the combination of increased groundwater extraction, which reached up to 11.4 MGD in 2002 (Kuniasky et al., 2010) contributed to lower groundwater levels and possibly shorten the aquifer recharge time. This has increased the risk for salt water intrusion into the aquifer (Kuniasky et al., 2010). The effect of this process on the mangrove ecosystem has not been documented; however, pivot irrigation is not used nowadays. In some farms, drip irrigation has been implemented.

CHAPTER 3 MODEL DESCRIPTION

3.1 RUNOFF AND HYDRAULIC SIMULATION

Runoff in the watershed of Jobos Bay area was simulated using PC Storm Water Management Model (PCSWMM¹) based upon the Environmental Protection Agency (EPA) model SWMM5² and including geographic information system (GIS) data formats. This modeling software simulates the surface runoff response of a given catchment to preloaded precipitation data by representing the subcatchments as an interconnected system of hydrologic and hydraulic components. SWMM contains a series of capabilities and limitations for the Jobos Bay project:

- The software PCSWMM allows inputs from Economic and Social Research Institute (ESRI) format shapefiles, images, and digital elevation models (DEM). This interaction let the user to use the remote sensing knowledge to create a scenario that fits more with the existent conditions. On this project, these features allow to recreate a possible future scenario of the proposed hydrologic conditions.
- The model was used to analyze historical rain fall data from 2002 to 2011. These periods contains only the maximum accumulative rain in 24 hours events for each year. Maximum annual 24-hr duration events from 2002 to 2011 were simulated with SWMM.
- Rainfall data was obtained from the JBNERR weather station of the main office which is located approximately 2.5 km east of the project area. The effect of the distance is not

¹ PCSWMM is a marketed software develop by Computational Hydraulics International (CHI).

² Storm Water Management Model (SWMM)

significant because most 24 hours events are associated with tropical storms covering the entire watershed.

- The model simulates the infiltration. The user could select the soil conservation service Curve Number, Horton or Green-Ampt models. Also the software let change from one method to another, but the data required by each method have to be available.
- The software allows defining a large variety of open channels geometries. It creates a connection of the rainfall runoff simulation with the hydraulics elements and is capable to simulate the water behavior on the system.
- Channel transitions (contraction or expansion) cannot be modeled on SWMM. There are no features which identify the transition elements. The lengths of the transitions are not considered by the model software.
- Channel bends analyses are not considered by SWMM. The superelevation effects in the water surface of the channel bend is not taken in consideration.

3.2 CONCEPTUAL MODEL.

This project consist in two differents modeling parts, the hydrology, which determines the surfaces runoff for the given subwatershed and the design of open channels with different features. The mathematical basis of the hydrological and hydraulic designs will be summarized in two sections following the EPA SWMM User Manual ³(James et al., 2011).

³ PCSWMM use the EPA SWMM User Manual.

3.2.1 HYDROLOGICAL COMPUTATIONS

The surface runoff in SWMM is computed using the water balance equation which takes in consideration the precipitation, storage, evaporation, infiltration, and runoff (see Figure 3.1). The modeling software treat the subcatchments as a nonlinear reservoir and the water input comes from precipitation or any upstream subcatchments. The storage capacity (d_p) in the subcatchments will depends on the ponding, surface wetting and interception information provided by the user. The surface runoff depends on the storage information and the Manning's equation (3.1). The outflows are integrated in the system as evaporation, infiltration, and runoff (Q). The water depth (d), which is continually changing depending of time and amount of inflows, will be computed with the runoff per unit area over the subcatchments (Rossman, 2010).

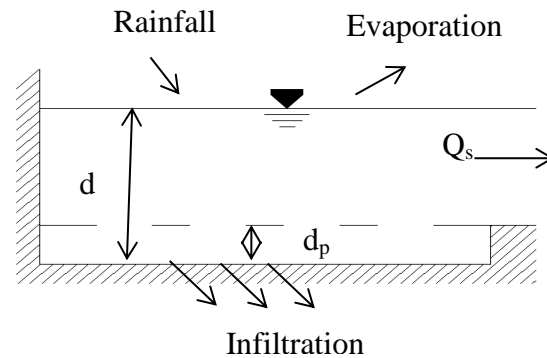


Figure 3.1. Illustration of the water balance variables and surface runoff computation.

The SWMM non-linear reservoir outflow equation is:

$$Q_s = W \frac{1}{n} (d - d_p)^{5/3} S^{1/2} \quad 3.1$$

where:

- Q_s = subcatchment outflow (m^3/s)
- W = subcatchment width (m),
- n = Manning roughness coefficient,
- d = water depth (m),
- d_p = Depth of depression storage or storage capacity (m), and
- S = longitudinal slope (m/m).

3.2.2 INFILTRATION

Infiltration is the process by which the water (from rainfall, snowmelt or irrigation) moves from ground surface into the soil (Rawis, et al., 1992). SWMM provides three alternatives of infiltration models: 1) The Curve Number method developed by Soil Conservation Services (SCS), 2) Horton model and 3) the modified Green-Ampt model. The Curve Number (CN) method, estimates the infiltration capacity of a subcatchment according to a tabulated CN index (James and James, 2000).

The computation of infiltration by the Curve Number method is explained in the SCS Urban Hydrology for Small Watershed, Technical Report (TR-55), published in June 1986 (NRCS, 1986). This method computes the runoff with the following relations:

$$Q_R = \frac{(P - I_a)^2}{(P - I_a) + S} \quad 3.2$$

$$I_a = 0.2S \quad 3.3$$

$$S = \frac{1000}{CN} - 10 \quad 3.4$$

where:

Q_R	=	runoff depth (in.),
P	=	Rainfall depth (in.),
S	=	potential maximum retention after runoff begins (in.),
I_a	=	initial abstraction (in), and,
CN	=	Curve Number.

The initial abstraction represents all the losses (Figure 3.1) before runoff begins which includes depression storage, interceptions, evaporation and infiltration.

The curve number is determined depending of the hydrologic soil group, cover type, treatment, hydrologic conditions, and antecedent conditions. Curve numbers values are generally provided in tables (0)

3.2.3 HYDRAULICS COMPUTATIONS

The hydraulics computations will depend on the flows generated by the hydrologic model. In general, SWMM represents the hydraulic system by different elements such as conduits, nodes (junction, outfall, and flow divider nodes), storage units, pumps, flow regulators and weirs. Some of these elements are used to model the hydraulic system proposed in this project.

A conduit in the current project represents the open channel that moves the water from SWMM node to another. Nodes are elements which links conduits. These elements are able to represent confluence of natural surface channels and they can receive external inflows into the channel system.

The conduits, in SWMM, can be represented in all geometric shapes. The user has the option to draw transects of the channel or cross section. For this project, the trapezoidal geometry was used for open channel simulation. This modeling software use the Manning equation to express the relation between flow rate, channel bottom slope, cross sectional area, and hydraulic radius. The principal input parameters for conduits are:

- 1) name of the inlet and outlet nodes,
- 2) offset height or elevation above the inlet and outlet node inverts,
- 3) conduit length
- 4) Manning's roughness coefficient,
- 5) cross sectional geometry,
- 6) entrance/exit losses coefficients (optional), and
- 7) presence of a flap gate to prevent reverse flow (optional).

A channel transition, according to Chow, 1959, is a structure designed to change the geometric shape or cross sectional area of the flow. A channel transition should avoid excessive energy losses and eliminate cross waves and turbulence in order to provide safety to channel walls. There are several types of transitions (that will be discussed on Chapter 5), and Chow

(1959) recommends a coefficient of inlet losses for each of those transitions. SWMM do not have a particular element to analyze the transition areas but, the conduits contain a section to include the loss coefficient value at the entrance or at the outlet of each of them.

Side or lateral weirs are part of the flow regulator section in the SWMM user manual. The manual describes the flow regulators as structures used to control or divert flows within a conveyance system. Side weirs are represented in SWMM as a link connecting two nodes, where the weir is placed upstream of the node. The principal inputs for side weirs are:

- name of its inlet and outlet node,
- shape and geometry,
- crest height or elevation above the inlet node invert, and
- discharge coefficient.

The equation used for side weirs in SWMM are represented by the general formula (see Figure 3.2):

$$Q_w = C_w L h^{3/2} \quad 3.5$$

where:

- C_w = weir discharge coefficient,
- L = length of the weir,
- h = head difference across the weir, and
- Q_w = output side weir flow.

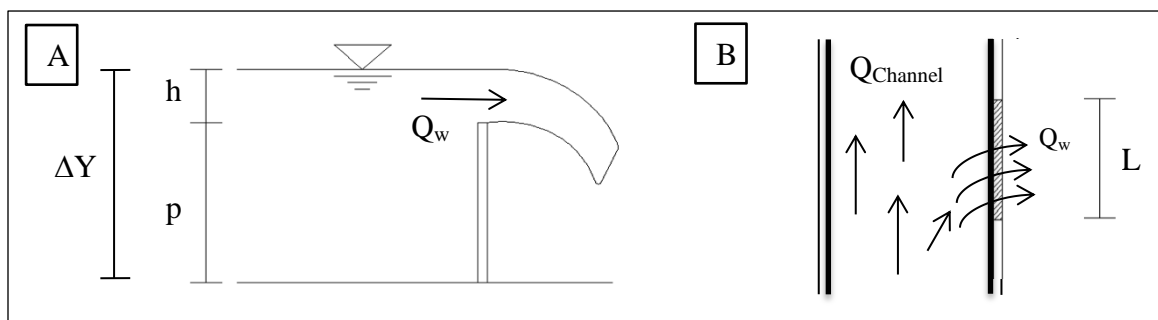


Figure 3.2. Weir schematics: A: lateral view of the weir; B: Top view of the wier.

Once the setup of the channel geometry is completed, SWMM can develop routing calculations using the conservation of mass and momentum equations for gradually varied flow. This software includes three different methods to solve previously mentioned equations; steady flow, kinematic wave routing and dynamic wave routing.

The steady flow routing method assumes that flow is uniform and steady. This routing method uses the inflow hydrographs at the channel upstream end to the downstream end without delay or change of shape. This method assumes that the channel longitudinal slope is equal to the friction slope of the channel.

The kinematic wave routing solves the continuity equation (3.6) and the simplified version of the momentum equation (3.7) for each reach of the channel. The only requirement for this method is that the slope of the water surface must be equal to the bottom slope of the channel. This method uses the discharge corresponding to normal depth as the maximum flow conveyed by the channel. Any amount of water that exceeds this value is considered lost from the system or ponded. This method cannot calculate the backwater effect, entrance/exits losses, or flow reversal.

Dynamic wave routing computes the complete one-dimensional Saint Venant flow equations, obtaining more accurate results. This method solves the unsteady momentum and continuity equations for each channel reach and computes the continuity equation in each node. This method can compute the backwater effect, entrance/exits losses, and flow reversal because it couples together the solution value of the water level from the channel conduits and the level at the nodes. The requirement of this method is to use smaller time step, usually minutes or less

The Saint Venant equations are:

$$\begin{array}{l} \text{Continuity} \\ \text{Equation :} \end{array} \quad \frac{\partial A}{\partial t} + \frac{\partial Q}{\partial x} = 0 \quad 3.6$$

Dynamic
Equation:
$$\frac{\partial(\frac{Q^2}{A})}{\partial x} + \frac{\partial Q}{\partial t} + gA \frac{\partial H}{\partial x} + gAS_f + gAh_L = 0$$
 3.7

Kinematic
Equation:
$$gAS_f + gAh_L = 0$$
 3.8

Steady State
Equation:
$$S_f - S_0 = 0$$
 3.9

where:

- A = cross-sectional area (m²),
- t = time (min),
- Q = flow rate (m³/s),
- H = hydraulic head of the water in the channel (m),
- S_f = friction slope = Q²n²/(A²R^{4/3}),
- S₀ = longitudinal slope (m/m),
- h_L = local energy loss per unit length of the channel (m), and
- g = acceleration of gravity (m/s²).

All these routing methods use the Manning equation to relate the flow rate to the channel depth or to compute the friction slope.

CHAPTER 4 HYDROLOGY

Hydrology is the study of water movement and distribution over catchment area. The prediction of a runoff in a watershed, will depends on the data of rainfall, discharging points, drainage areas, flow length, longitudinal slope, infiltration, ponding, evaporation, losses and soil characteristics.

4.1 STORM RAINFALL EVENTS

Two sources of information were used to obtain precipitation data for this project. From NERRS website (National Estuarine Research Reserve System, 2012), the historic data were obtained from 2002 to 2011 at Jobos Bay Reserve. The second source of information comes from NOAA Atlas 14 (NOAA, 2010). Atlas 14 provides the storm depths for different recurrence intervals and rainfall duration (see Table 4.1 and). Return period or recurrence interval is the reciprocal of the probability that an event will be equaled or exceeded in any day of the year (Bedient et al., 2008). In other words, a 10 year storm event has a probability of 10% of being equaled or exceeded any single year.

4.2 WATERSHED

The area of interest (AOI) in Jobos Bay is a region that does not have perennial water bodies. The runoff of the zone depends of rainfall events and from the agricultural irrigation excess. The AOI has two ditches that collect the water from upstream watershed and drain it to the mangrove area at Mar Negro. The east channel drains water from the water pump release at the center of irrigation pivot. The irrigation system is not operational and there is no agricultural activity.

Table 4.1 Precipitation partial duration series–based precipitation frequency estimates (in millimeters) at Salinas, P.R. Lat. 17.9702; Long.-66.2061– Guayama-Salinas, P.R

Duration	Average recurrence interval (years)						
	1	2	5	10	25	50	100
5-mi	9	12	15	17	19	21	23
10-min	12	17	20	23	26	29	32
15-mi	16	21	26	29	34	37	41
30 - min	25	34	41	47	54	59	65
60 min	38	51	61	69	80	88	97
2-hr	46	65	82	95	113	127	141
3-hr	55	71	92	108	131	148	167
6-hr	67	88	118	143	177	205	234
12-hr	79	105	146	180	229	271	314
24-hr	93	123	176	221	287	343	403

The west channel collects water from other places due to topographic features. Both channels collect excess water from irrigation during agricultural activities and also drain waters from nearby places. These two channels serve as starting point of watershed delineation (see Figure 4.1). The watershed contributing to these channels starts in the AOI and extends 4.6 km to the north along the valley with an area of about 4.0 km².

The watershed delineation was prepared using ArcGIS 10 with a 1962 USGS digital topographic map (Central Aguirre Quadrangle). The subwatersheds (see Figure 4.1) details were obtained using overlapping of aerial photos⁴ from 2007 with a digital USGS topographic maps and fieldwork. A total of 22 subcatchments were delineated according to the existing land use and land cover of the area. Table 4.2 shows the area of each subcatchment.

⁴ Aerial photos from Central Aguirre and Salinas; United State Corps of Engineers, Spatial Resolution of 30 m.

Table 4.2 Areas per subcatchment

Subcatchment	Area (km ²)	Area %
1	0.082	2.04%
2	0.274	6.79%
3	0.014	0.34%
4	0.073	1.82%
5	0.101	2.51%
6	0.243	6.04%
7	0.359	8.90%
8	0.020	0.49%
9	0.089	2.21%
10	0.045	1.12%
11	0.010	0.24%
12	0.207	5.14%
13	0.747	18.53%
14	0.008	0.20%
15	0.056	1.38%
16	0.207	5.12%
17	0.044	1.10%
18	0.066	1.63%
19	0.121	2.99%
20	0.327	8.10%
21	0.622	15.43%
22	0.318	7.88%

Total Area = 4.031 Km²

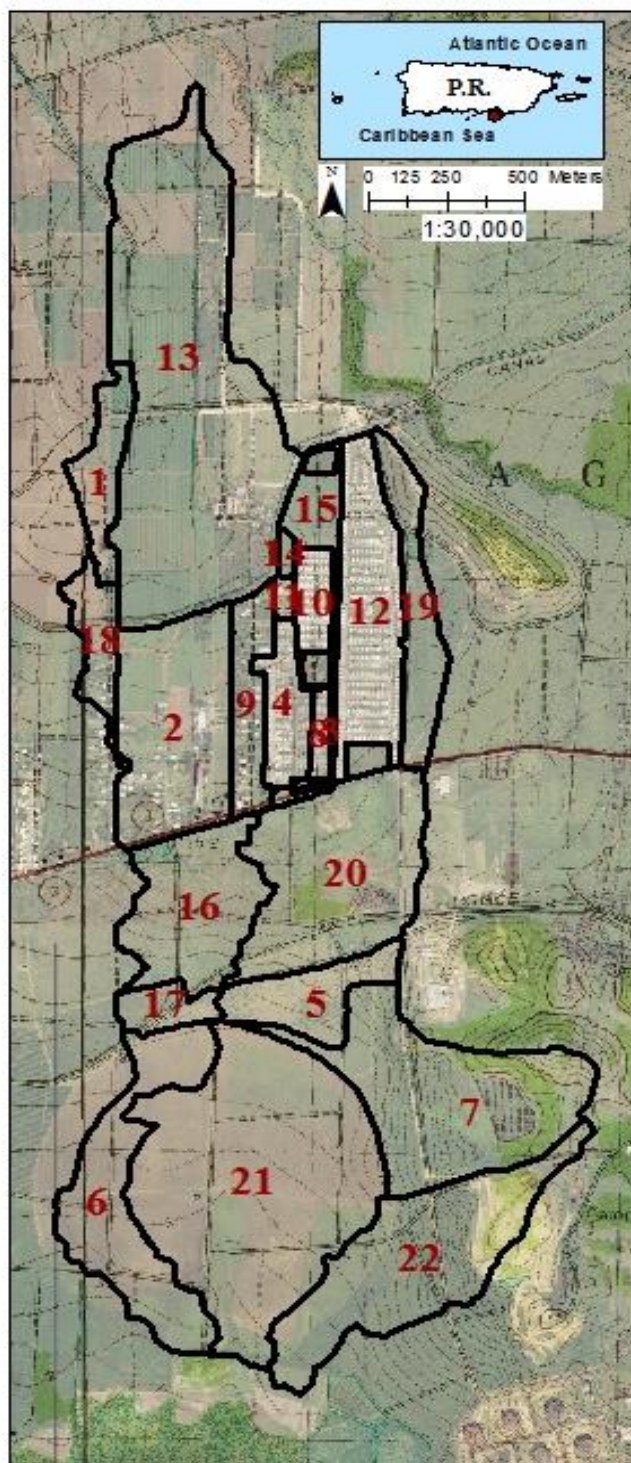


Figure 4.1. Delineated watershed of AOI .

4.3 OVERLAND FLOW ROUGHNESS

The overland roughness indicates the resistance of the land surface to the water movement. The resistance is provided by the friction of different types of impervious surfaces and pervious surfaces as natural vegetation and agriculture among others. The overland roughness is measured by the n value in Manning's equation. The Table 4.3 shows the roughness coefficients values used in this project. Field observations and remote sensing media (aerial images) were used to select the roughness coefficient of each watershed.

Table 4.3. Roughness Coefficient for flood plains (NRCS, 1986).

	Description	Roughness Coefficient (n)
Impervious	Fallow (no residue)	0.05
	Cultivated soils	
	Residue Cover \leq 20%	0.06
	Residue Cover $>$ 20%	0.17
	Grass	
	Short grass prairie	0.15
	Dense Grass	0.24
	Bermuda Grass (patios, lawns)	0.41
	Range (natural)	0.13
	Woods	
	Lights Underbrush	0.40
	Dense Underbrush	0.80
Long term Landfill*	0.10 - 0.14	
Pervious	Concrete, asphalt, gravel or bare soil	0.011

* (Bagchi, 2004)

4.4 HYDROLOGIC ABSTRACTION

The hydrologic abstractions consist of the withdrawal of water from the hydrologic cycle by evapotranspiration, ponding and infiltration. Evapotranspiration data was ignored for this project due of the lack of information during analyzed periods. Evaporation data was not available for this project. The watershed does not have natural ponding areas. There are three small manmade retention ponds that have no effects on routing.

The infiltration is the capacity of the soil to let the water enter into it. Infiltration depends on the soil properties determined mainly by the grain size distribution. Small grains size corresponds to less infiltration. Infiltration can be also affected by a change in the bulk density, and organic matter. If the bulk density increases, the amount of water retention decreases (Rawis, et al. 1992). Infiltration is the major component of hydrologic abstractions.

The Curve Number (CN) method is used to estimate the runoff obtained from rainfall after subtracting the hydrologic abstraction. The CNs were calculated by using the NRCS Web Soil Survey (WSS, N.R.C.S., 2013) to obtain the hydrologic soil group and detailed land uses. The hydrologic soil group was obtained through the input of the AOI delineated watershed to the WSS webpage, using a watershed shapefile created in ArcGIS (see Figure 4.1). The subcatchment (see Figure 4.2) has three hydrologic groups which are: sandy loam - group A with a 16% of the watershed, silty clay loam – group B with a 42% and clay soil – group D with the 42% of the watershed. According to NRCS the predominant type of soil in the delineated watershed are clay soils but each subcatchment can contain their own subdivision of hydrologic soils rating as shown in Table 4.4. Details of the distribution of the hydrologic groups by subwatersheds in percentage are shown in the Table 4.5.

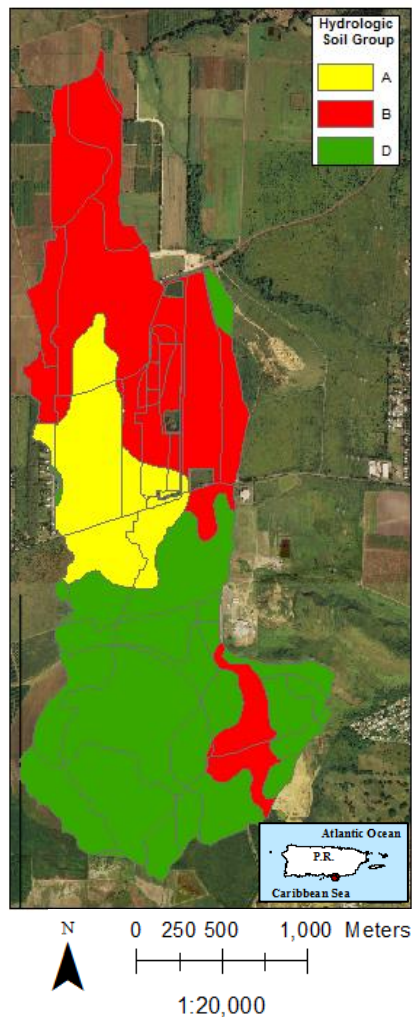


Figure 4.2. Representation of the hydrologic group.

Table 4.4. Hydrologic group percentages of the watershed (Soil Conservation Service, 2013).

SCS Soil Rating	Percentage by Watershed
A	16.0
B	42.0
D	42.0

Table 4.5. Hydrologic group percentages by subcatchment.

Subwatersheds	SCS Soil Rating in Percentage		
	A	B	D
1	0.0	100.0	0.0
2	94.8	4.2	1.0
3	75.5	24.5	0.0
4	31.0	69.0	0.0
5	0.0	0.0	100.0
6	0.0	0.0	100.0
7	0.0	26.7	73.3
8	39.4	60.6	0.0
9	42.1	57.9	0.0
10	0.0	100.0	0.0
11	0.0	100.0	0.0
12	1.7	98.3	0.0
13	10.1	89.9	0.0
14	0.0	100.0	0.0
15	0.0	100.0	0.0
16	58.5	0.0	41.5
17	0.0	0.0	100.0
18	25.5	70.5	4.0
19	0.0	73.8	26.2
20	22.1	13.8	64.1
21	0.0	0.4	99.6
22	0.0	0.0	100.0

The land uses were obtained from the WSS webpage, satellite imagery and field work inspections. This field inspection involved recognition of the land use in the area, especially those communities located at the north of the AOI watershed. Also, the field work helped to recognize the communities' water drain direction, water drainage outfalls, and which communities collect the water in retention ponds.

The unit soil groups were obtained from the WSS which are described in Table 4.6 and Figure 4.3. The SCS National Engineering Handbook (Mockus, 2004) was used for identification of the CN value by subcatchments. After obtained all the values of CN of each subcatchment, the weighted CN method was used to compute the CN values using a composite weighted CN as shown in Equation 4.1. The distribution of CN values in the watershed is shown in Figure 4.4. In general the watershed has a minimum CN value of 50 a maximum of 84 which represent the 25% of the area (see Table 4.7).

$$\text{Weighted CN} = \frac{\sum_i A_i \times CN_i}{A_T} \quad 4.1$$

where A_i is the area of each hydrologic unit inside one subcatchment and A_T is the entire area of that catchment.

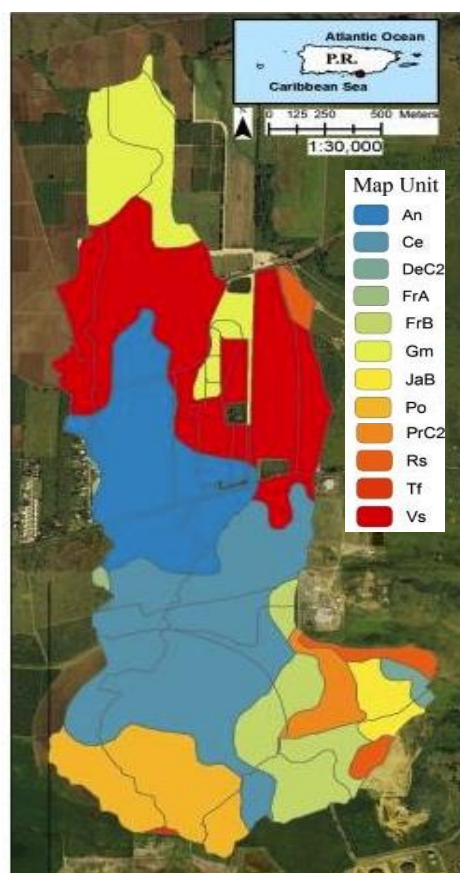


Figure 4.3. SCS map units.

Table 4.6 Hydrologic Unit (Soil Conservation Service, 2013).

Map Unit Symbol	Map Unit Name	Area in km ²	Percentages
An	Arenales Sandy Loam	0.6265	15.54%
PrC2	Pozo Blanco clay Loam, 5 to 12% slopes, erode	0.0981	2.43%
Vs	Vives Silty Clay Loam, high Bottom	0.9870	24.49%
Gm	Guamani Silty Clay Loam	0.3987	9.89%
Ce	Cartagena Clay	0.9651	23.94%
FrB	Fraternidad Clay, 2 to 5 percent slopes	0.3287	8.15%
Po	Ponce Clay	0.3860	9.58%
DeC2	Descalabrado clay, 5 to 12 percent slopes, erode	0.0294	0.73%
JaB	Jacana Clay, 2 to percent slopes	0.0906	2.25%
Tf	Tidal Flat	0.0041	0.10%
FrA	Fraternidad Clay, 2 to 5 % slopes	0.0131	0.33%
Rs	Rock Land	0.1036	2.57%



Table 4.7. Curve number distribution percentages of the watershed

CN	Watershed Percentage CN coverage areas
50	2.3%
54	0.3%
61	2.2%
63	21.5%
64	1.6%
65	5.1%
69	16.9%
73	8.1%
79	8.9%
83	7.9%
84	25.2%

Figure 4.4 Weighted curve number by watershed

4.5 HISTORICAL RAINFALL

Historical rainfall data was obtained from NOAA National Estuarine Research Reserve website for the meteorological Station Jobos Bay weather (SJB) located in latitude $17^{\circ}57'23.25''\text{N}$ and longitude $66^{\circ}13'22.69''\text{W}$ (National Estuarine Research Reserve System, 2012). The SJB is situated approximately 2.5 kilometers to the east of the study area. This station provides information from 2002 to present in periods of 15 minutes. Only the data from 2002 to 2011 was analyzed. These data was processed to obtain the maximum accumulation of rain in a period of 24 hours every year.

Figure 4.5 shows an example of a 24-hour duration rainstorm from hurricane Kyle on 2008. This period starts in September 22 at 12:00AM and ends 24 hours later. Section 4.8 provides a detailed explanation of this event and modeling results from this storm.

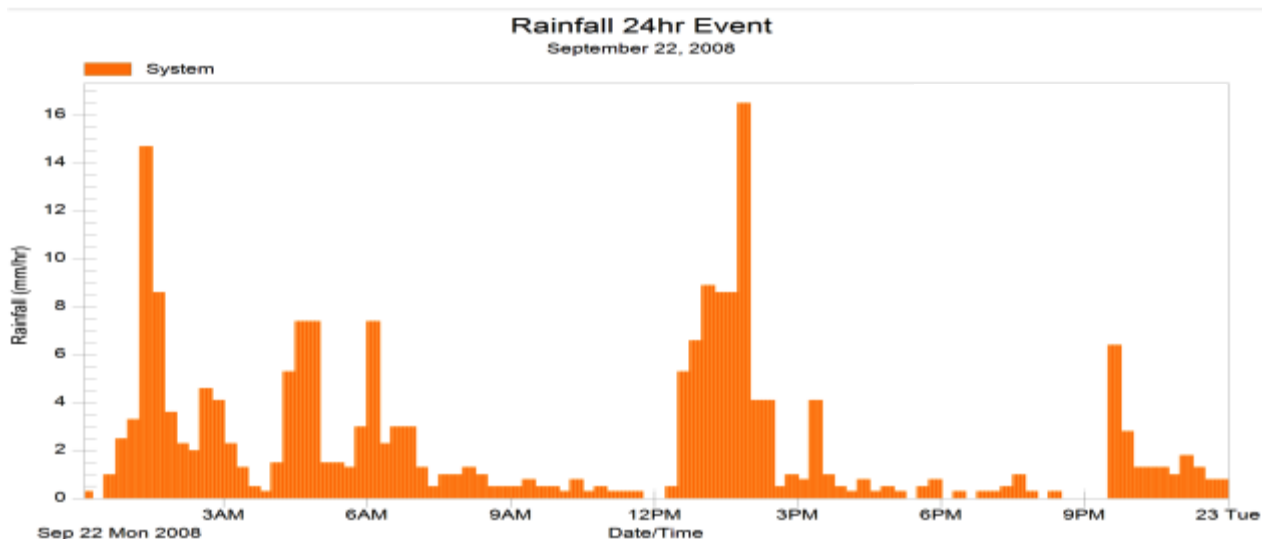


Figure 4.5. Hyetograph of historical storm of September 22, 2008 showing the distribution of the rain along 24 hours.

4.6 AGRICULTURAL IRRIGATION

In Addition to the rain storms, the excess of agricultural irrigation produces a water runoff that may have an impact in the JBNERR. The irrigation circle at north of the study site is the main area of irrigation which could create some runoff that reach the AOI. This circle has an area of 101.2 hectares (1.012 km²) which was divided in 4 subareas of 25.3 hectares each (see Figure 4.6). According to the NRCS (NRCS, 2009) the farmer only uses half of circle area for cropping and leaves the other half at rest and ready for the next sow season.

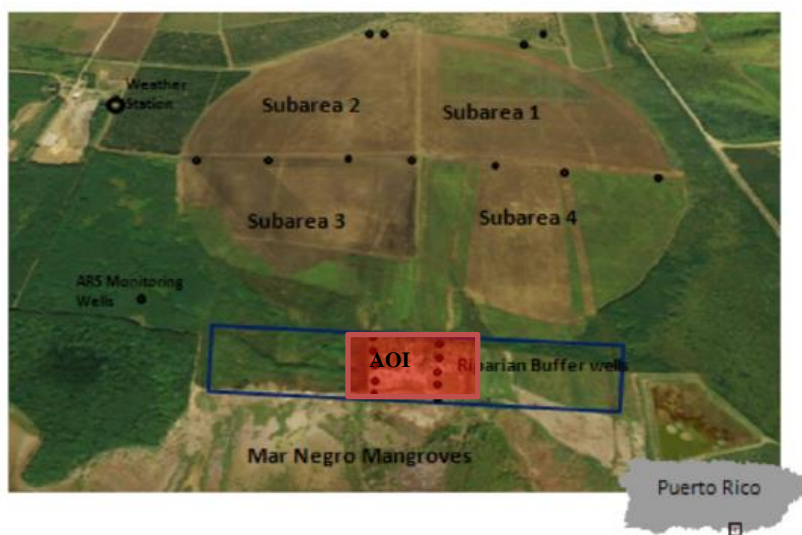


Figure 4.6. Irrigation subareas for the pivot area at north of Jobos Bay (William C. O. et al., 2012).

During the operation of the center pivot unit, the farmers only irrigate one quarter of the circle at a time. This method of cropping allows the farmers to choose any two quarters of the circle in which they desire to sow. The irrigation system operational time was set depending of the crop type with an established time of 13 or 22 hours for each independent circle quarter. Also the irrigation time was chosen depending of the size of the sowing in the quarter of the circle.

The corn crops were the only sow, which requires an irrigation of 22 hours twice a week (NRCS, 2009).

During the years of 2008 and 2009 crops of corn, cowpea and sorghum were sowed and irrigated using the pivot unit system (Williams et al., 2012). The sorghum crops require an irrigation of 9.14 millimeters per day, while the corn crops needs 9.89 millimeters per day (NRCS, 2009). The irrigation data correspond to the peak season during the months of July and August. The annual irrigation amount for 2008 and 2009 were 553 millimeters and 1270 millimeters, respectively (William C. O. et al., 2012). Also the amounts of rain for the same years were 1059 mm and 670 mm, respectively. Irrigation flows were considered as inflow in the design as explained in Section 4.8.

4.7 SWMM HYDROLOGY SETTING AND MODELING

The Storm Water Management Model (SWMM) developed by U.S. Environmental Protection Agency (EPA) was selected as design tool for this project. SWMM allows full integration of hydrology and hydraulic design on detailed scale and complex spatially, and temporal varied flow conditions (Environmental Protection Agency, 2013). SWMM is an enhanced version of US EPA storm water management model (CHI, 2011) that includes a self-contained GIS interphase for spatial analysis.

The watershed system in SWMM consists of 22 (see Figure 4.1) subcatchments draining from north bound to Mar Negro. Figure 4.7 shows the connection between the preset outlets of each subcatment with a red line. Additional to the subcatchments, there are three retention ponds, marked with green color in Figure 4.7, which regulate urban storm discharge from communities at the northeast side of the basin (large blue colored area in the Figure 4.7).

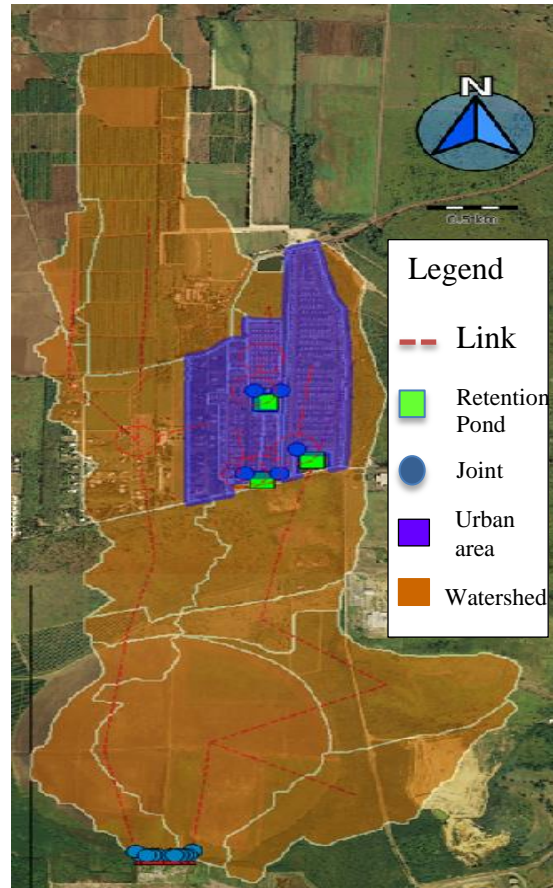


Figure 4.7. PCSWMM maximum surface runoff by subcatchment.

4.8 HYDROLOGIC ANALYSIS

The basin has two principal subcatchments, one at the east side which includes the communities and the west side which has low density communities and more agricultural areas. Both watersheds drain toward the south discharging into the two earth channels named West Channel and East Channel (see Figure 1.2).

Historic rainfall data gives an idea of the amount of precipitation occurring in the area. The last ten years rainfall data was chosen for this analysis, (2002 -2011); The first step was to find the highest cumulative precipitation in 24hrs by year, starting at 12:00 AM (see hyetographs in Appendix B). With the sorted data, identify if the storm date was related to a meteorological system was performed (as a tropical storm, hurricane, etc.). If the storm has relation with a

meteorological event, a new database was created with the rain data of the complete event (see hyetographs in Appendix C). The infiltration was computed using the Curve Number model to estimate the amount of runoff.

4.8.1 RUNOFF BY CN METHOD

Table 4.9 shows the highest rainfall accumulation in 24 hours each year and the inflow peak runoff obtained by the model at the West Channel and the East Channel. The maximum 24 hrs runoff obtained during these ten years was in September 22, 2008 producing a total runoff of $12.80 \text{ m}^3/\text{s}$. This event corresponds to a tropical wave that affected Puerto Rico from September 21 to 23. This tropical wave became later hurricane Kyle. The complete duration of the storm and hurricane were simulated and the results from SWMM are shown in Table 4.8.

The 2008 storm event produced a rain depth of 204 mm in 24 hours. This event represents a return period of less than 10 years according to the depth-duration frequency curve (DDF) obtained in NOAA, Atlas 14, 2012 (see Appendix D). The 2011 hurricane event is under the curve of a return period of 1 year, according to the DDF curve. The estimated runoff by the CN Method for this event was $1.45 \text{ m}^3/\text{s}$.

4.8.2 IRRIGATION DATA

Based on NRCS (2009) the irrigation data used from the 2008 sorghum sowing represents the historically maximum discharge produce by irrigation. The daily irrigation peak was $9.14 \text{ mm}/\text{day}$. This flow occurred over an area equal to a quarter of the circle (equal to 0.18 to 0.25 km^2), during a period of 13 hours. Therefore, for these conditions, the irrigation intensity corresponds to $0.70 \text{ mm}/\text{hr}$. The results from SWMM showed a peak runoff of $0.01 \text{ m}^3/\text{s}$ at the outlet of the subcatchment. The irrigation flow is negligible when compared with the rainfall runoff used for design.

Table 4.9. Storms; 10 Years Historical Events and 24 hours duration

Year	2002	2003 ^a	2004 ^b	2005	2006	2007 ^c	2008 ^d	2009 ^e	2010 ^f	2011 ^g
Month	Sept.	Nov.	Nov.	May.	June	Oct.	Sept.	Sept.	Jun.	Aug.
Day	9	11	16	17	14	27	22	5	23	22
24 hr Accum. Rainfall (mm)	49.7	108.0	65.1	94.9	59.7	101.2	204.6	99.3	64.3	48.7
West Channel (m ³ /s)	0.42	2.04	0.48	1.39	0.52	1.68	3.86	1.43	0.65	0.36
East Channel (m ³ /s)	1.76	5.76	1.61	4.50	2.04	5.47	8.94	4.16	2.78	1.09

- a. Tropical Wave
- b. Hurricane Jean
- c. Tropical Storm Noel
- d. Tropical Wave, became hurricane Kyle
- e. Tropical Depression - Remnants of Tropical Storm Erika
- f. Hurricane Otto
- g. Hurricane Irene

Table 4.8. Complete Storms; 10 Years Historical Events.

Year	2003 ^a	2004 ^b	2007 ^c	2008 ^d	2010 ^e	2011 ^f
Month	Nov.	Nov.	Oct.	Sept.	Oct.	Aug.
Day	10-13	14-18	26-28	21-23	5-8	21-24
Accum. Rainfall (mm)	475.2	153.2	217	442.9	156.9	187.1
West Channel (m ³ /s)	9.15	1.15	2.61	5.82	1.51	1.94
East Channel (m ³ /s)	20.57	3.29	7.47	14.07	2.65	4.79

- a. Tropical Wave
- b. Hurricane Jean
- c. Tropical Storm Noel
- d. Tropical Wave, became hurricane Kyle
- e. Hurricane Otto
- f. Hurricane Irene

CHAPTER 5 HYDRAULICS

The rainfall chosen for hydraulic design was the 2011 maximum 24 hr duration storm event with an accumulative rainfall of 48.7 mm. This rainfall event produced a peak runoff of 0.36 m³/s for the West Channel and 1.09 m³/s for the East Channel (see last column of Table 4.9). This event produced the minimum flow among the 10 rainfall events analyzed in SWMM. Larger events flooded the area completely making unnecessary a design for peak flows exceeding one-year frequency.

The Jobos watershed has multiple irrigation channels which drains the excess water from the crops areas to Jobos Bay (see Figure 2.1.B). They were excavated by the P.R. Land Authority to control the excess of water from furrow irrigation systems during the sugar cane production times (Gregory L. Morris & Associates, 2000). Two of these channels (see Figure 1.2) drain water from a pivot irrigation system to Mar Negro.

These channels were named East Channel and West Channel, due to their location, from the center of the area of interest. The West Channel collects water which drains from the west side of the pivot. The length of this channel is 220 m until it reaches the area of interest (AOI). This channel has a trapezoidal geometry with a variable depth which increases approximately 1.5 m in the transition zone between the JBNERR region and PRLA lands. In the JBNERR area, the channel depth is 0.4 meter depth before it discharges into the Mar Negro. The top width of the channels varies from 5.5 m in the deepest areas to 3 m in the outlet to Mar Negro. The bottom of the existing channels is composed of silt and clay, organic material and some areas are covered with vegetation. Most of this vegetation can be found in the transition zone upstream of the study area.

The East Channel starts in the center of the pivot and collects water from the east side of the pivot region. The length of this channel is 730 m from its origin until it reaches the mangroves in the Mar Negro Area. The channel depth is 0.9 m from the beginning of the area of interest to downstream until it reaches the outlet to Mar Negro. The top width varied from 7m in the deepest areas to 3 m in the outlet. The bottom is composed of the same material as the West Channel and it is mostly full of vegetation along the channel.

5.1 GENERAL HYDRAULIC PROCEDURES

The hydraulic design requirements includes a channel revetment, channel bend, channel contractions and side weirs. Figure 5.1 shows a general flowchart of the design sequence, each step will be discussed next.

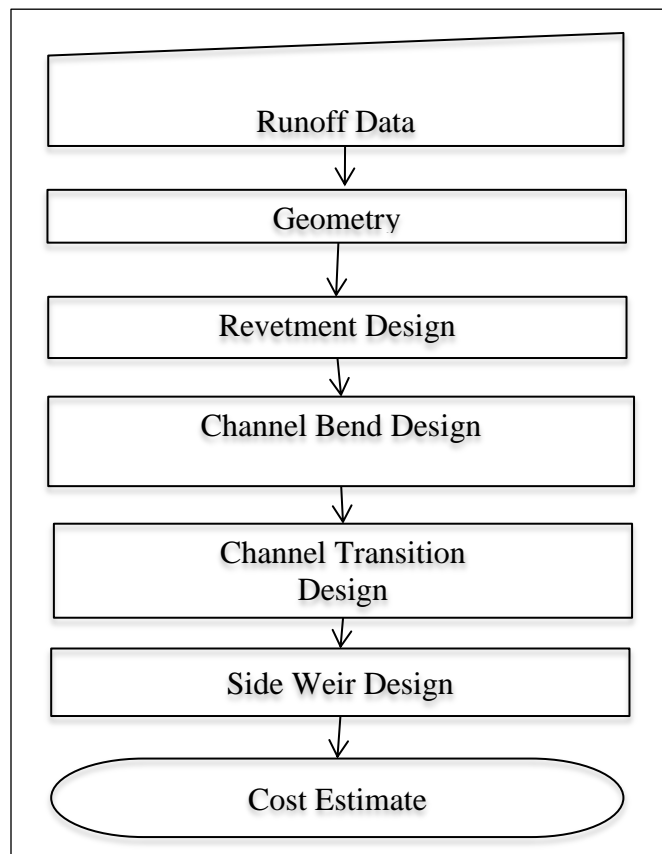


Figure 5.1. General flowchart of the hydraulic Design.

5.2 CHANNELS CHARACTERISTICS AND SIDE WEIRS DESIGN

The project watershed does not have any perennial water stream network. The only drainage system that has the watershed is a series of channels that were built to discharge the excess of agricultural irrigation.

Water from the East and West Channel will be collected in two independent new channels. Each new channel will redirect the water parallel to the bay coastline and spread it as overland flow by using a set of lateral weirs. Channel dimensions were adjusted such that an almost equal amount of water can be spreaded along the channel. The system will distribute runoff and irrigation water over the AOI, promoting vegetation, filtrating pesticides and fertilizers from agricultural activities and reducing impact of chemicals reaching the mangrove area by spreading the discharge from the farmlands.

The new design consist of a variable geometry channel, reducing channel bottom width from three meters to one half meter. All sections are trapezoidal with a side slope of 1:1.5 for stability purposes. There is a transition between each section and three lateral weirs are designed at each channel reach. Figure 5.2 and Table 5.1 presents the description of the general geometry along both channels, East and West Channel.

The flow varies gradually along of the channel, due to the side weirs and transition sections produce a water depth variation along the channel section. The computation of the water depth starts at the last downstream side weir (see Figure 5.2), where a known depth is fixed at 0.37 m for the West Channel and 0.62 m for East Channel, as a boundaries condition. These initial depths were obtained by the computation of the normal depth in the upstream side of the weir. Computation continues to the next upstream section.

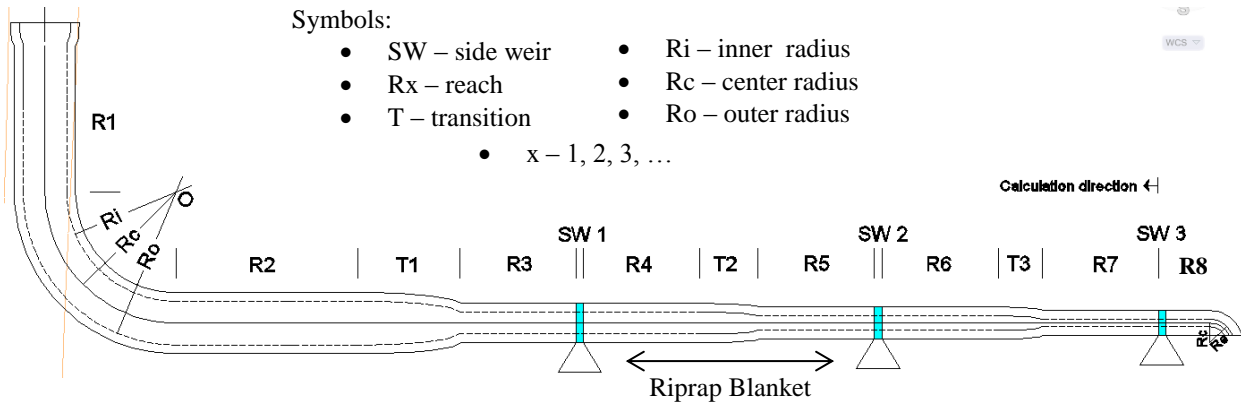


Figure 5.2. Channel Design Setup.

Table 5.1. West Channel and East Channel general geometric data.

Sections	West Channel			East Channel		
	Length	Bottom Width	Side Slope	Length	Bottom Width	Side Slope
	m	m	m/m	m	m	m/m
R1	10.00	3.00	1.50	10.00	3.00	1.50
Bend	14.14	3.00	1.50	14.14	3.00	1.50
R2	13.50	3.00	1.50	13.50	3.00	1.50
T1	7.00	1.50	1.50	6.00	1.50	1.50
R3	8.00	1.50	1.50	8.00	1.50	1.50
SW1	0.37	1.50	1.50	0.69	1.50	1.50
R4	8.00	1.50	1.50	8.00	1.50	1.50
T2	4.00	1.00	1.50	4.00	1.00	1.50
R5	8.00	1.00	1.50	8.00	1.00	1.50
SW2	0.37	1.00	1.50	0.73	1.00	1.50
R6	8.00	1.00	1.50	8.00	1.00	1.50
T3	3.00	0.50	1.50	3.00	0.50	1.50
R7	7.00	0.50	1.50	7.00	0.50	1.50
SW3	0.37	0.50	1.50	0.93	0.50	1.50
R8	2.00	0.50	1.50	2.00	0.50	1.50

5.3 CHANNEL LINING

During an open channel design it is important to consider the channel bed and banks protection from erosion. The channel lining can provide the protection to walls and the channel bed from erosion and decrease its maintenance cost. Unlined natural channels are generally susceptible to erosion and development of vegetation inside the channel, increasing the maintenance cost and deteriorating the operation of the channel. Other factor that needs to be verified during the lining selection is the maximum velocity allowed by the type of lining. In other words, the maximum water velocity allowed by the lining to prevent erosion (Chow, 1959) or damage to the channel walls and bed. This section will introduce the types of linings that were considered on this project.

Earth lining

This lining will depends to the soil type, flow velocity and requires continued maintenance among other factors. Earth lining will be affected by erosion especially if the mean velocity exceeds the 0.9 meter per second and the side slopes are less than 3H: 1V (City of EL Paso, Engineering Department, 2008).

With this lining the East and West channels will experiment failures due to intermittent drying and watering conditions. This type of channel requires constant maintenance which increases the operational cost. Also, spill flow during some events will erode the channels walls and alter the geometry of the side wall.

Concrete lining

The concrete lining channels may be constructed of reinforced concrete and is generally used in rectangular channels or in trapezoidal channels. The use of steel to reinforce the structure represents a cost increase in materials and construction of the system. This type of lining is

generally designed for supercritical flow conditions or velocities greater than 1.5 meter per second. Side wall angles could be steeper than 2:1 (City of EL Paso, Engineering Department, 2008). This lining was not chosen for this project because this type of lining represents a high construction cost. The channel will need to be reinforced completely specially in the areas of the side weirs and at the transition. Velocity in this project are low, therefore, concrete lined is not justified.

Riprap Lining

The riprap is used as erosion control lining for natural channels. The surface of this lining is composed of rocks which increase channel roughness depending of rock size. This increase in roughness allows the channel to handle more pronounced longitudinal gradients (Federal Highway Administration, 1988). During a lack of maintenance, the riprap is susceptible to growth of vegetation which represents an increase in flow resistance and decreases the channel capacity. The maximum allowed side slope is 3H: 1V. The riprap lining is one option for this project but, the channel will be exposed to vegetation growth. As previously mentioned the vegetation can offer a resistance to the water and affect the operation of the weirs channel and the rest of the channel.

Grouted riprap lining

This type of lining provides a rigid surface because the riprap is grouted. The benefit to have a grouted material is that the lining can use a smaller size of riprap. Also the maintenance of the channel is less than other linings. Since the walls and the channel bed are grouted an impermeable layer is created which do not allow the groundwater pressure being released between the rocks (WEF and ASCE, 1992). This lining prevents channel erosion and the grouted produces an impermeable layer which protects the channel bed and sidewall from vegetation

growth. This option of lining has the best characteristics for the design purposes of this project and was selected.

5.4 RIPRAP – LINING CHANNEL DESIGN PROCEDURES

Riprap is a lining formed by large angular rocks which provide soil protection from erosion and decreases the runoff velocities. The lining design calculations are based on a trapezoidal shape channel covered of cement mortar. The cement mortar layer increases the shear stress resistance, provides stability, and prevents vegetation growth inside of the channel. This is called grouted riprap lining, which is recommended for this project. This type of lining provides stability to the walls and bottom of the channel and reduce maintenance cost. Also, the use of a concrete mortar to stick the rocks to the channel surface allows to use a smaller riprap size.

There are several methods for riprap design. This project used the method proposed by the National Cooperative Highway Research Program (NCHRP) Report 108, 1970 (Anderson et al., 1970 and Sturm, 2011). This method describes step by step the design of riprap lining to prevent erosion of highway drainage channels. This method involves channel geometry, longitudinal slope, roughness coefficient, the mean riprap size, shear stress exerted on the channel bed and the sidewalls, and the design discharge.

5.4.1 RIPRAP DESIGN CRITERIA

The riprap design criteria are that the maximum shear stress (MSS) exerted by the water on the channel walls (τ_o^W) and bed (τ_o), does not exceed the critical shear stress (CSS) at both places. Figure 5.3 shows a flowchart with the procedure to select a riprap size. Each step of the flow chart will be discussed in detail in this section.

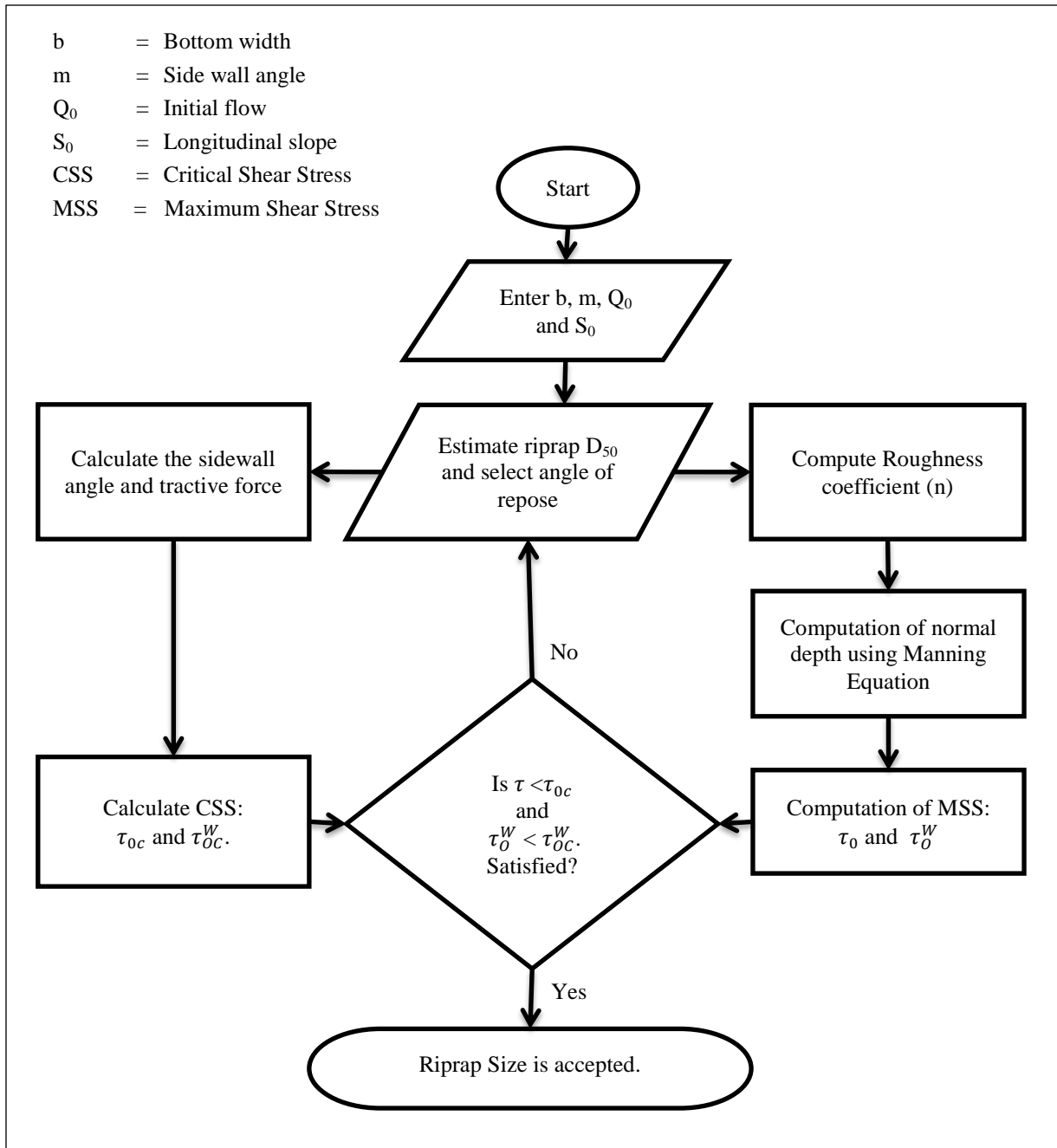


Figure 5.3. Flow chart of the riprap design procedure (Anderson et al., 1970).

Critical Shear Ratios

A riprap size must be estimated as part of the proposed design procedure. The computations consist of a series of trial and error calculations until the critical shear stress turns greater than the maximum shear stress ($\tau_{0c} > \tau_0$ and $\tau_{0c}^W > \tau_0^W$) applied on the channel. The iteration process starts assuming the average rock size D_{50} . As first trial, $D_{50} = 0.09$ m and crushed rock type are proposed. The next step is to calculate the critical shear for the bed and the wall as follows:

$$\text{Critical shear stress in the bed:} \quad \tau_{0c} = 4D_{50} \text{ (lbs/ft}^2\text{)} \quad 5.1$$

$$\text{Critical shear stress in the side wall:} \quad \tau_{0c}^W = K_r * \tau_{0c} \text{ (lbs/ft}^2\text{)} \quad 5.2$$

The critical shear stress on the side wall will depend on tractive force ratio which is defined as:

$$K_r = \frac{\tau_{0c}^W}{\tau_{0c}} = \sqrt{1 - \frac{\sin^2 \theta}{\sin^2 \emptyset}} \quad 5.3$$

where; \emptyset = angle of repose of riprap, and θ = channel side slope angle.

The angle of repose of a rock is the maximum angle in which the rock can be placed without sliding due to gravity (Sturm, 2011). This angle of repose can be obtained using the Figure 5.4. In order to reduce impact on soil conditions the preferred channel side slope selected was 1.5H: 1V. This angle allows to use the majority of the lining types (Chow, 1959). The angle of the sides can be calculated using the following equation:

$$\theta = \tan^{-1} y/x \quad 5.4$$

where: y/x is the ratio of horizontal to vertical distance. For this case 1.5 H : 1 V.

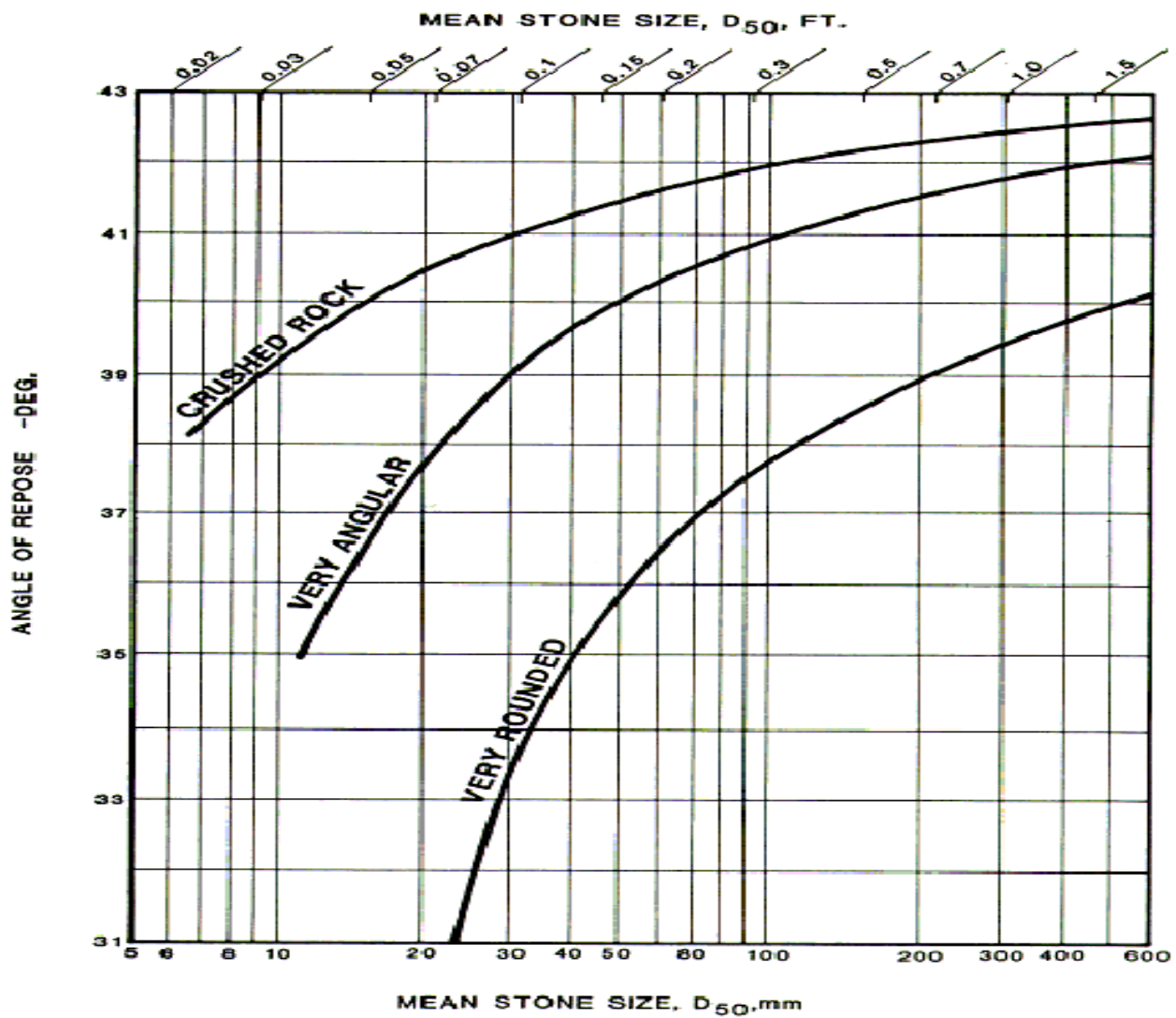


Figure 5.4. Chart to determine the angle of repose of riprap in terms of the stone diameter chosen and the shape (Anderson et al., 1970).

Roughness Coefficient

The roughness coefficient was estimated based on the texture of the proposed channel surface. The Manning’s n-value or the roughness coefficient was determined using the effective size (D_{50}) of the riprap and equation 5.5 (Anderson et al., 1970). The D_{50} represents the size for which 50% of the particles are smaller than the diameter established. A higher riprap D_{50} is translated into a higher roughness.

$$n = 0.0395 * D_{50}^{1/6} \quad 5.5$$

The Manning's coefficient calculated by equation 5.5 is for United States Customary System (USCS). For that reason the calculation examples involves a conversion from USCS to metric system (SI).

Manning's equation and normal depth for West Channel

The normal depth depends on the amount of flow and the geometry of the channel. The Manning's equation 5.6 was used to compute the normal depth of the channel:

$$AR^{2/3} = \frac{Qn}{k\sqrt{S_0}} \quad 5.6$$

where:

- Y = water depth (m)*,
- b = bottom width (m)*,
- m = side slope of the channel *,
- B = top width (m)* = $b + 2Ym$,
- A = trapezoidal area (m²) = $Y(b + Ym)$,
- P_r = wetted perimeter (m) = $b + 2Y(1 + m^2)^{1/2}$,
- R = hydraulic radius (m) = A/P_r ,
- Q = discharge (m³/s),
- n = Manning's roughness coefficient,
- k = 1 (metric units), and
- S_0 = longitudinal slope.

* See Figure 5.5 for variable references.

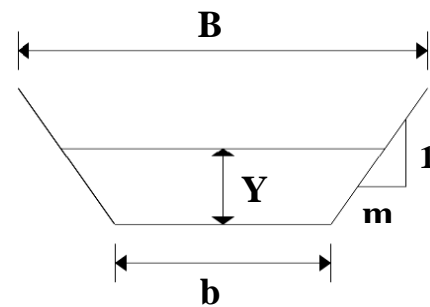


Figure 5.5. Trapezoidal channel diagram.

To calculate the maximum shear stress on the bottom and the side walls of the channels, Sturm, (2011) and Anderson, et al., (1970), recommends to use:

$$\text{Maximum shear stress in the bed} \quad \tau_0 = 1.5\gamma RS_0 \quad 5.7$$

$$\text{Maximum shear stress in the wall} \quad \tau_0^W = 1.2\gamma RS_0 \quad 5.8$$

where γ is the specific weight of water given as 9810 N/m³ and R is the hydraulic radius. The normal depth is obtained from equation 5.6.

After the calculation of the normal depth, the hydraulic radius (R) can be calculated. The right hand term in equation 5.6 is known. The left hand side is a function of depth (Y). The equation is solved for the normal depth (Y) for a given bottom width (b), and side slope (m). The verification consists in comparing the maximum shear stress in the walls and in the bed of the channel with the critical shear stress at the same places. If the actual maximum shear stress is lower than the critical shear stress in both sides, the channel will meet the design requirements.

5.4.2 RESULTS AND DISCUSSION

The first iteration for the riprap design used a D_{50} of 0.09 m. This size met the shear stress requirements. This riprap size was chosen considering the effect of the rock size in the water depth and velocity. An increase in the rock size, produces an increase in roughness (see equation 5.5), decreases the water velocity flow of the channel and increases the water depth.

The roughness coefficient (n) for the riprap $D_{50} = 0.09$ m is $n = 0.032$. To increase the channel wall and bed stability, a mortar layer will be added to the riprap. This mixing between the riprap and mortar is known as grouted riprap. The roughness coefficient for grouted riprap lining is between 0.040 maximum and 0.028 minimum (Ghere, 2011). Therefore, the n – value for grouted riprap is in the same range of the value for riprap.

The critical shear was calculated using the rock size (D_{50}) from equation 5.1 and 5.2 resulting in values of 56.6 Pa for channel bed and 31.4 Pa for side walls. A summary of results is presented in Table 5.2.

Figure 5.6 shows the cross-section of the riprap channel. This cross section represents the most upstream part at the beginning of the project of each channel. The channel bottom width varies along the channel until it reaches 0.5 m wide. Each channel, East and West, have the same setup of the bottom width but different channel depths (ΔZ) due to the flows variation before and

after weir. The West Channel is recommended to have a depth of 0.40 meters and East Channel is recommended a depth of 0.80 m. The riprap wall thickness is .18 m and the bottom thickness of 0.30 m. This information will be detailed in Chapter 7.

Table 5.2. Channel riprap lining design configuration data

	West Channel	East Channel
Channel flow (m^3/s)	0.35	1.09
Y_n = Channel normal depth (m) =	0.35	0.66
b = Bottom width (m) =	3.00	3.00
m = Side wall angle =	1.50	1.50
Longitudinal slope =	0.001	0.001
B = Top width (m) =	4.04	4.99
Manning roughness coefficient =	0.03	0.03
D_{50} (m) =	0.09	0.09
Angle of repose =	41.80	41.80
Sidewall angle =	33.69	33.69
Tractive force ratio =	0.55	0.55
Critical shear stress on bed (Pa) =	56.55	56.55
Maximum shear stress on bed (Pa) =	3.38	5.63
Critical shear stress on wall (Pa) =	31.36	31.36
Maximum shear stress on wall (Pa) =	2.70	4.50
Bottom thickness (m)* =	0.30	0.30
Bank thickness (m)** =	0.18	0.18
Free Board (m)*** =	0.40	0.47

* $3.00D_{50}$.

** $1.75D_{50}$.

*** $\sqrt{mY_n}$ or Appendix E

Note: D_{50} must be in feet.

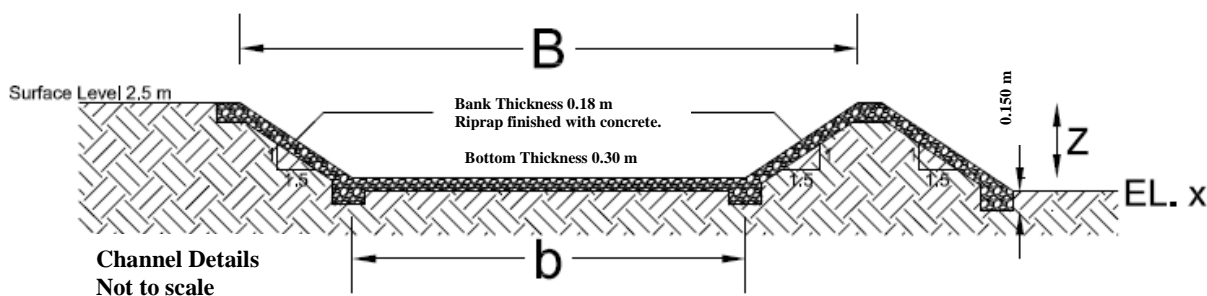


Figure 5.6. Riprap channel design, not at scale. For dimension of b and B please see the Table 5.2

5.5 CHANNEL BEND

The existing channels are straights and discharge directly to the Mar Negro area. The new design includes a 90° bend which will redirect the flow parallel to the coast line. Once the flow reaches these new channels, the weirs will be in charge of flooding the area at different location to promote a more distributed overland flow.

When a change of direction occurs in an open channel a series of centrifugal forces occurs in the bend resulting in a superelevation of the water surface (Akan, (2006) and Chow, (1959)). This superelevation consist in an increment of water depth at the outside boundary of the bend. This difference in elevation of water surface can be computed using the following equation (Akan, 2006):

$$\Delta y = \frac{V^2 T}{g R_c} \quad 5.9$$

where:

Δy	=	difference in water surface elevation at the outside and inside of the bend (superelevation, see Figure 5.7),
g	=	gravitational acceleration (9.81 m/s ²),
R_c	=	mean radius of the bend (m),
V	=	average cross-sectional velocity (m/s), and
T	=	water surface width (m).

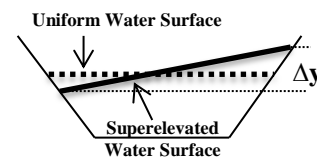


Figure 5.7. Superelevation profile.

Chow (1959) recommends a ratio of mean radius (R_c) to bottom width of three ($R_c/b=3$).

The internal (R_i) and outer radius (R_o) can be computed as:

$$\begin{aligned} R_i &= R_c - \frac{T}{2} \\ R_o &= R_c + \frac{T}{2} \end{aligned} \quad 5.10$$

A channel bend suffers a higher shear stress at the bottom and sides due to secondary currents (Akan, 2006). This secondary current is produced by the frictional forces of the channel

boundaries (Ippen et al., 1961). The secondary current is translated as cross-stream circulation (see Figure 5.8) which is composed of a helical motion and a weaker counter rotation at the outer bank cell (Blanckaert et al., 2004). All channel velocity vectors, included in the stream-wise direction and the cross-stream circulation, causes a variation in boundary shear stress (Thornton et al., 2011). Ippen et al., (1961) remarked four factors in which the higher velocities contributes in the shear stress of the outer bank downstream from the bend.

- a) as soon the flow passes the bend, it returns from free vortex pattern to normal, producing a flow acceleration in outer bank,
- b) separation zone decreases effectiveness of the area,
- c) center region cell (see Figure 5.8) move to the outer bank, and
- d) the shear stress distribution on the outer bank downstream corresponds to the velocity patterns and flow depths.

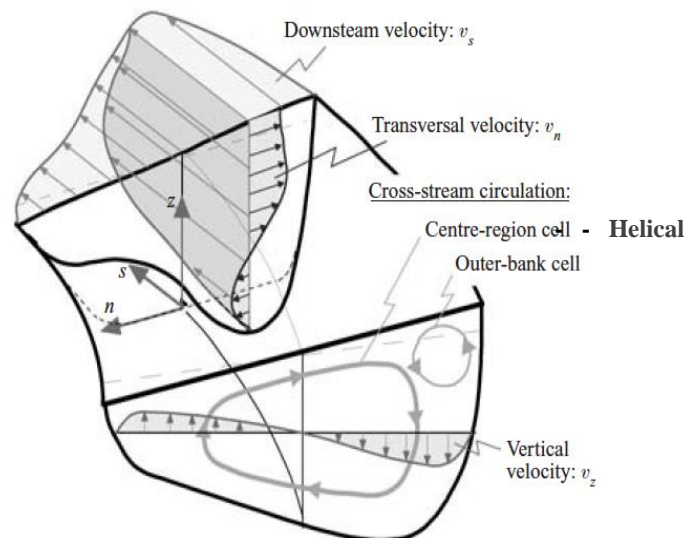


Figure 5.8. Cross section sketch of secondary flow characteristics in a channel bend (Blanckaert et al., 2004).

A minimum protection length is necessary to prevent a geometrical erosion after the channel bend. The protection length can be computed as follows (Akan, 2006):

$$L_p = K_p \frac{R^{7/6}}{n_b} \quad 5.11$$

where:

$$\begin{aligned} L_p &= \text{protection length (m),} \\ K_p &= 0.736 \text{ m}^{-1/6}, \\ n_b &= \text{Manning roughness coefficient, and} \\ R &= \text{hydraulic radius (m).} \end{aligned}$$

Strictly speaking, lined channel should be able to resist increased shear stress due to bends geometry. The length used in this design was 13.5 m, which exceeds the length recommended by the equation 5.11 (see Table 5.3). Figure 5.9 shows the shear stress zones produced by the flow in the channel bend and the protection length that must be used to prevent erosion in the channel. The increase on shear stress on the bend will depend on the critical shear stress allowed by the channel lining. If the shear stress caused by the channel bend is higher than the critical shear stress, the channel lining must be changed in order to complete an effective design. The increase of shear stress in the channel will be dictated by a coefficient K_{bend} which can be found using Figure 5.9 with the R_c/b . The R_c/b is the ratio of the radius at the center by the bottom width of the channel.

This shear stress on the bottom and the sidewalls caused by the channel bend can be calculated using the following equations:

$$\tau_{bs} = K_{\text{bend}} \tau_s \quad 5.12$$

and

$$\tau_{bb} = K_{\text{bend}} \tau_b \quad 5.13$$

where:

- τ_{bs} = side shear stress at channel bend,
- τ_s = side shear stress for straight channel (Table 5.3),
- K_{bend} = dimensionless coefficient obtained in Figure 5.9,
- τ_{bb} = bottom shear stress at channel bend, and
- τ_b = bottom shear stress.

The superelevation for both channels is less than five centimeters which means that can be ignored. The dimensionless coefficient obtained, using a R_c/b ratio of three (3), is 1.86. If τ_{bs} and τ_{bb} are lower than the critical shear stress calculated in the riprap design (see Table 5.3) the curve will satisfy the design and no further changes has to be done to complete this part of the channel design. This condition is satisfied in this case.

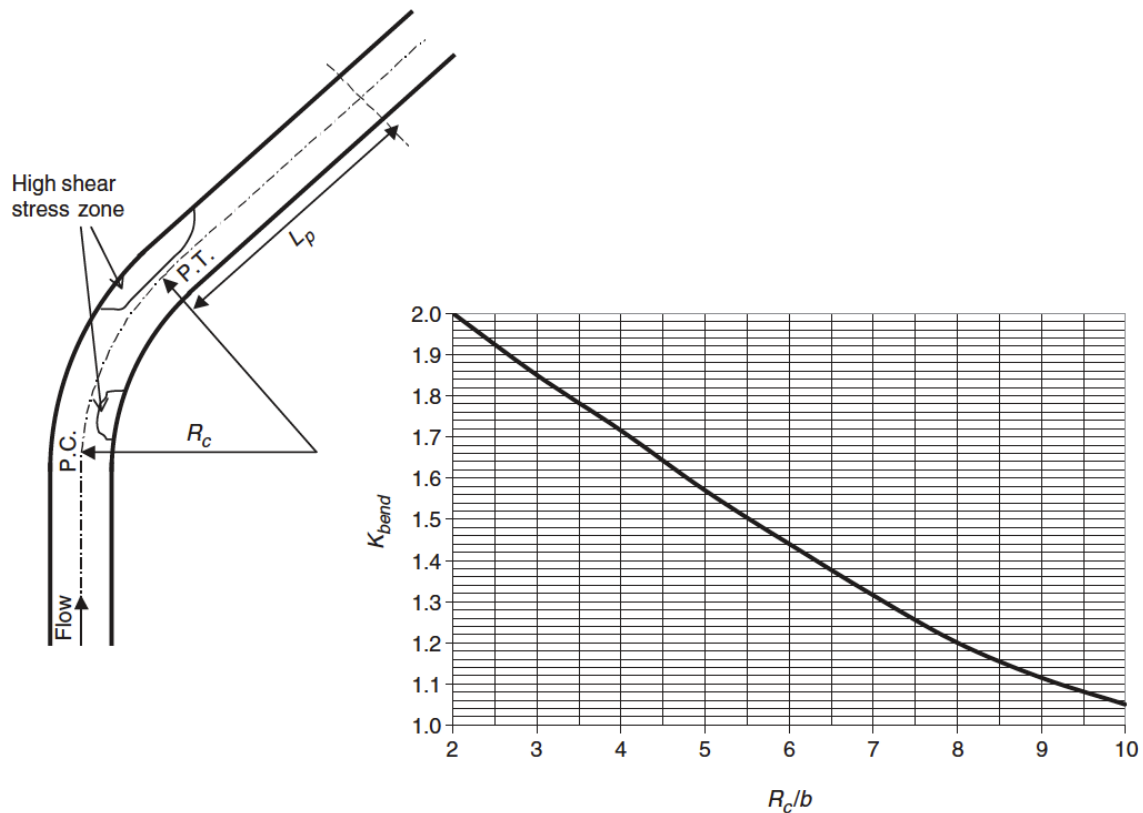


Figure 5.9. A: Channel diagram. B: Dimensionless coefficient for shear stress caused by channel bends calculation (Akan, 2006).

Table 5.3. Channel bend design data.

	90 degrees curve	
	West Channel	East Channel
Outer Radius , R_o (m)	11.13	11.63
Center Radius , R_c (m)	9.00	9.00
Inner Radius, R_i (m)	6.87	6.37
Super Elevation (m)	0.003	0.01
Protection length (m)	7.00	12.00
Bend Coefficient, B_{end}	1.86	1.86
Bend Sidewall Shear stress , τ_{bs} (Pa)	5.02	5.02
Bend Bed Shear stress , τ_{bb} (Pa)	6.28	6.28
Riprap Critical shear stress on bottom (Pa)	31.35	31.35
Riprap Critical shear stress on wall (Pa)	56.55	56.55

5.6 CHANNEL TRANSITION

The proposed channel involves a system of three weirs (weirs will be discussed in the next section) which will affect the water depth and the amount of flow that will be in the channel. If the channel keeps the original shape downstream, each withdrawal of water means that the water flow depth will decrease until a certain point in which the operation of the channel can be affected. To improve the channel operation, three inlet transitions were designed before each weir. The inlet channel transition is a design to change the cross sectional area of the flow (Chow, 1959).

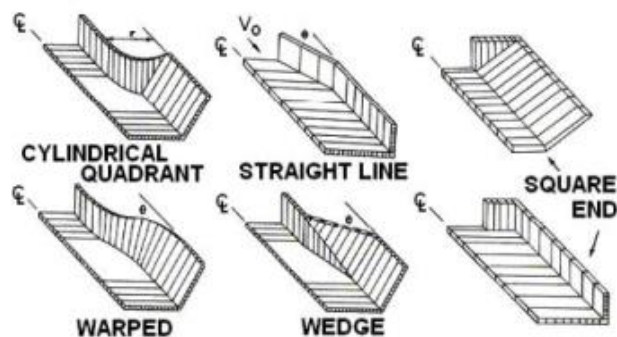


Figure 5.10. Transition types (Federal Highway Administration, 2012).

The channel inlet transition or constriction increases the flow velocity and maintains the water depth. This constriction keeps the water depth at a level more appropriate for the operation of the channel system and reduces the losses of energy. The transition design is also required to maintain subcritical flow in the channel. There are different types of transitions (see Figure 5.10). The Federal Highway Administration (FHWA, 2012) recommends the straight line transition or wedge transition for design purpose. The warped and cylindrical quadrant transitions are more efficient but, their cost of constructions high.

The difference in velocities between the entrance and the exit of the transitions results in a change in velocity head. The water surface is affected by the velocity head. Therefore, a loss factor known as inlet loss coefficient is introduced to account for this effect (Chow, 1959). This can be expressed using the following equation (Chow, 1959; French, 1987):

$$\Delta y' = \Delta h_u(1 + C_c) \quad 5.14$$

where:

- $\Delta y'$ = change in water surface elevation,
- Δh_u = difference in velocity head across the transition ($\frac{(U_{i+1}^2 - U_i^2)}{2g}$),
- U_i = flow velocity at section i,
- g = acceleration by gravity, and
- C_c = inlet loss coefficient.

Each transition type has a different inlet loss coefficient, Chow, (1959) recommends the use of coefficient presented in Table 5.4. The straight line transition was chosen for this design. For this type of transition the contraction coefficient (C_c) or outlet loss coefficient is 0.30.

In transitions design it is required to know the energy changes along the transition. Using the energy equation 5.15, between two continuous sections, the differences in elevation on the water surface and the headloss through the transition can be obtained as:

Table 5.4. Inlet loss coefficient (Chow, 1959).

Transition type	Contraction C_C
Warped	0.10
Cylindrical Quadrant	0.15
Wedge*	0.30
Straight Line	0.30
Square End	0.30

* Established by the USACE, (1994).

$$E_0 = E_A + \Delta z - h_L \quad 5.15$$

where:

- E_i = specific energy = $Y_i + \frac{U_i^2}{2g}$
 i = subindex (0 or A)
 Δz = change in elevation of the channel bottom and,
 h_L = head loss through the transition.

The head loss (h_L) can be computed using equation 5.16:

$$h_L = C_c \Delta h_u \quad 5.16$$

The water depth along the transition is obtained using the energy equation 5.15. The length of the transition (FHWA, 2012) can be computed by the following equation:

$$L = \frac{b_i - b_{i+1}}{2 \tan \theta} \quad 5.17$$

where:

- b_i = bottom width before (i) and after (i+1) the transition, and
 θ = flare angle (see Figure 5.11.A) of the transition walls, should be a maximum of 12.5° (FHWA, 2012).

The change of bottom width during a transition is computed as follows:

$$b = b_i + \frac{(b_{i+1} - b_i)x}{TL} \left[1 - \left(1 - \frac{x}{TL} \right)^t \right] \quad 5.18$$

$$L = 2.35(b_i - b_{i+1}) + 1.65mY \quad 5.19$$

$$t = 0.80 - 0.26\sqrt{m} \quad 5.20$$

where:

- b = bottom width at the section,
- b_i = bottom width upstream,
- b_{i+1} = bottom width downstream,
- L = computed transition length (see equation 5.19),
- x = variation in transition length, $0 \leq x \leq L$,
- TL = length rounded up to the nearest whole number,
- m = channel side slope, and
- Y = channel depth.

Figure 5.11 shows the schematic of the transition and the energy grade line .

The transitions were designed to reduce the bottom width of the channel gradually. This was achieved by designing three different transitions in which the channel bottom width reduces from 3 m to 0.5 m. Figure 5.12 shows the steps followed during the design process, which is a representation an adaptation of the standard step method (Chow, 1959).

The channel design involves gradually variable flow conditions due to the change on geometry. The computations start downstream and continues in the upstream direction. The energy equation between two sections is :

$$Y_D + \frac{U_d^2}{2g} + z_d = Y_u + \frac{U_u^2}{2g} + z_u - h_L - h_f \quad 5.21$$

where: z is the elevation from a datum to the channel bottom, U is the average velocity in the channel, Y is the channel depth, g is acelleration by gravity, and h_L and h_f total head loss and friction loss in the channel between the two sections, respectively.

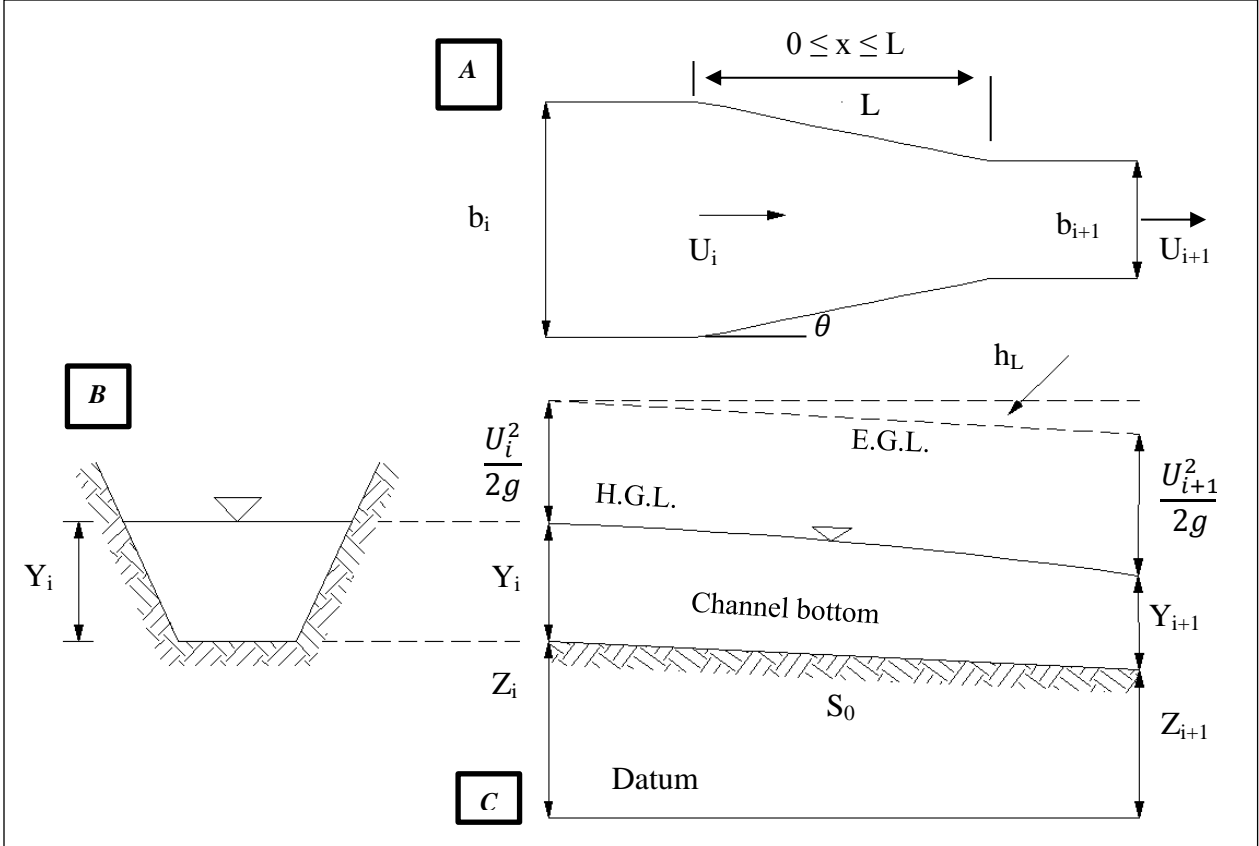


Figure 5.11. Energy diagram in gradually varied flow in open channel. A: Transition top view; B: Channel Cross section; C: Channel lateral cross section.

After calculation of the downstream specific energy, compute the specific energy upstream E_i by adding the specific energy downstream (known value) plus the difference of channel bottom elevation between two sections Δz .

$$E_u = E_d + \Delta z \tag{5.22}$$

The upstream water depth can be computed by trial and error from equation 5.22. With the upstream water depth, the upstream velocity friction loss (h_f), and the energy loss in the contraction (h_L) can be computed.

At this point, the upstream water depth needs to be corrected by both, velocity and friction loss. It is necessary to recalculate the upstream specific energy (see equation 5.15) but

considering the velocity head loss and friction head loss. Once this process is completed, a new trial and error is required to recalculate a new water depth corrected. With the new depth, the head losses are recalculated and compared with the first ones that were computed. If the differences between both head losses are 1 mm or less no further trials are required.

The length of the transition was computed using the equation 5.19 and it is required for the friction headloss computation. In this case, the length was rounded up to the nearest whole number for design purposes.

To maintain a subcritical flow in the transition it is required a flare angle less or equal to 12.5° . Equation 5.17 verifies if the transition length meets this requirement.

Results

The East and West channels have identical geometry, a total of six (6) transitions, three (3) in each channel. The West channel transitions were named T1 to T3, where T1 is located upstream and T3 is the last transition downstream. For reference of the transition location in the channel please see Figure 5.2. The East channel will follow the same sequence with transitions T4 to T6. Higher numbers belongs to downstream and the T4 is located upstream.

The following tables present general information about the change in the channel bottom width, transition length, and the change in water depth along the transition.

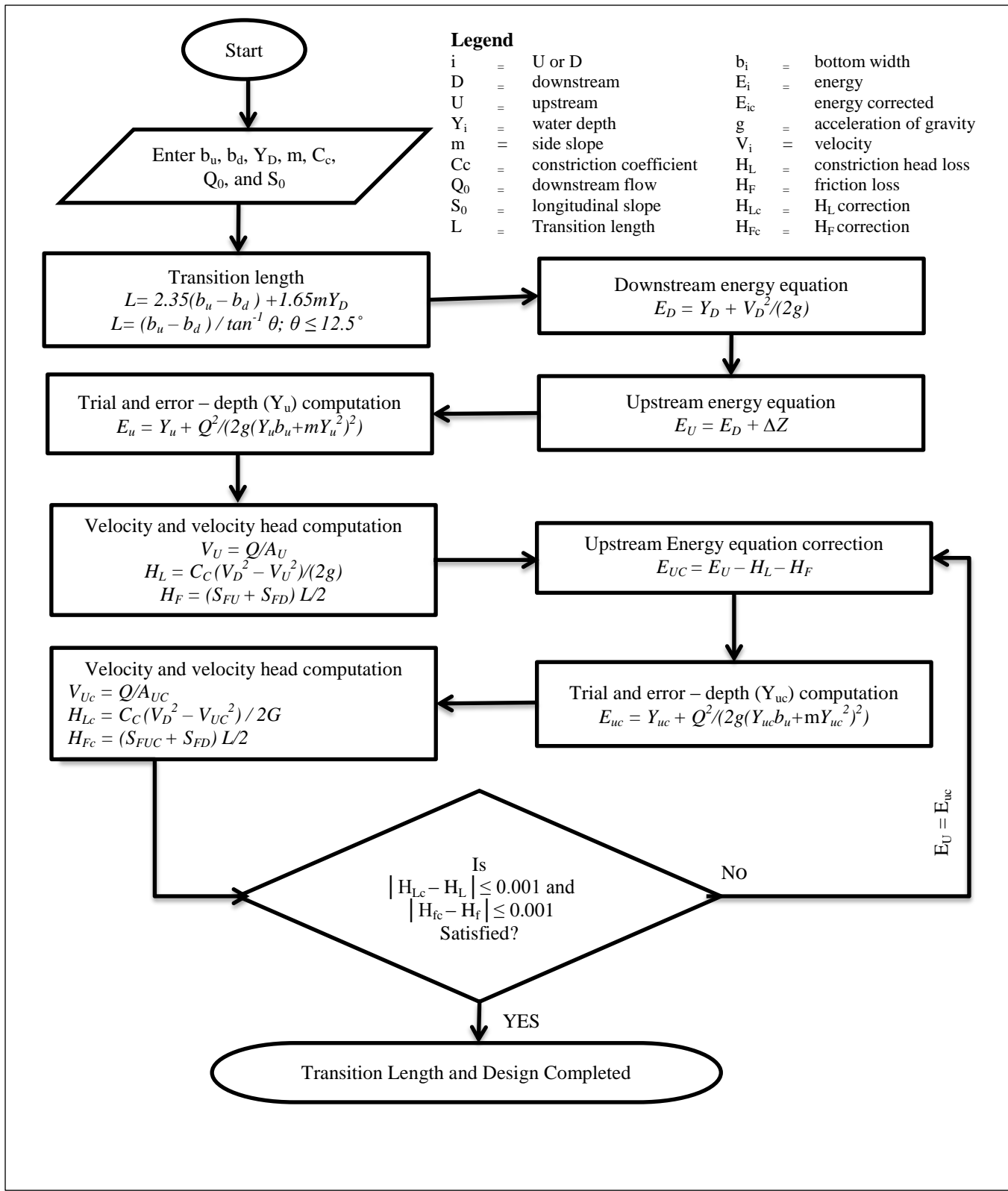


Figure 5.12. Channel Transition design flow chart.

West Channel Transition Data

From Table 5.5 to Table 5.7 are the numerical descriptions of the profiles shown in Figure 5.13 to Figure 5.14.

Table 5.5. Design computations for Transition T1, length of 7 m. $Q_{\text{design}} = 0.35 \text{ m}^3/\text{s}$.

Section	Transition Length (X)	Channel Width (b)	Bottom Channel Elevation (Z)	Water Depth (Y)
	(m)	(m)	(m)	(m)
Downstream	7	1.50	0.0000	0.3850
1	6.3	1.65	0.0007	0.3986
2	5.6	1.80	0.0014	0.4102
3	4.9	1.95	0.0021	0.4191
4	4.2	2.10	0.0028	0.4260
5	3.5	2.25	0.0035	0.4316
6	2.8	2.40	0.0042	0.4362
7	2.1	2.55	0.0049	0.4400
8	1.4	2.70	0.0056	0.4433
9	0.7	2.85	0.0063	0.4461
Upstream	0	3.00	0.0070	0.4485

Table 5.6. Design computation for T2, length of 4 m. $Q_{\text{design}} = 0.23 \text{ m}^3/\text{s}$.

Section	Transition Length (X)	Channel Width (b)	Bottom Channel Elevation (Z)	Water Depth (Y)
	(m)	(m)	(m)	(m)
Downstream	4	1.00	0.0000	0.3863
1	3.6	1.05	0.0004	0.3947
2	3.2	1.10	0.0008	0.4026
3	2.8	1.15	0.0012	0.4095
4	2.4	1.20	0.0016	0.4154
5	2	1.25	0.0020	0.4206
6	1.6	1.30	0.0024	0.4253
7	1.2	1.35	0.0028	0.4295
8	0.8	1.40	0.0032	0.4332
9	0.4	1.45	0.0036	0.4366
Upstream	0	1.50	0.0040	0.4398

Table 5.7. Design computations for T3, length of 3 m. $Q_{\text{design}} = 0.12 \text{ m}^3/\text{s}$.

Section	Transition Length (X)	Channel Width (b)	Bottom Channel Elevation (Z)	Water Depth (Y)
	(m)	(m)	(m)	(m)
Downstream	3	0.50	0.0000	0.3536
1	2.7	0.55	0.0003	0.3595
2	2.4	0.60	0.0006	0.3648
3	2.1	0.65	0.0009	0.3693
4	1.8	0.70	0.0012	0.3731
5	1.5	0.75	0.0015	0.3764
6	1.2	0.80	0.0018	0.3792
7	0.9	0.85	0.0021	0.3817
8	0.6	0.90	0.0024	0.3840
9	0.3	0.95	0.0027	0.3860
Upstream	0	1.00	0.0030	0.3878

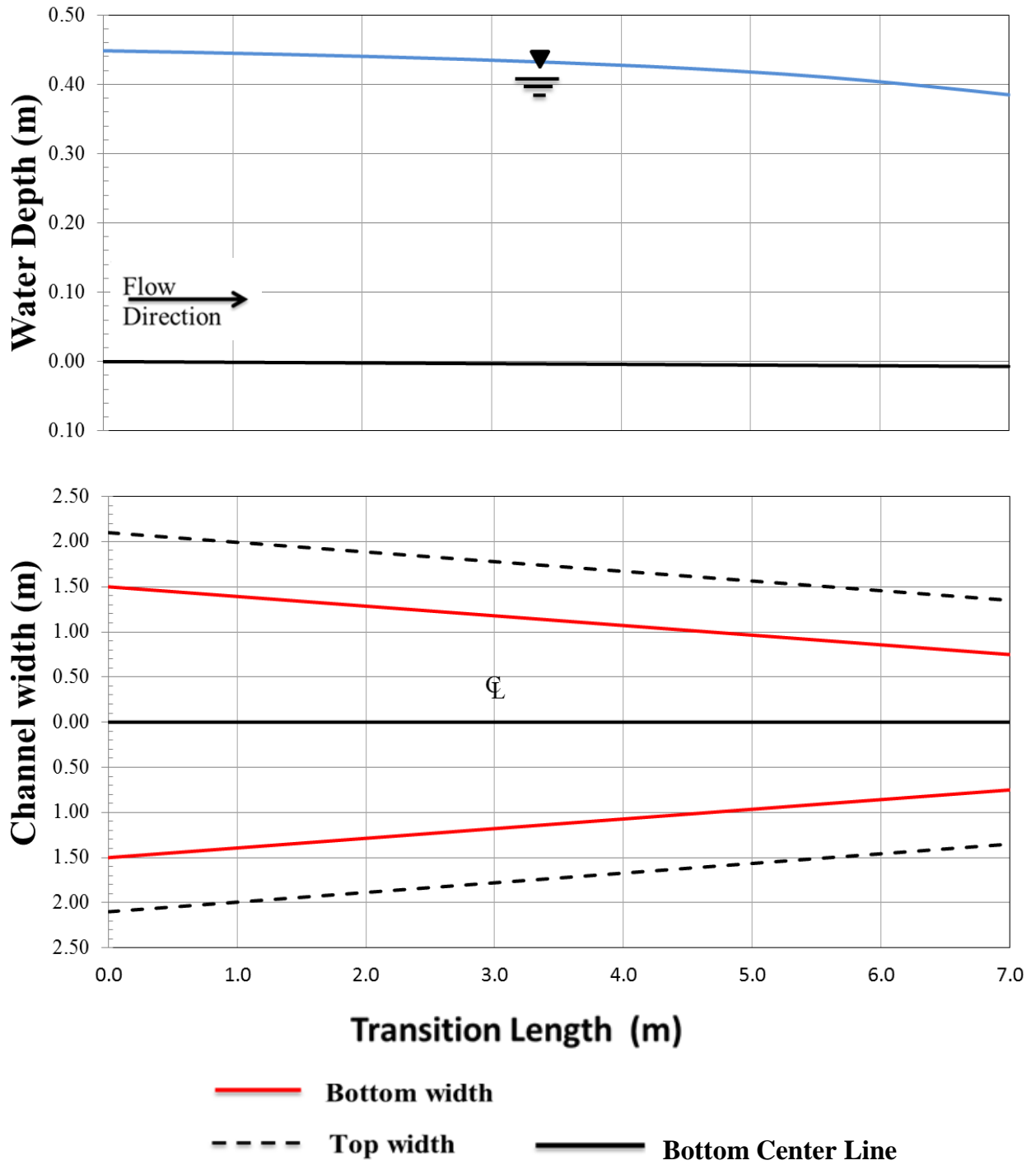


Figure 5.13. Water depth and channel width variation along the T1 length.

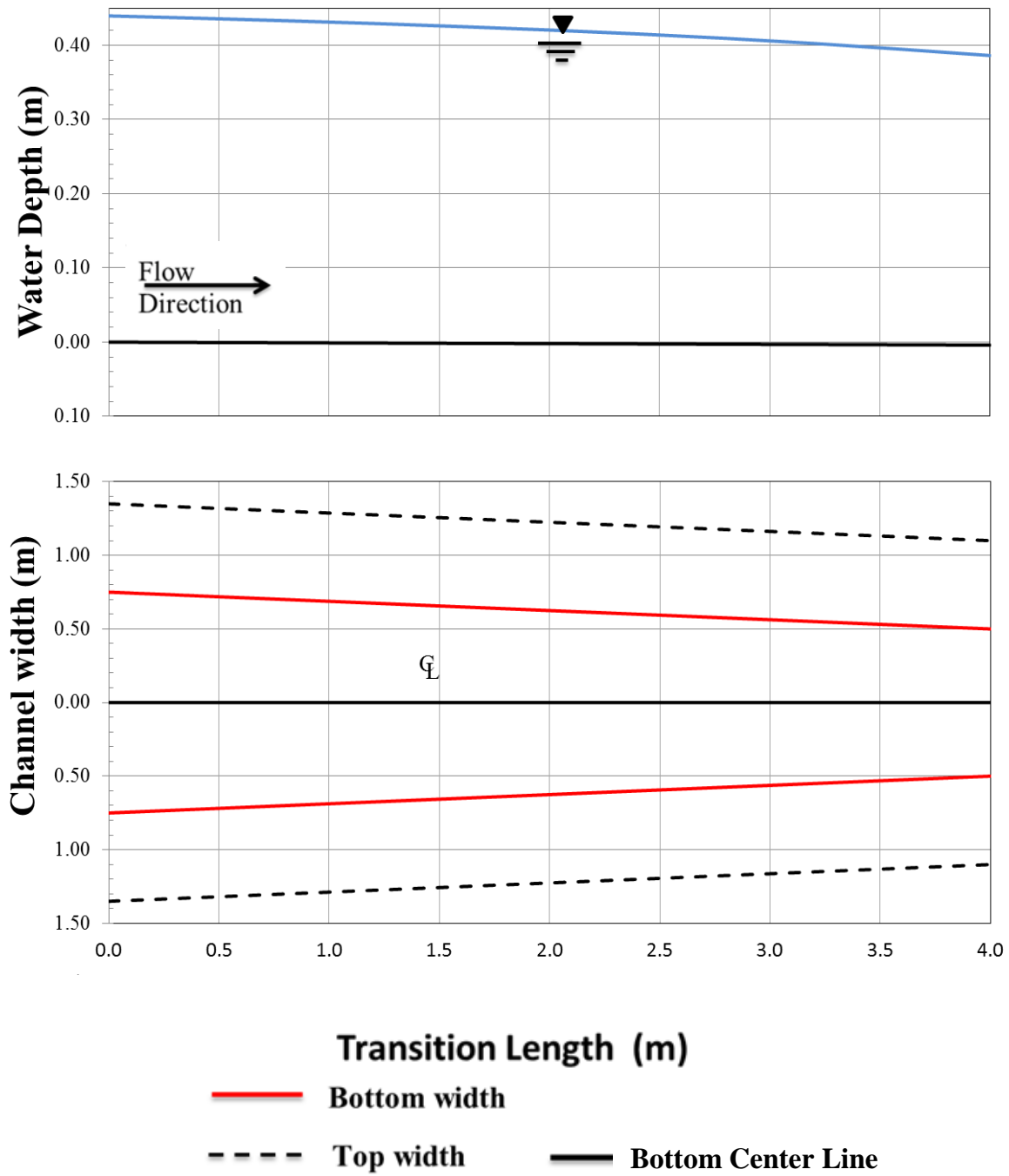


Figure 5.14. Water depth and channel width variation along the T2 length.

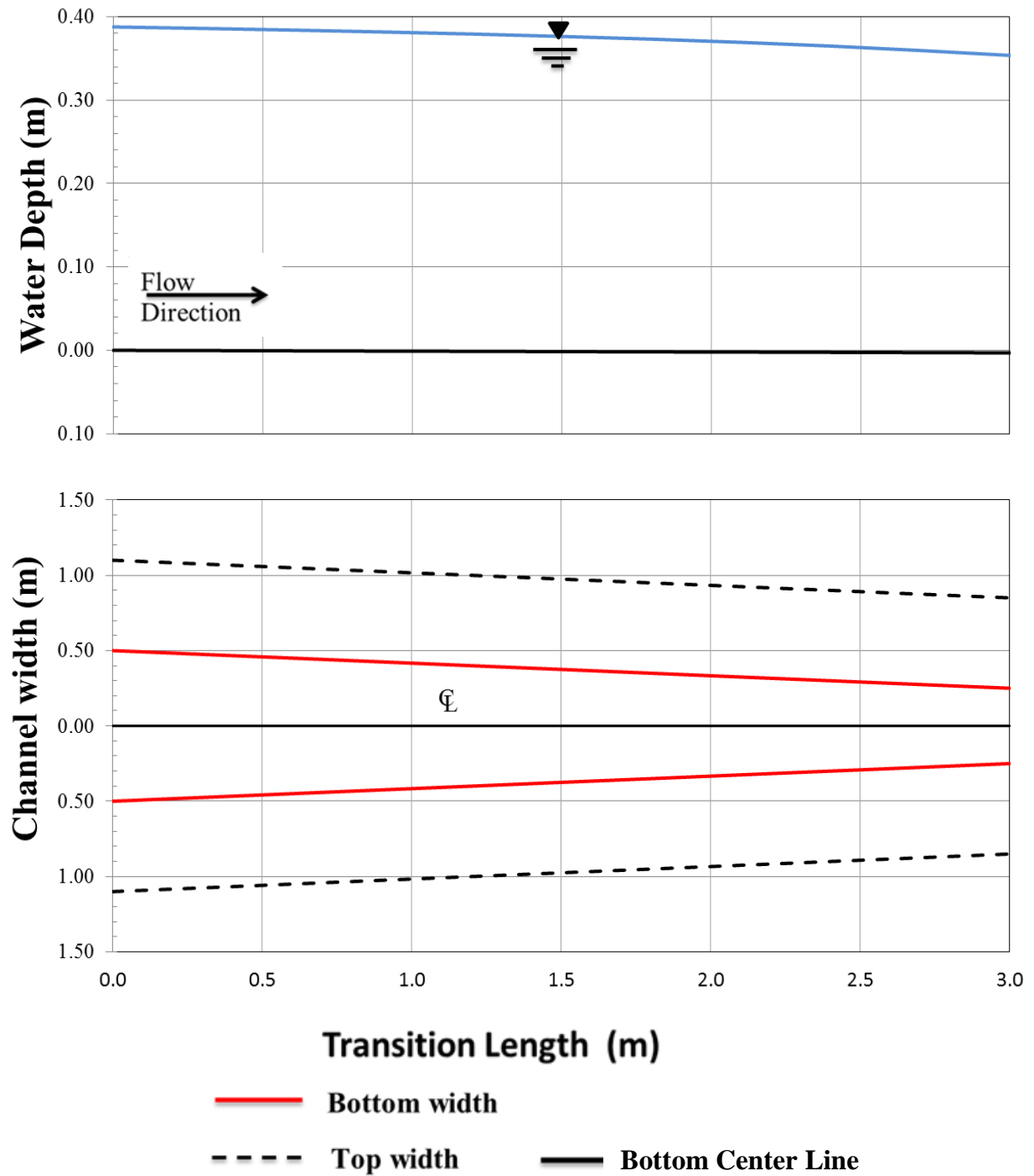


Figure 5.15. Water depth and channel width variation along the T3 length.

East Channel Transition Data

From Table 5.8 to Table 5.10 are the numerical results for the East Transitions. The profiles are shown in Figure 5.16 to Figure 5.18.

Table 5.8. Design computation for T4, length of 6 m. $Q = 1.09 \text{ m}^3/\text{s}$

Section	Transition Length (X)	Channel Width (b)	Bottom Channel Elevation (Z)	Water Depth (Y)
	(m)	(m)	(m)	(m)
Downstream	6	1.50	0.0000	0.6769
1	5.4	1.65	0.0006	0.7002
2	4.8	1.80	0.0012	0.7213
3	4.2	1.95	0.0018	0.7377
4	3.6	2.10	0.0024	0.7508
5	3	2.25	0.0030	0.7616
6	2.4	2.40	0.0036	0.7707
7	1.8	2.55	0.0042	0.7785
8	1.2	2.70	0.0048	0.7853
9	0.6	2.85	0.0054	0.7913
Upstream	0	3.00	0.0060	0.7966

Table 5.9. Design computation for T5, length of 4 m.

Section	Transition Length (X)	Channel Width (b)	Bottom Channel Elevation (Z)	Water Depth (Y)
	(m)	(m)	(m)	(m)
Downstream	4	1.0000	0.0000	0.6723
1	3.6	1.0500	0.0004	0.6869
2	3.2	1.1000	0.0008	0.7012
3	2.8	1.1500	0.0012	0.7136
4	2.4	1.2000	0.0016	0.7245
5	2	1.2500	0.0020	0.7342
6	1.6	1.3000	0.0024	0.7429
7	1.2	1.3500	0.0028	0.7508
8	0.8	1.4000	0.0032	0.7580
9	0.4	1.4500	0.0036	0.7646
Upstream	0	1.5000	0.0040	0.7707

Table 5.10. Design computation for T6, length of 3 m.

Section	Transition Length (X)	Channel Width (b)	Bottom Channel Elevation (Z)	Water Depth (Y)
	(m)	(m)	(m)	(m)
Downstream	3	0.50	0.0000	0.6092
1	2.7	0.55	0.0003	0.6097
2	2.4	0.60	0.0006	0.6102
3	2.1	0.65	0.0009	0.6107
4	1.8	0.70	0.0012	0.6111
5	1.5	0.75	0.0015	0.6114
6	1.2	0.80	0.0018	0.6117
7	0.9	0.85	0.0021	0.6119
8	0.6	0.90	0.0024	0.6122
9	0.3	0.95	0.0027	0.6123
Upstream	0	1.00	0.0030	0.6125

Table 5.11 summaries the transition geometry for both channels. Columns 2 and 3 show the variation in bottom width from upstream (b_U) to downstream (b_D). The Column 4 and 5 shows the computed transition length and the used length, which is the rounded value the column 4. The equation 5.17. This flare angle must be less than 12.5 as mention previously.

Table 5.11. Transition length and flare angle.

Transition	b_U	b_D	Computed Length	Used Length	Flare Angle
	(m)	(m)	(m)	(m)	($^{\circ}$)
(1)	(2)	(3)	(4)	(5)	(6)
T1	3.00	1.50	3.44	4.00	9.89
T2	1.50	1.00	2.01	3.00	4.76
T3	1.00	0.50	6.31	7.00	10.85
T4	3.00	1.50	5.65	6.00	11.33
T5	1.50	1.00	3.54	4.00	9.12
T6	1.00	0.50	2.65	3.00	4.76

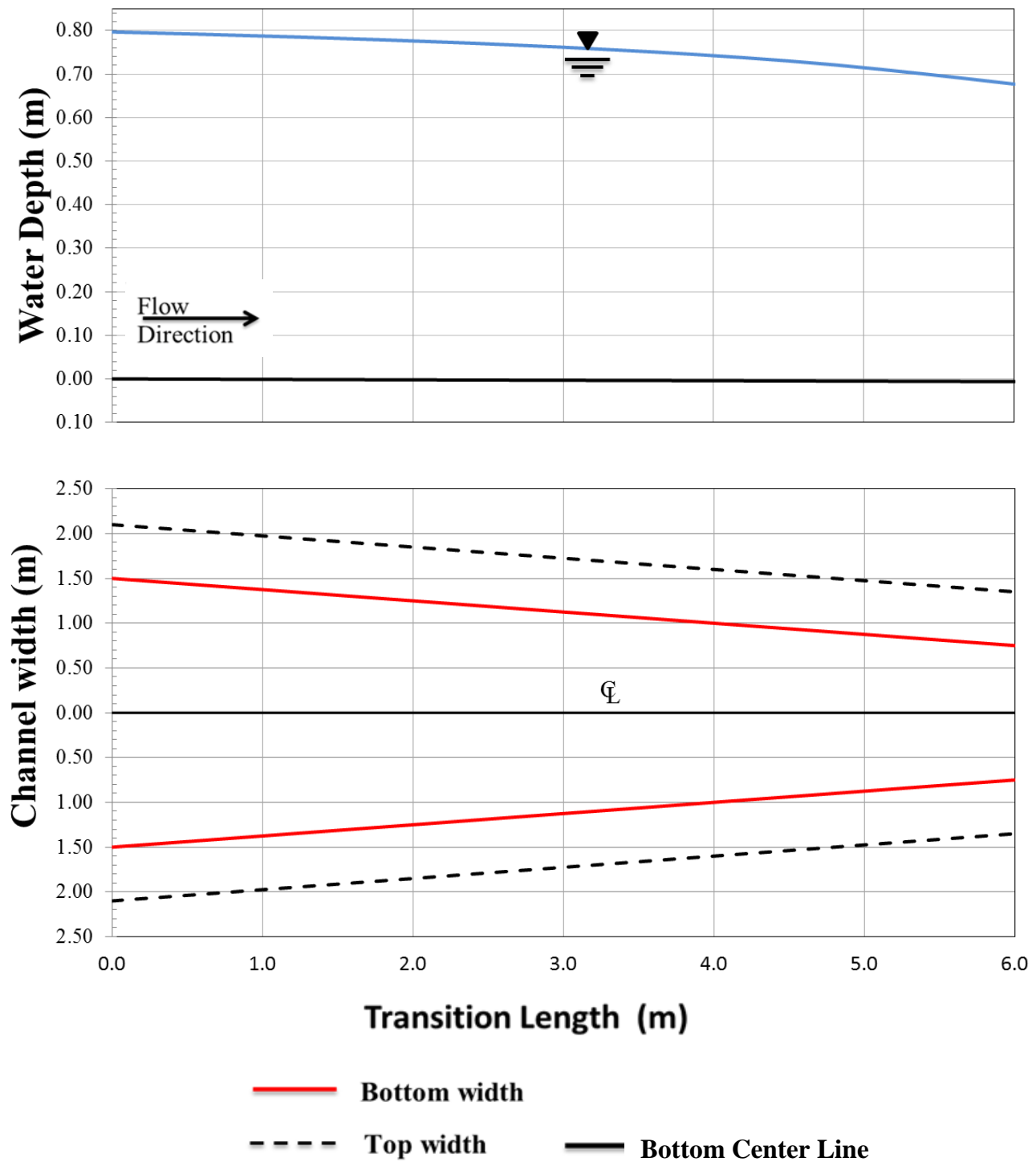


Figure 5.16. Water depth and channel width variation along the T4 length.

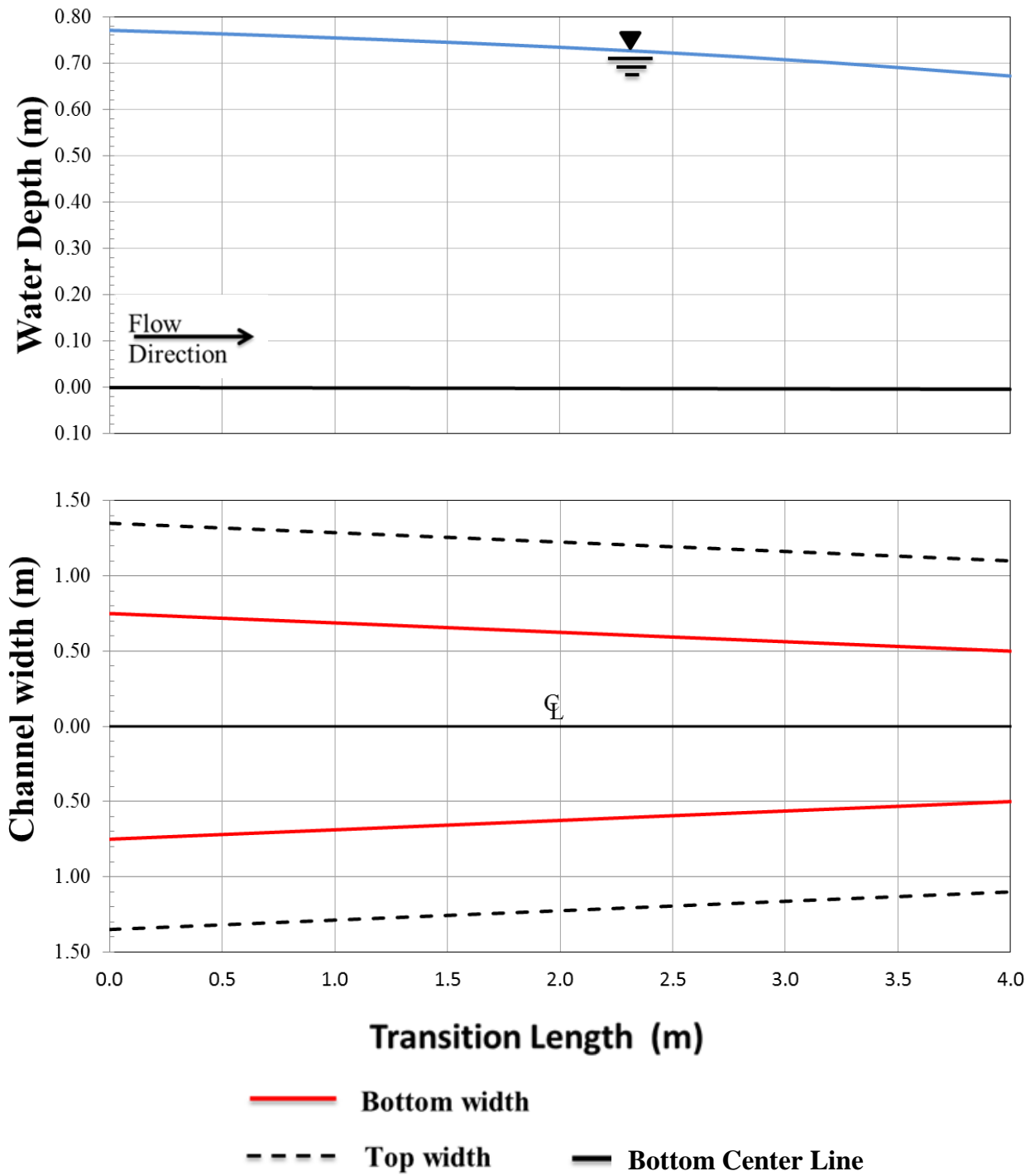


Figure 5.17. Water depth and channel width variation along the T5 length.

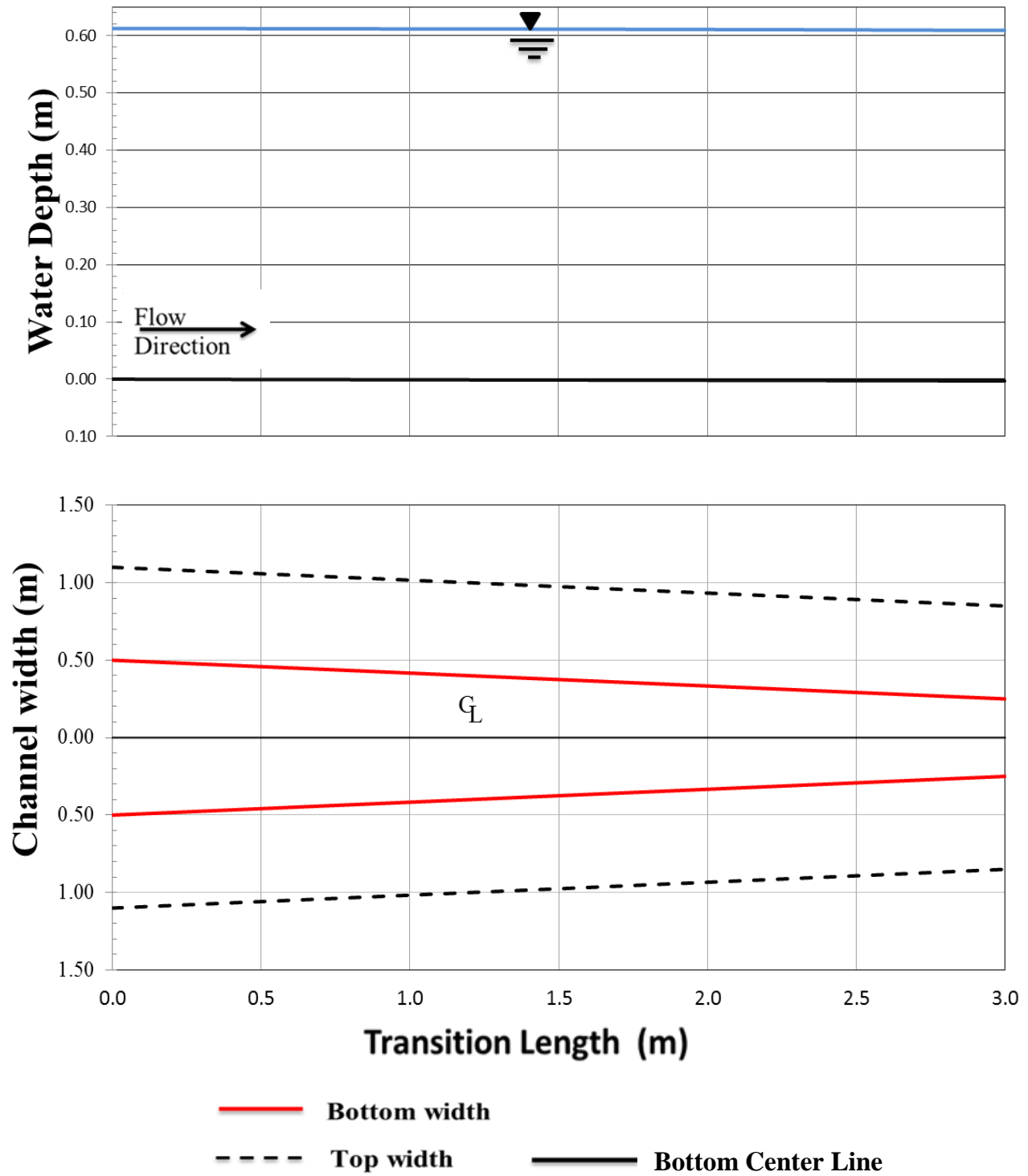


Figure 5.18. Water depth and channel width variation along the T6 length.

5.7 SIDE WEIRS DESIGN

A lateral weir, also called side weir, is a hydraulic control structure whose function is to divert excess flow from the main channel reducing the amount of downstream flow. This structure could operate as a water diversion device into another channel, a secondary reservoir or overland runoff area. The side weirs are commonly build-up to remove flow and controls the water depth in the main channel in order to prevent the flow to exceed the channel level downstream. The side weirs could also be used as a channel level control. However, the most common use of this structure is as a flood control device which divert the excess flow to a secondary stream or to a possible temporary off stream storage (May et al., 2003; Ka-Leung et al., 2002).

In irrigation canals, weirs can be used to divert the flow into sub-canals branch and distribute the water to irrigated areas. This type of hydraulic structure has other applications such as in river control structures, navigable canals to maintain reasonably constant water level, sewerage and wastewater treatments, and trash screens bypass, among others (May et al., 2003). In the proposed project, side weirs will be designed to create a uniformly distributed flow over the area of interest shown in Figure 5.19.

Weir Geometry

The West and the East channel shown in Figure 5.19 begin with the same geometry of the original channel and will be divided in 3 sections each having a side weir and a channel transition. The contraction will help to reduce the width of the channel while keeping the water depth at the same level along the channel.

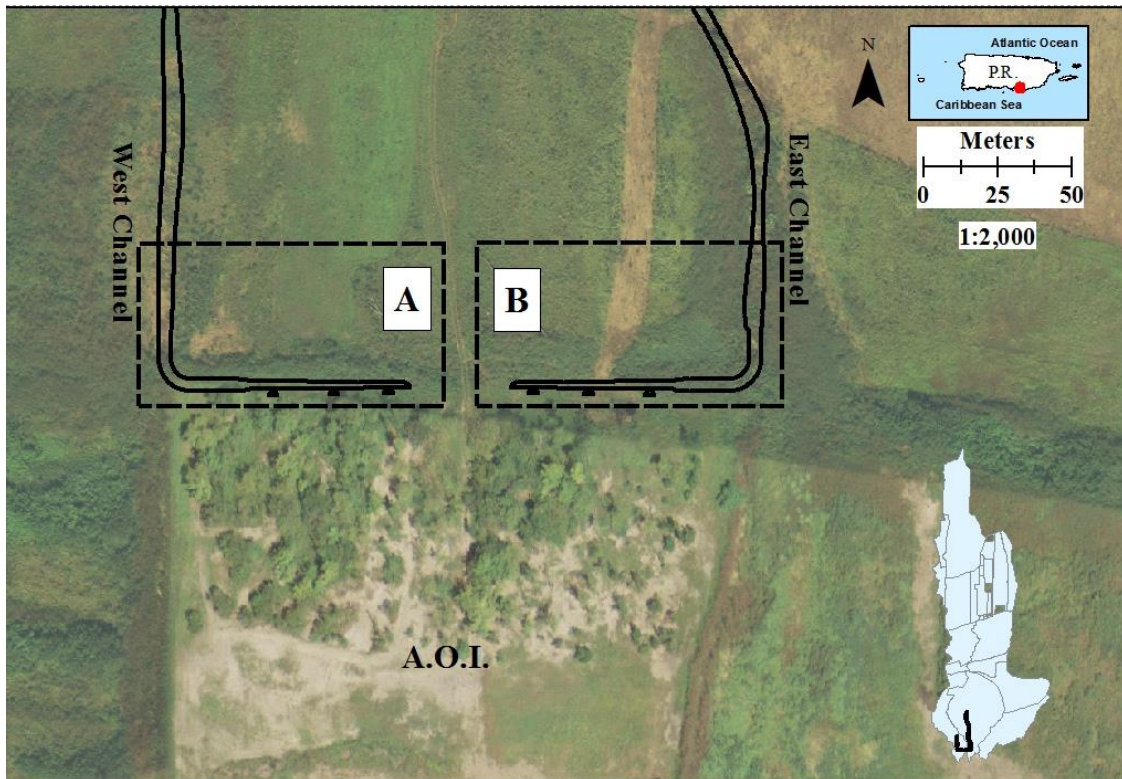


Figure 5.19. Proposed Channel and Location of the Side Weirs.

The weirs geometry (see Figure 5.20) is composed of two principal elements; a crest (P) elevation and the length of the crest (L_w). The design was prepared considering a sharp crest that will remain at the same level along the channel. Each weir has different crest elevation and length.

The side weir design depends on the water depth, computed at the preceding transition section. The first step is the calculation of the wetted area (A_w) and channel top width (B_w). For the height of the spillway crest, May et al., (2003), recommend to use the ratio of wetted area to the top width $P = (A_w/B_w)$ as initial estimate. The head at the weir is calculated subtracting the water depth from the crest level ($P_0 = Y_0 - h_0$). The h_0 represents the elevation of the crest according to Figure 5.20. The head of the water is related to the discharge, higher water head means an increase in the flow of the spillway. The proposed channel system was designed to

discharge approximately the same amount of water over each of the first two (2) weirs and the remaining flow in the last.

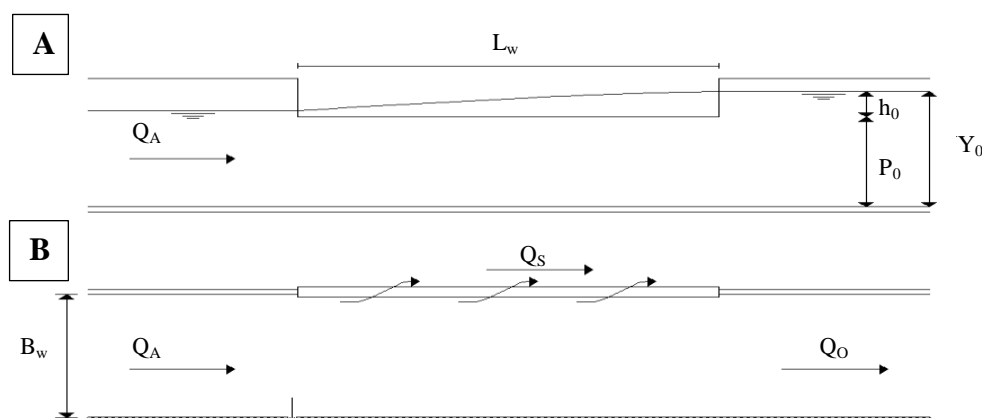


Figure 5.20. Typical operation of side weir: A: Water depth across the side weir. B: Top view of the side weir (May et al., 2003).

Froude Number

The Froude number is a non-dimensional parameter which helps to determine the flow conditions upstream and downstream of the side weir. Froude number can have a direct influence on the operation of the weir flow. When the value of this parameter is equal to one the flow is considered critical. If the value is greater than one, the flow is considered fast or supercritical. Furthermore, if the value is less than one, it implies a slow or tranquil flow, called subcritical flow.

The Froude number is calculated using the following equation:

$$F = \frac{Q}{A\sqrt{gD}} \quad 5.23$$

where:

- Q = Discharge (m^3/s),
- A = Area (m^2),
- g = acceleration by gravity (9.81 m/s^2), and
- D = hydraulic depth (m) = A/B .

Figure 5.21 shows different side weirs profiles in which the flow profiles are affected by the Froude number value. The subscripts A and O denote the flow conditions upstream and downstream respectively; likewise F is Froude number, Y is the water depth and Y_c is the channel critical depth.

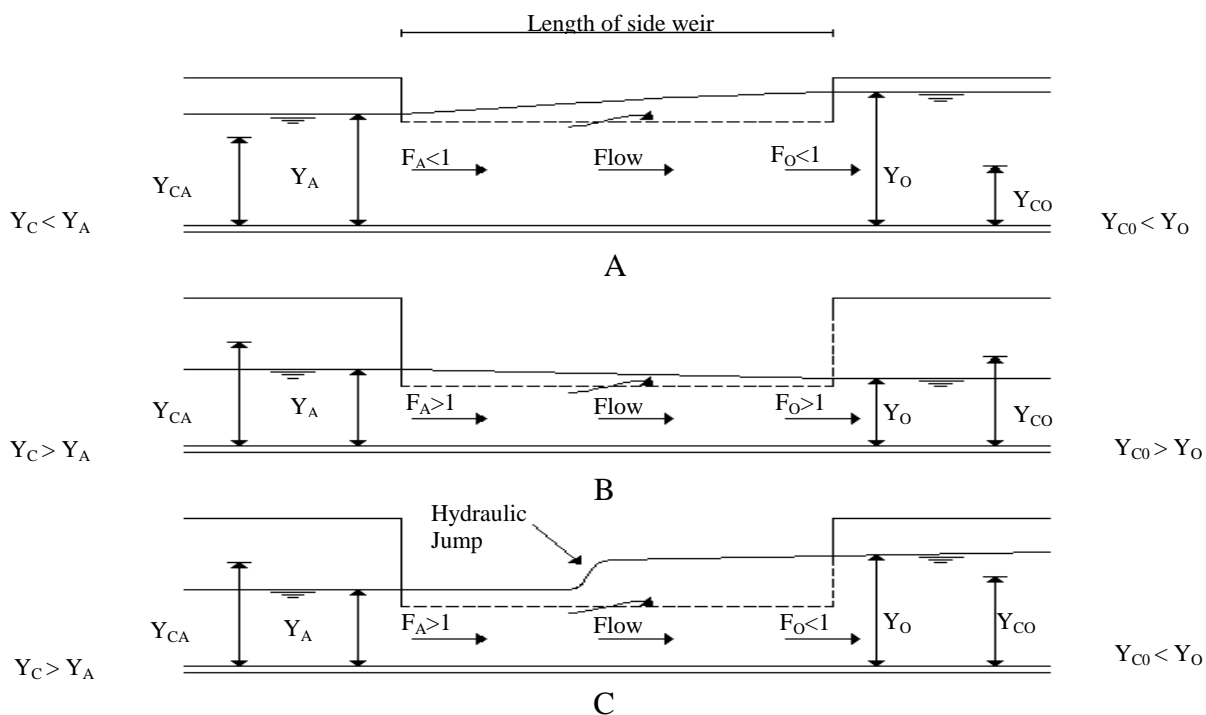


Figure 5.21. Flow conditions on a side weir: A: Subcritical flow profile. B: Supercritical flow profile. C: Mixed flow. (May et al., 2003; Henderson F. M., 1966)

The flow over the weirs is preferable subcritical (Figure 5.21.a). Under subcritical flow conditions the water depth increases downstream along the length of the side weir. This condition will remain if the channel maintain uniform longitudinal slope in the channel (Ka-Leung et al, 2002 and May et al., 2003). The result will be a flow which is not constant but increases downstream along the weir length.

If the Froude number is greater than one (Figure 5.21.b), the water depth and weir flow will decrease along the length of the side weir. Depending on the tailwater conditions, a

hydraulic jump could exist within the lateral weir length as shown in Figure 5.21.c. This is called mixed flow conditions. This mixed flow is characterized for having a supercritical condition upstream and subcritical conditions downstream. Mixed flow conditions in the lateral weir should not be allowed in the design because it will preclude a uniform spread of flow in an area along the channel.

Spillflow equation and discharge coefficient

With the previous design of the upstream channel geometry, it is necessary to choose the best equation to design the lateral weirs. Several equations have been proposed to calculate the spillflow along a lateral weir (Chaudhry, (2008); Chow, (1959); and Henderson, (1966)). The base formula for discharge over weirs is:

$$Q_w = C_e L_w h^{\frac{3}{2}} \quad 5.24$$

where:

- Q_w = total flow rate discharged by the side weir (m^3/s),
- C_e = effective discharge coefficient,
- L_w = effective length of crest of side weir (m), and
- h = head on weir crest (m) = $(h_0 - Y)$.

Other equations can be found in the literature with multiple variations and different discharge coefficients. An accurate discharge coefficient is necessary for the estimation of the weir design discharge. The discharge coefficients for different types of weirs (transverse, side flow, v-notch, and trapezoidal) have been obtained through different experiments. As a result, multiple equations have been developed and tailored to their individual scenarios. A summary of formulas for estimation of discharge coefficient for side weir found in literature are presented in Table 5.12.

Table 5.12. Discharge coefficient equations for rectangular sharp crest side weirs reported by Emiroglu. et. al. 2011.

Author	Discharge coefficient (C_d) equation*	Eqn. Number
Nadesamoorthy, T. and Thomson, A.	$C_d = 0.432 \left(\frac{2 - F_A^2}{1 + 2F_A^2} \right)^{0.5}$	5.25
Subramayan, K. and Awasthy, S. C.	$C_d = 0.864 \left(\frac{1 - F_A^2}{2 + F_A^2} \right)^{0.5}$	5.26
Hager, W.H.	$C_d = 0.485 \left(\frac{2 - F_A^2}{2 + 3F_A^2} \right)^{0.5}$	5.27
Sing R, Manivanna, T and Satynarayana, T.	$C_d = 0.33 - 0.18F_A + 0.49 \left(\frac{P}{h_1} \right)$	5.28
Jalili, M.R. and Borghei, M.R.	$C_d = 0.71 - 0.41F_A + 0.22 \left(\frac{P}{h_1} \right)$	5.29
Borghei M, Jalili M.R. and Ghodsian M.	$C_d = 0.7 - 0.48F_A + 0.3 \left(\frac{P}{h_1} \right) + 0.06 \left(\frac{L_w}{B} \right)$	5.30
Ranga Raju et al.	$C_d = 0.54 - 0.40F_A$	5.31
May. R.W.P., Bromwich, B.C., Gasowski, Y. and Rickard, C.E.	$C_e = n\sqrt{g} \left(J - K \left(\frac{L_w}{b} \right) F_A \right)$	**5.32

* $C_e = \frac{2}{3} C_d \sqrt{2g}$

** (May et.al, 2003).

The variables in Table 5.12 can be described as follows:

- C_u = coefficient of discharge,
- n = 1 for sharp weir crest,
- g = acceleration of gravity (m/s^2),
- L_w = effective length of crest of side weir (m),
- P = crest level from bottom of the channel (m) = A_w/B_w ,
- h_1 = height of the water surface above weir crest in parent channel at downstream end, of the weir (m) = $y - P$,
- J = coefficient depending on the ratio h_0/L and h_0/P (see equation 5.33),
- K = coefficient depending on the ratio h_0/P (see equation 5.34),
- b = width of the channel (m),
- B = top width of the channel (m), and
- F_A = Froude number at upstream of the lateral weir location (see Figure 5.21).

Coefficients J and K develop by (May, Bromwich, Gasowski, and Rickard, 2003) from sharp crest weirs data. This coefficients are computed by using the following equation:

$$J = c_1 + c_2 \left(\frac{1}{1 + \left(4 \times \frac{h_0}{L_w} \right)} \right) \quad 5.33$$

where: c_1 and c_2 are defined as equation 5.33:

$$\begin{aligned} c_1 &= 0.5212 - 0.1752\Omega \\ c_2 &= 0.1041 + 0.1462\Omega \end{aligned} \quad 5.34$$

where: Ω is defined as:

$$\Omega = \frac{h_0/p}{1.5 + \left(h_0/p \right)} \quad 5.35$$

and coefficient K is given by:

$$K = 0.018 + 0.149 \left(\frac{\frac{h_0}{p}}{0.27 + (h_0/p)} \right) \quad 5.36$$

Coefficient K and J were developed by Mays et al. (2003) using data from sharp crested weirs. Appendix F shows a graphical option to obtain K and J values using the h_0/p ratio.

The discharge coefficient equations, shown in Table 5.12, depend on the following dimensionless parameters (Emiroglu et. al, 2011):

$$C_d = f \left(F_A, \frac{L}{b}, \frac{h}{p}, \frac{h}{L} \right). \quad 5.37$$

where: F_A is the upstream Froude number, the side weir length-bottom width ratio which represents the lateral contraction ratio, the vertical contraction ratio (water head–crest height ratio) of the side weir, and water head – weir length ratio.

Usually, the change in water depth during the side weir operation is small and can be ignored. Also the water depth upstream can be approximate as normal depth. For that reason, the

Froude number can be calculated using normal depth (Rosier B., 2007). All discharge coefficients (C_d) were developed for subcritical flows; this means that upstream Froude number must be less than one. This consideration was used only for the last side weir downstream. The current project use gradually varied flow computations for the channel design.

5.7.1 SPILLFLOW CALCULATIONS

The side weirs are structures which produces a reduction of water flow along the length of the structure. This reduction of water affects the energy as gradient. The energy change during the operation of this type of structure is a characteristic of a spatially varied flow. The side weirs design computation will depend on the conservation of mass (Equation 5.38), the conservation of energy (Equation 5.21) and the Froude number (Equation 5.23) which defines the flow regime. The continuity equation along the lateral weir is:

$$Q_{in} = Q_{spill} + Q_{out}. \quad 5.38$$

where:

- Q_{in} = flow entering to the weir system,
- Q_{spill} = spill flow over the weir crest, and
- Q_{out} = remainder flow which continues in the system.

Figure 5.22 is a descriptive flowchart of the design procedure. The computation starts downstream of the last side weir in the channel. Subcritical flow is considered in the design. The downstream boundary condition depth was assumed as normal depth. The discharge coefficient was computed with the Equation 5.25 in Table 5.12 of Subramayan, K. and Awasthy, S. C. This equation is commonly used in the literature (Hager et al., 1986 and Rowlings, 2010) for side weirs with sharp crest.

5.7.2 RESULTS

The discharge coefficient is the parameter which controls the amount of flow discharging over the weir. The SWMM user's manual (Rossman, 2010) recommends to use for sharp crest transverse side weirs a constant discharge coefficient (C_e) of 1.84. It is important to mention this detail because on SWMM the transverse weir replaces the side weir. On the software, the transverse weirs use equation 5.24 to describe the weir spill flow.

Table 5.13 and Table 5.14 show the discharges coefficients (C_d) from equations in Table 5.12 and the effective discharge coefficient (C_e) computed with the equation $C_e = \frac{2}{3} C_d \sqrt{2g}$. Also these tables show the calculation of the discharge coefficient using Mays et al. (2003). This equation represents the value of the effective discharge coefficient. consequently low coefficients provide longer weir length and viceversa. Equation 5.26 (equation two in Table 5.3) produces the maximum discharge coefficient with the weir length less than one meter. The crest height for the West channel are 0.12, 0.14 and 0.16 m and in the East channel the crest height is 0.20, 0.22, and 0.24 m. All weir crests are at the same elevation from the top of the channel surface.

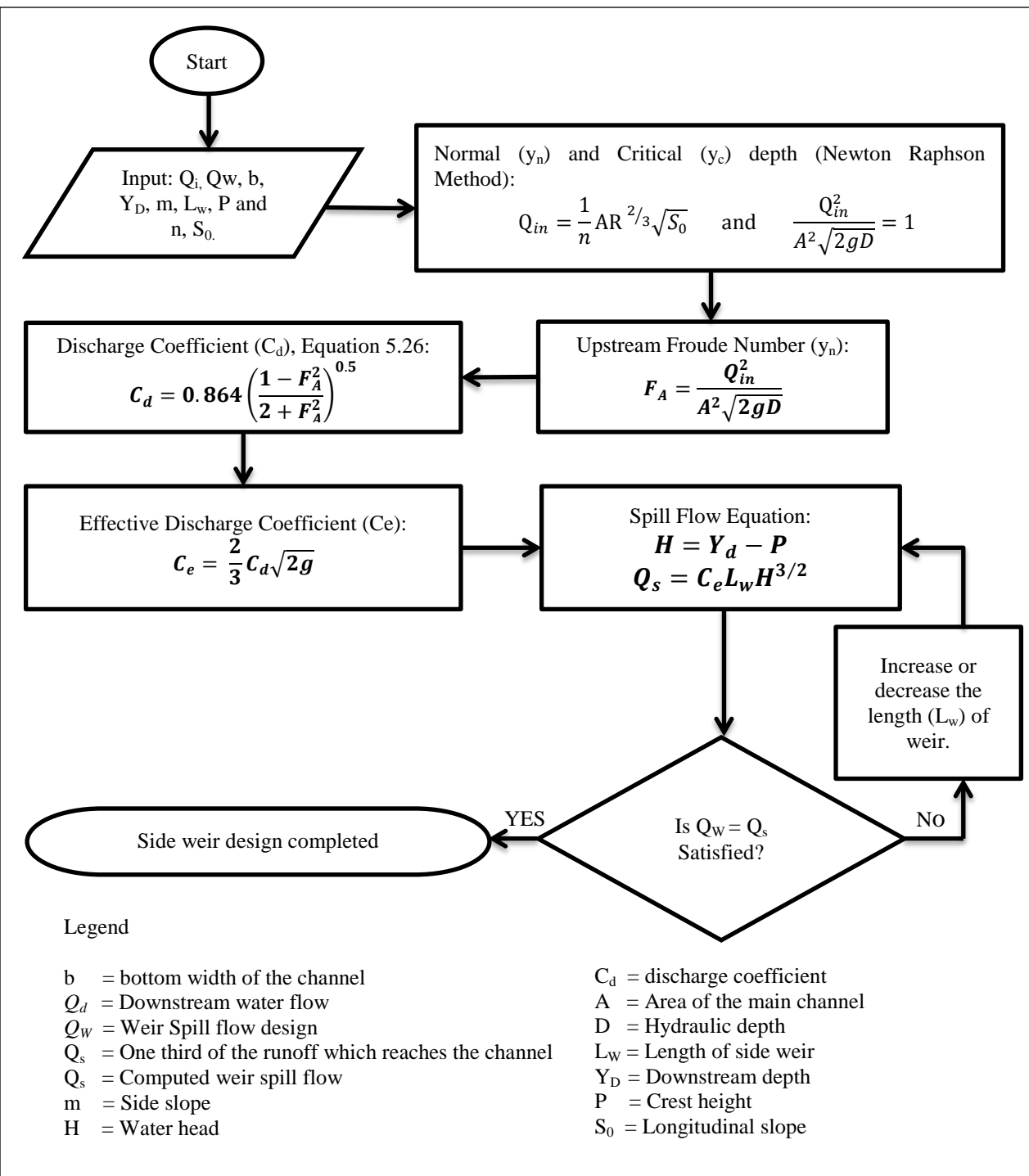


Figure 5.22. Side weir design flowchart.

However, the crest height changes downstream due the depth difference produced by the longitudinal slope. Froude number, which is necessary to compute the discharge coefficients, was less than 0.4 for both channels and a minimum of 0.14 occurred in West Channel. It is important to maintain a Froude number below on ($F < 1$) upstream of the weir. Mays, et. al, 2003 recommends F_A less than 0.6 for optimal operation of the side weir.

The goal of the design is to develop a system in which the side weirs, during normal operation, spill approximately the same discharge (Q_w) in each of the weirs. The results presented in Table 5.15 and Table 5.16 demonstrate the success of the design to achieve constant discharge outflow from each weir.

Table 5.13. Discharge coefficient (C_d) and effective discharge coefficient (C_e) for West Channel side weirs (3rd weir belongs to downstream weir).

West Channel							
Author	Equation Number	3 rd Side Weir		2 nd Side Weir		1 st Side Weir	
		C_d	C_e	C_d	C_e	C_d	C_e
Nandesamoorthy et al.	5.25	0.386	1.140	1.121	0.380	0.374	1.105
Subramanya et al.	5.26	0.591	1.744	0.584	1.726	0.578	1.708
Hager	5.27	0.475	1.403	0.472	1.393	0.469	1.385
Sing et al.	5.28	0.69	2.037	0.565	1.668	0.513	1.513
Jalili and Borghei.	5.29	0.445	1.314	0.486	1.435	0.497	1.467
Borghei et al.	5.30	0.384	1.134	0.425	1.256	0.438	1.295
Ranga Raju et al.	5.31	0.456	1.346	0.443	1.309	0.433	1.279
Mays:	-	-	-	-	-	-	-
Omega	5.35	0.451	0.540	0.540	0.586	0.586	0.586
c_1	5.34	0.442	0.427	0.427	0.419	0.419	0.419
c_2	5.34	0.168	0.181	0.181	0.188	0.188	0.188
K	5.36	0.140	0.147	0.147	0.150	0.150	0.150
J	5.33	0.525	0.491	0.491	0.480	0.480	0.480
C_e	5.32	1.600	1.518	1.518	1.488	1.488	1.488

Table 5.14. Discharge coefficient (C_d) and effective discharge coefficient (C_e) for East Channel side weirs (3rd weir belongs to downstream).

East Channel							
Author	Equation Number	3 rd Side Weir		2 nd Side Weir		1 st Side Weir	
		C_d	C_e	C_d	C_e	C_d	C_e
Nandesamoorthy et al.	5.25	0.383	1.130	0.371	1.095	0.361	1.065
Subramanya et al.	5.26	0.587	1.735	0.575	1.697	0.564	1.665
Hager	5.27	0.449	1.327	0.427	1.261	0.411	1.213
Sing et al.	5.28	0.473	1.398	0.467	1.380	0.463	1.366
Jalili and Borghei.	5.29	0.603	1.780	0.518	1.530	0.483	1.426
Borghei et al.	5.30	0.476	1.406	0.487	1.438	0.483	1.426
Ranga Raju et al.	5.31	0.417	1.232	0.427	1.261	0.422	1.247
Mays:	-	-	-	-	-	-	-
Omega	5.35	0.510	0.578	0.607			
c_1	5.34	0.432	0.420	0.415			
c_2	5.34	0.177	0.186	0.191			
K	5.36	0.145	0.150	0.151			
J	5.33	0.500	0.474	0.466			
C_e	5.32	1.533	1.465	1.445			

Table 5.15. West side weirs design data.

West Side Weirs				
Downstream to upstream				
Details	3rd Side Weir	2nd Side Weir	1st Side Weir	
Downstream	Flow (m^3/s)	0.000	0.117	0.233
	Flow Velocity (m/s)	0.000	0.382	0.292
	Water depth (m)*	0.360	0.389	0.384
	Critical depth (m)	0.000	0.106	0.129
	Froude Number (m)	0.000	0.120	0.177
Side Weir	Design Spillway flow (m^3/s)	0.117	0.117	0.117
	Discharge Coefficients	1.744	1.726	1.708
	Weir Length (L; m)	0.760	0.550	0.500
	Crest Level (P; m)	0.160	0.140	0.120
	Lateral Contraction Ratio (L/b)	1.520	0.550	0.333
	Vertical Contraction Ratio (H/P)	1.214	1.769	2.203
	Average Water Depth (m)	0.357	0.324	0.345
	Water Head (H; m)	0.197	0.246	0.255
Upstream	Flow (m^3/s)	0.117	0.233	0.350
	Flow Velocity (m/s)	0.319	0.382	0.440
	Water Depth	0.354	0.386	0.375
	Froude Number (m)	0.211	0.242	0.267
Channel Slope	0.001	0.001	0.001	
Area (m^2)	0.365	0.610	0.773	
Top Width (m)	1.596	2.831	3.820	
Channel Bottom width (m)	0.500	1.000	1.500	

Table 5.16. East side weirs design data.

West Side Weirs				
Downstream to upstream				
Details	3rd Side Weir	2nd Side Weir	1st Side Weir	
Downstream	Flow (m ³ /s)	0.000	0.375	0.747
	Flow Velocity (m/s)	0.000	0.554	0.439
	Water depth (m)*	0.620	0.676	0.673
	Normal depth (m)	0.000	0.485	0.595
	Critical depth (m)	0.000	0.216	0.267
	Froude Number (m)	0.000	0.140	0.213
Side Weir	Design Spillway flow (m ³ /s)	0.373	0.373	0.373
	Discharge Coefficients	1.735	1.697	1.665
	Weir Length (L; m)	0.930	0.730	0.690
	Crest Level (P; m)	0.240	0.220	0.200
	Lateral Contraction Ratio (L/b)	1.860	0.730	0.460
	Vertical Contraction Ratio (H/P)	1.541	2.061	2.373
	Average Water Depth (m)	0.615	0.578	0.630
	Water Head (H; m)	0.375	0.451	0.464
Upstream	Flow (m ³ /s)	0.373	0.747	1.120
	Flow Velocity (m/s)	0.433	0.554	0.663
	Water Depth	0.610	0.671	0.664
	Froude Number (m)	0.227	0.282	0.323
Channel Slope	0.001	0.001	0.001	
Area (m ²)	0.863	1.347	1.658	
Top Width (m)	3.088	5.040	6.473	
Channel Bottom width (m)	0.500	1.000	1.500	

5.7.3 SIDE WEIR PROFILE

A sketch of the cross section at the side weir can be seen in Figure 5.23 and Figure 5.24. The riprap geometry design will continue with the same setup as discussed in Section 5.4, but the weir will be located at the south wall of the channel. The weir will consist of a non-corrosive material with a determined crest height. The foundation buried at one foot below the channel base, filled with concrete. At the downstream of the spillway, it is recommended to add 50 millimeters thick riprap blanket, 2 meter length minimum. This blanket will prevent the erosion on the side of spillway to reduce the velocity and distributing the water flow into the vegetation.

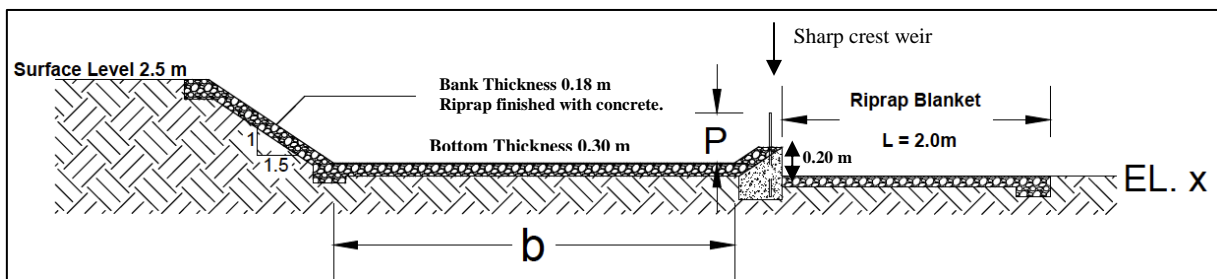


Figure 5.23. Side Weir Channel sketch (No to scale).

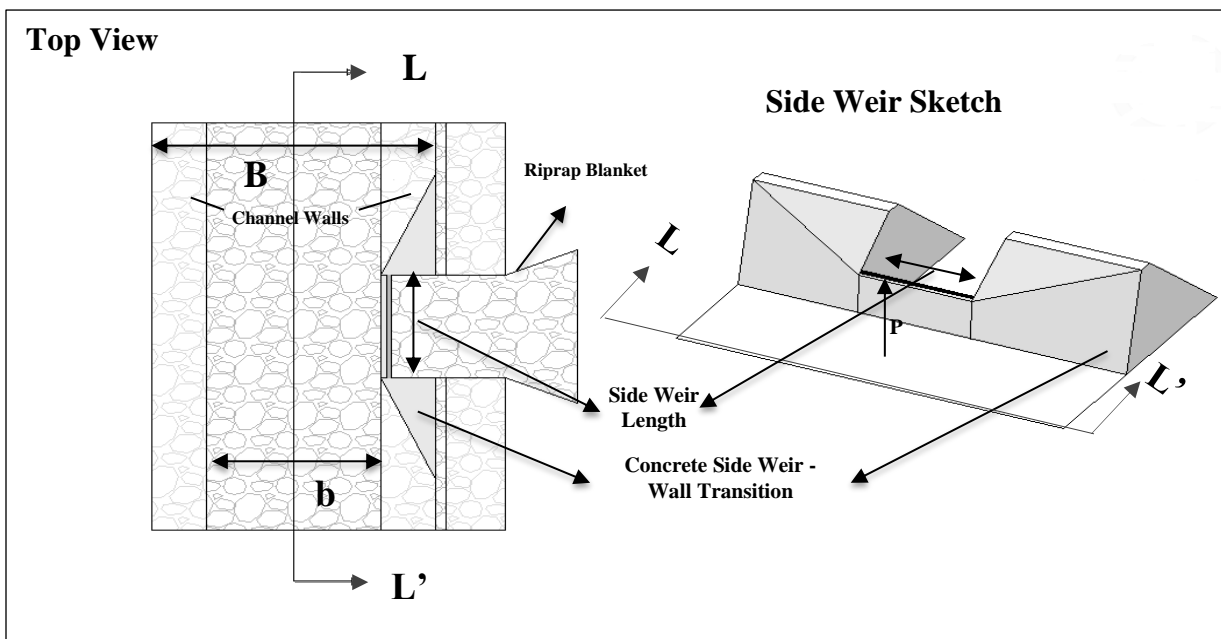


Figure 5.24. Side weir - wall transition details. (No to scale, exaggerate vertical axis)

5.7.4 VERIFICATION OF WATER SURFACE PROFILE

It is important to identify and verify the shapes of the water surface before start modeling any system. This water surface shapes will determine the relationship between the stage and the discharge (Sturm, 2011). This shapes also, helps to determine if the water depth is decreasing downstream. The tool that helps to determine water depth changes is the equation of gradually varied flow (Chow, 1959, and Sturm, 2011):

$$\frac{dy}{dx} = \frac{S_0 - S_f - Q_w}{1 - F^2} \quad 5.39$$

where:

- S_0 = channel bottom slope,
- S_f = energy slope or friction slope,
- Q_w = $\alpha Q q_{weir} / (gA^2)$,
- Q = weir discharge,
- α = energy coefficient (assume 1),
- q_{weir} = discharge ratio per unit length (dQ/dx),
- g = acceleration of gravity,
- A = area, and
- F = Froude number (equation 5.23).

The importance to predict the water surface profile on the side weirs is that it helps to determine the increase or decrease of water depth along the effective length of the weir. Figure 5.25 shows several types of water depth profiles and they will depend on the local depth (Y), the normal depth (Y_n) and the critical depth (Y_c). Also the Froude number, the bottom slope and the energy slope of the system have a big role to determine the type of profile required.

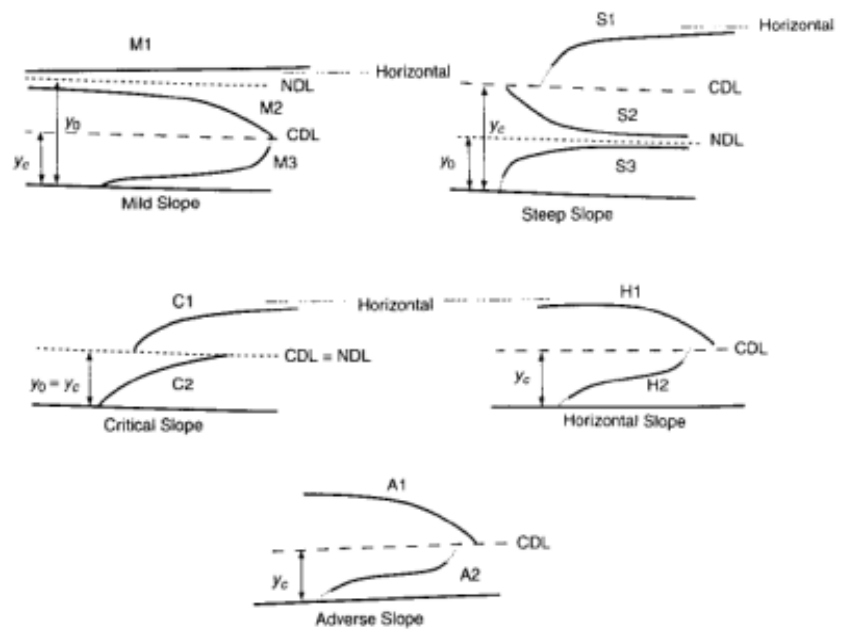


Figure 5.25. Gradually varied flow profiles (NDL = normal depth line; CDL = critical depth line) (Sturm, 2011).

Each profile is subdivided in basically three zones in which the comparison between the local depth, normal depth, and critical depth take place. Figure 5.26 shows a mild slope profile and the different zones with the water depths relation. Substituting the values of the bed slope (S_0), energy slope (S_f) and Froude number on the equation of gradually varied flow will determine the zone in the mild slope.

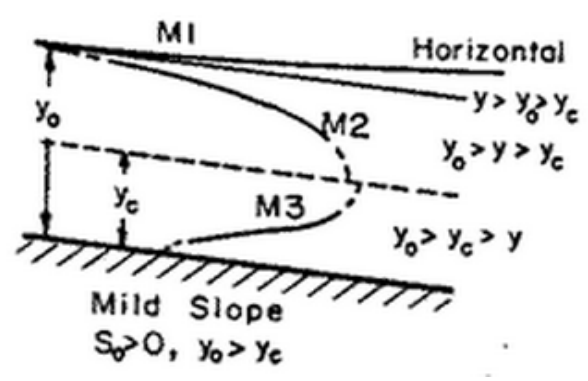


Figure 5.26. Mild slope profile (Chow, 1959)

According to Chow, 1959, the M1 zone can have the upstream local depth value equal to normal depth ($Y=Y_n$) since $dy/dx=0$ and at downstream end the surface will be tangent to the horizontal pool surface (see Figure 5.26), since $dy/dx=S_0$ as local depth go to infinite value.

To identify the type of water surface profile of the weir, the Improved Euler method was executed. This method uses equation 5.39 to compute the water profile along the side weirs. This algorithm was prepared in the VBA - Excel and it can be found in Appendix G.

Most of the data to compute the side weir profile were obtained from Table 5.15 and Table 5.16. The weir discharge per unit length (q_{weir}) must be entered in negative values to run the algorithm. The computed side weir profiles are shown in Figure 5.27 for West Channel and Figure 5.28 to the East Channel. The profiles are shown for the downstream, middle and upstream weirs, (See Figure 5.19 for visualization of side weir locations).

Comparing water depth (Y) in the profiles of the six weirs, normal (Y_n) depth and critical (Y_c) depth (see Table 5.15 and Table 5.16) it is observed that $Y > Y_n > Y_c$. This relation is typical of a mild profile slope in zone one (M1) which means that the profile shape is a backwater curve for a subcritical flow (Chow, 1959). Very small variation in the water profiles occurs along the side weirs, no larger than 1 cm.

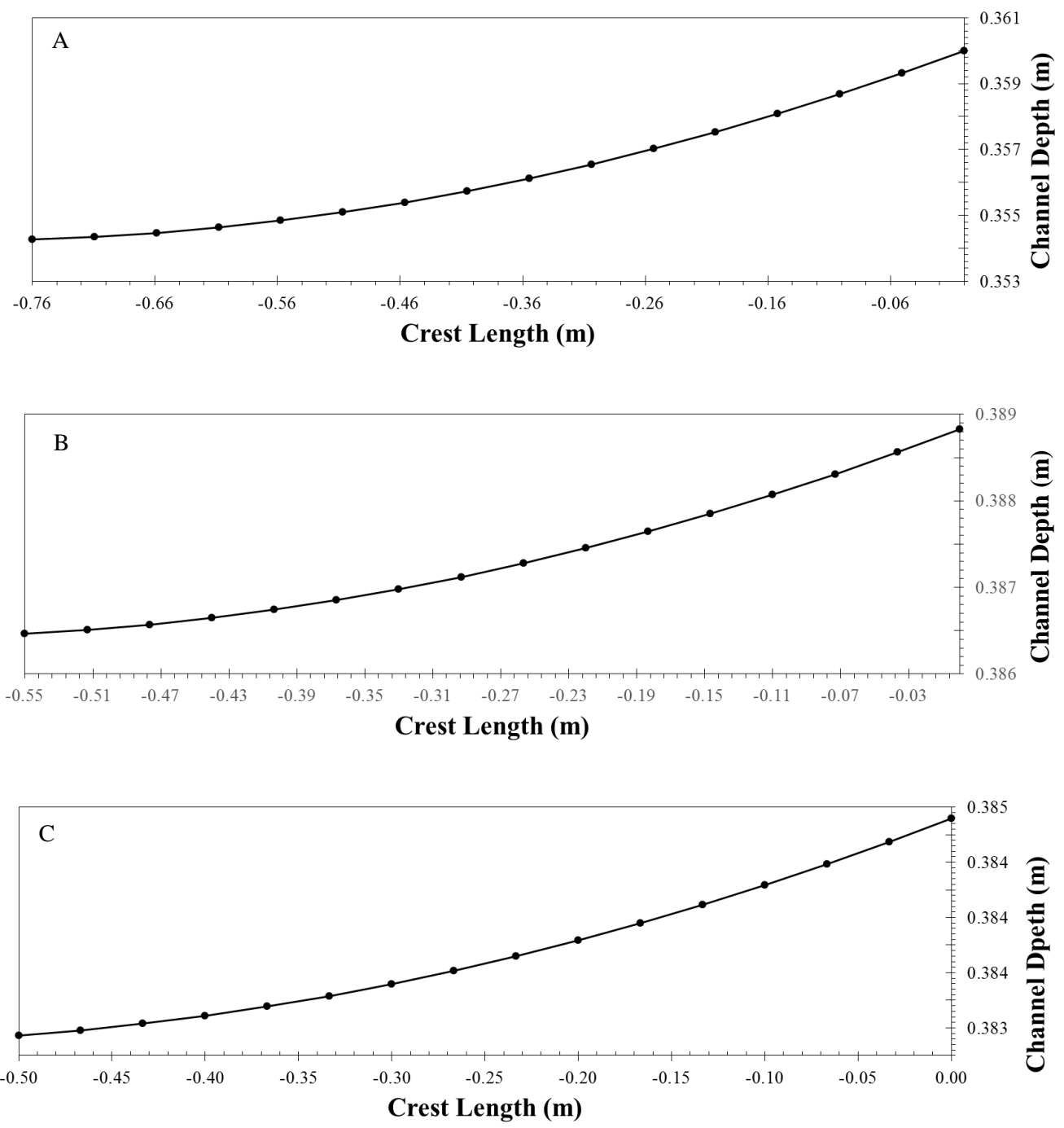


Figure 5.27. West channel side weir water profile: A: SW3, B: SW2 and C: SW1

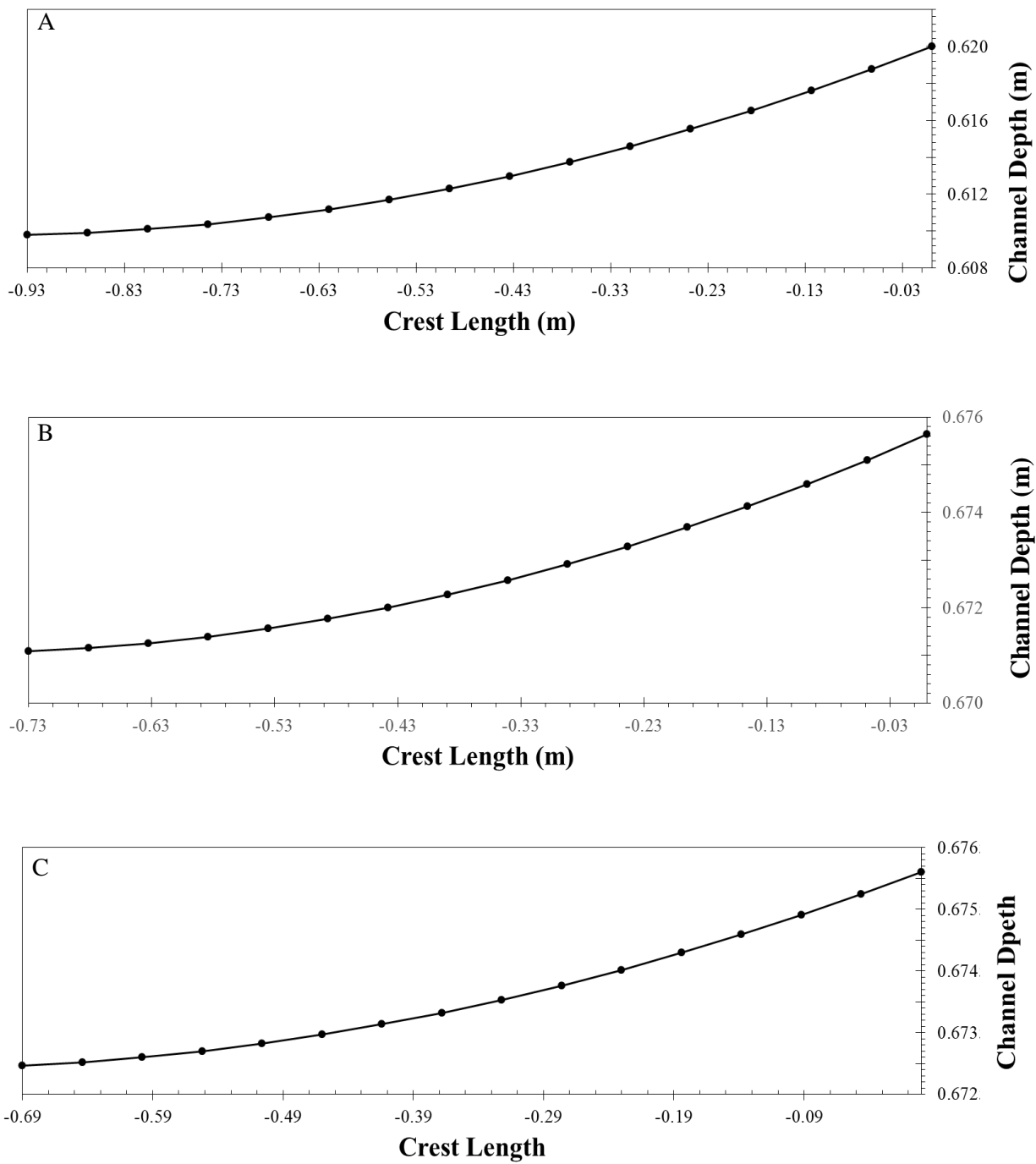


Figure 5.28. East channel side weir water profile. A: SW6, B: SW5 and C: SW4.

5.8 RECOMMENDED CHANNEL DIMENSIONS

Table 5.17 and Table 5.18, show the computed water depths at each of the sections along the channel for the design flow without any freeboard overflow occur under design conditions. In the West Channel, the maximum depth is 0.39 meters and the East Channel has a maximum depth of 0.77 meters.

The designed channels have a recommended depth of 0.40 m and 0.80 m for channels West and East, respectively. No provision for freeboard is given because there is no risk in case of channel overflows. Both channel depths were chosen based on the maximum water depths obtained in the computation. The channel is designed to distribute the flow through side weirs as long as the discharge is less than the design value. The geometry design has to ensure that flooding does not occur upstream, but flooding downstream into the AOI would be acceptable for large events because that is the purpose of the design and operation of the channels. In the discussion of the modeling of the channels, there will be a sensitivity analysis to see the flow behavior caused by different events.

Table 5.17. West Channel length and depth by section.

	Channel Sections	Section:		
		Downstream Depth	Upstream depth	Length
		(m)	(m)	(m)
Downstream to Upstream	SW3	0.360	0.354	0.76
	R7	0.354	0.354	7.00
	T3	0.354	0.356	3.00
	R6	0.356	0.389	8.00
	SW2	0.389	0.386	0.55
	R5	0.386	0.386	8.00
	T2	0.386	0.389	4.00
	R4	0.389	0.385	8.00
	SW1	0.385	0.384	0.35
	R3	0.384	0.385	8.00
	T1	0.385	0.391	7.00
	R2	0.391	0.382	13.50
	C1	0.382	0.367	14.14
	R1	0.367	0.357	10.00

Total: 92.30 m

Legend:

SW_i = Side Weir
 R_i = Reach
 T_i = Transition
 C_i = Bend
 i = 1,2,3, ..., n

Table 5.18. East Channel length and depth by section.

	Channel Sections	Section:		
		Downstream Depth	Upstream depth	Length
		(m)	(m)	(m)
Downstream to Upstream	SW6	0.620	0.610	0.93
	R14	0.610	0.609	7.00
	T6	0.609	0.614	3.00
	R13	0.614	0.676	8.00
	SW5	0.676	0.671	0.73
	R12	0.671	0.672	8.00
	T5	0.672	0.679	4.00
	R11	0.679	0.676	8.00
	SW4	0.676	0.673	0.69
	R10	0.673	0.677	8.00
	T4	0.677	0.690	6.00
	R9	0.690	0.766	13.50
	C2	0.766	0.744	14.14
	R8	0.744	0.737	10.00

Total:: 91.99 m

Legend:

SW_i = Side Weir
 R_i = Reach
 T_i = Transition
 C_i = Bend
 i = 1,2,3, ..., n

CHAPTER 6 PROJECT REPRESENTATION IN SWMM

This chapter explains the setup that has been used in SWMM for modeling of the channel hydraulics. Figure 6.1 shows details of the elements used. East and West channels were modeled through conduits (yellow) and junctions (dark blue). The main input data in conduits are channel roughness, full depth, lateral slope, channel slope and bottom width. The junction serves only as a link between conduits. No conduit exists without two junctions. The side weirs (light blue) begin from the junctions and extend until links with the outlet (red triangles). The weirs have a rectangular crest and the lateral weirs option was selected for modeling. The outlets represent boundaries at the downstream end of the side weir. SWMM is not able to model the contraction. Therefore, they were modeled as junctions dividing the changes in bottom width. The upstream side of the junction has greater width than the downstream side. These contractions can be found as a junction before each weir. The upstream side of the junction has greater width than the downstream side. These contractions can be found as a junction before each weir.

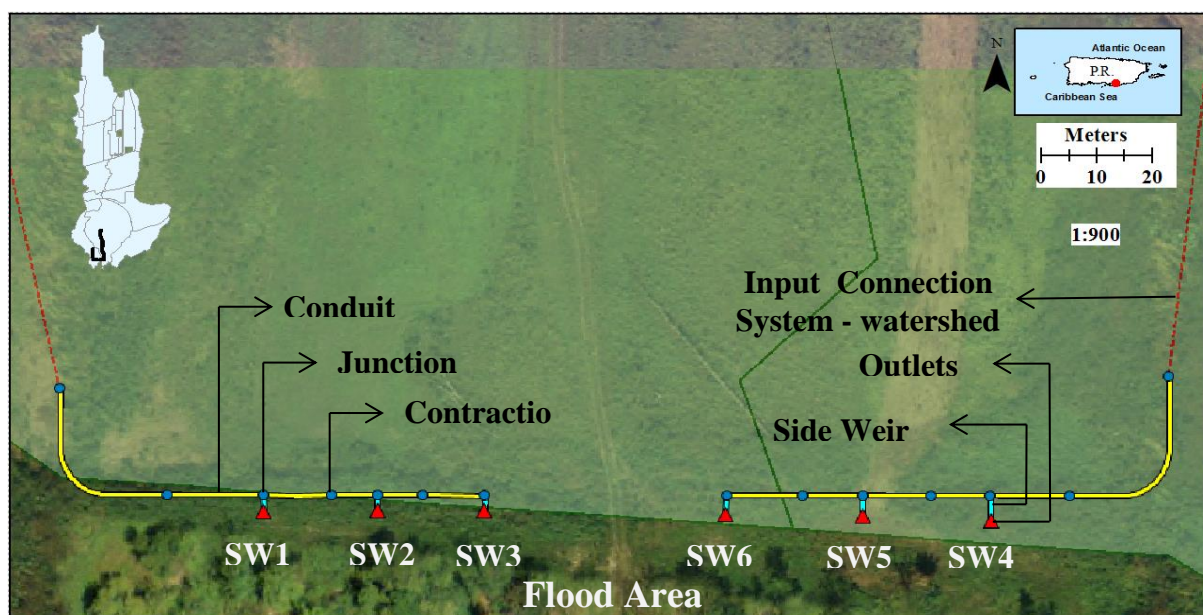


Figure 6.1. SWMM Modeling setup and features identification.

The Simulation Option window in SWMM allows the selection of the computation method for infiltration and routing. Dynamic Wave flow routing was selected as routing method. The SCS Curve Number Method was selected as the infiltration method. As previously mentioned, the historical event of August 8, 2011 was used as design event. Additional details about the subwatersheds areas, roughness values and other parameters can be found in previous sections.

6.1 MODELING DESIGN

The hydraulic model of SWMM will dictate the flow behavior in the design system for given conditions. The objective of this design is to distribute evenly the spill flow through three side weirs. This objective is applicable to the East and West Channels. Figure 6.2 and Figure 6.3 shows the flow distribution for each weir for the design storm measured in August 22, 2011. Both channels have a similar distribution pattern. When the rain intensity stays less than 10 mm/hr all weirs have the same pattern of distribution. Approximately at 2:45 PM there was an increase the amount of rain. The flow at that moment for the West channel was an average of 0.022 m³/s over each side weir. Furthermore, the East Channel, for the same time period, has an average of 0.085 m³/s.

The maximum spill flow over the weirs occurs at 11:00 P.M. which produces output discharges of 0.102, 0.099, and 1.29 m³/s (weirs spill flow upstream to downstream) in West Channel weir. The East channel have similar spill flow pattern, the flows produced by the models are 0.328, 0.325, and 0.402 m³/s (weirs spill flow from upstream to downstream).

The spill flows values obtained in SWMM do not match with the design weir flows. The design was computed using the energy equations, mass balance, and side weir equation along the channel from downstream to upstream. The design spill flow for each side weirs were 0.117 for the West Channel and 0.373 for the East Channel. These differences in values between modeling and design values are associated to the computation equations used in each method. The modeling

software uses the 1-D Saint Venant Equation which involves computations of the continuity equation, momentum equation, and side weir equation. Saint Venant equation considers the dynamic wave which involves the local acceleration, convective acceleration, pressure force, friction force, and the gravity force affecting the flow in the channel. The energy equation involves in the computation the elevation of the channel bottom with respect to a datum, pressure head, and the velocity head between two points. The computation of the energy equation is simpler when computed to the solution of the Saint Venant equation. The values from Saint Venant are expected to be more accurate if the input data was entered correctly.

6.2 SENSITIVITY ANALYSIS

This section will be divided in two types of rainfall data; synthetic rain and the historical rain. Both rainfalls types were modeled in SWMM to visualize the operation of the hydraulic design under variable rainfalls. A hyetograph of the synthetic rainfall were prepared using data obtained from the Atlas 14 (NOAA, Atlas 14, 2012) and the NOAA Technical Paper No.53 (Miller, 1965). The hyetographs correspond to an event with a returning interval of 2 years and durations of 3 and 6 hours.

The synthetic rain was modeled in SWMM and the runoff generated has values higher than historical rain data. Synthetic rains of a returning period of 2 years for durations of 3, and 6 hours were modeled. The runoffs produced by the modeling of those returning periods are shown in Table 6.1.

West Channel Side Weirs Discharge

Rainfall event August 22, 2011

8/23/2011 0:28, 32.994

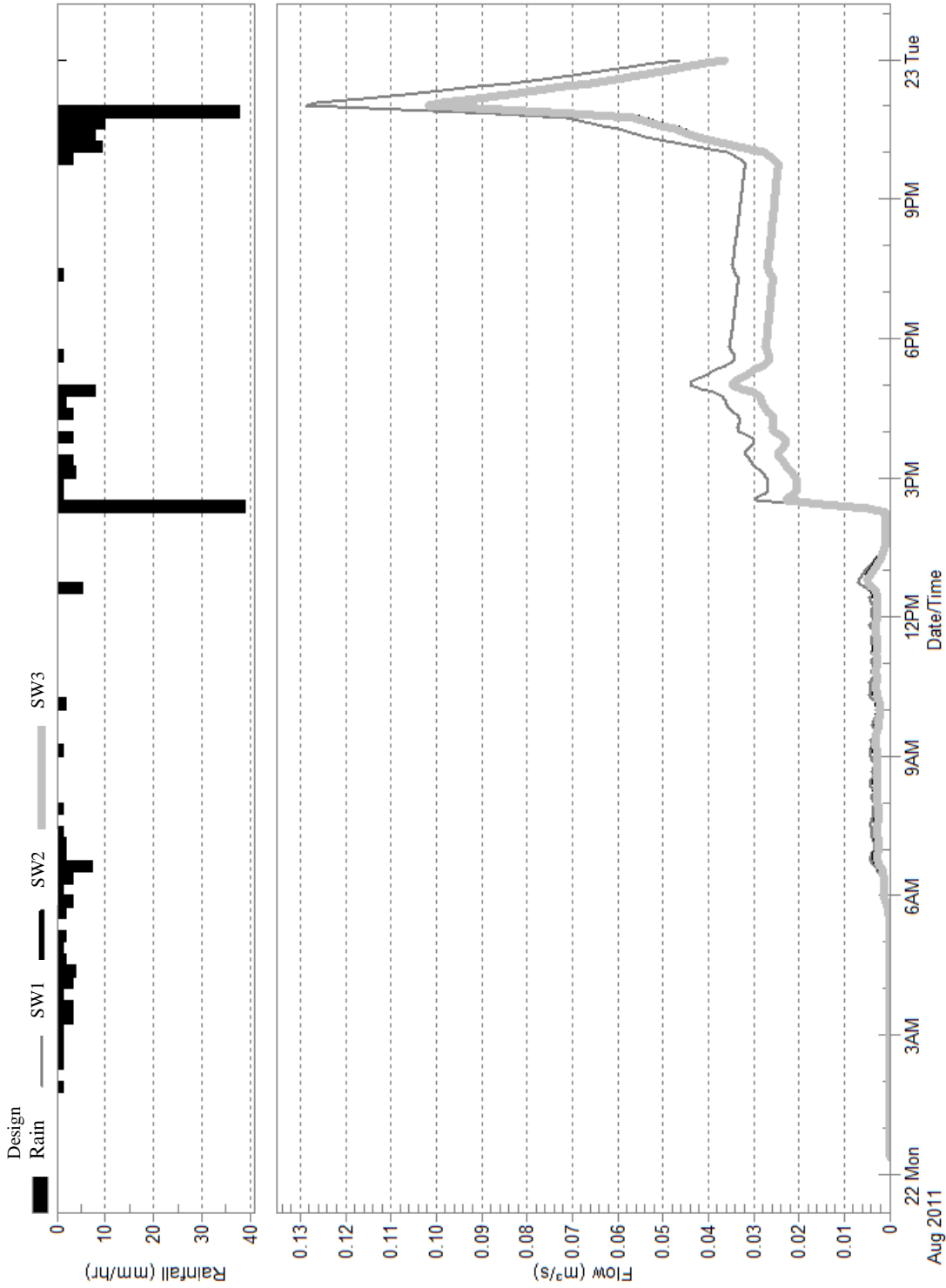


Figure 6.2. West Channel flow distributions of the side weir during the design rainfall event.

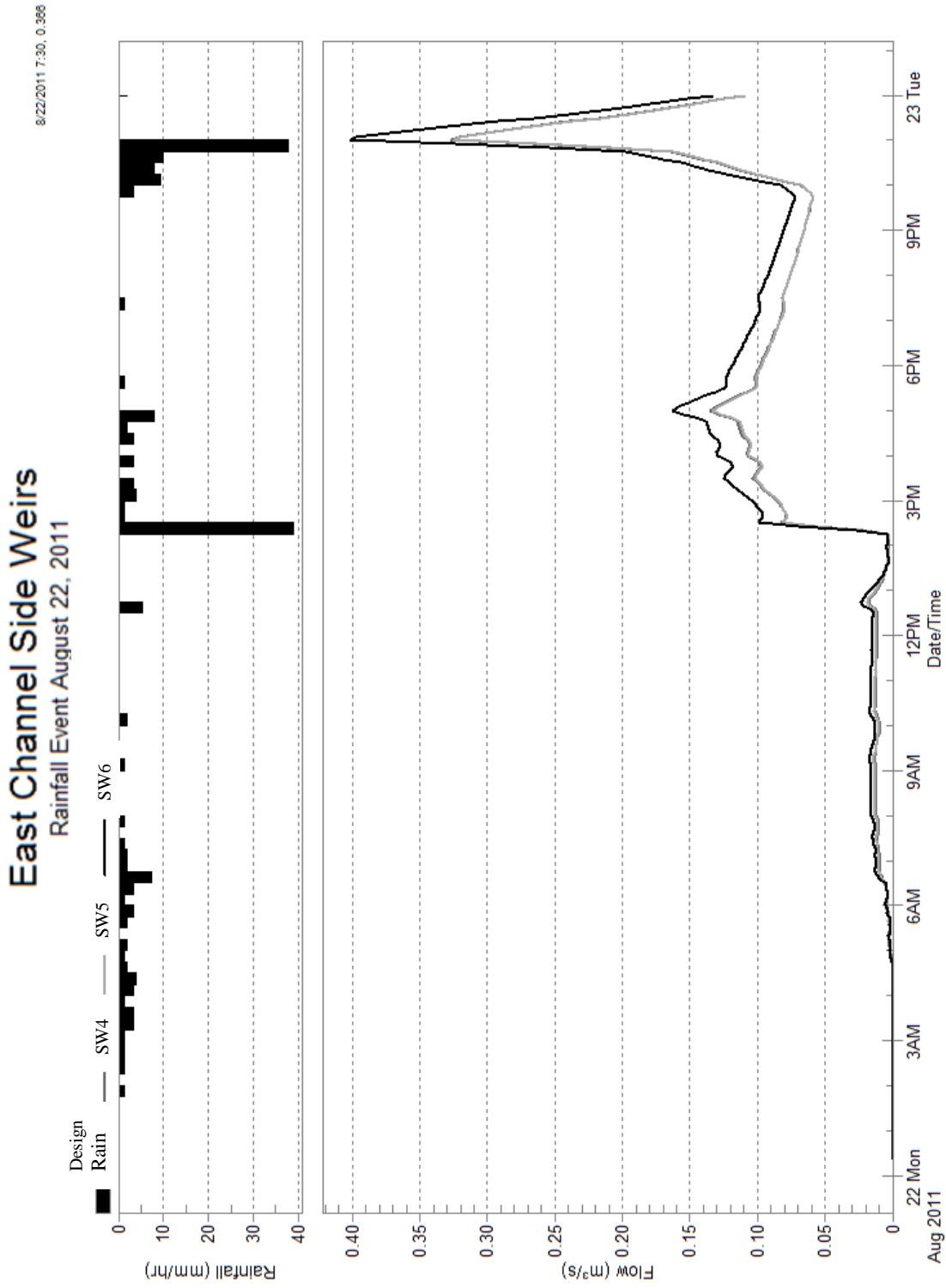


Figure 6.3. East Channel flow distributions of the side weir during the design rainfall event.

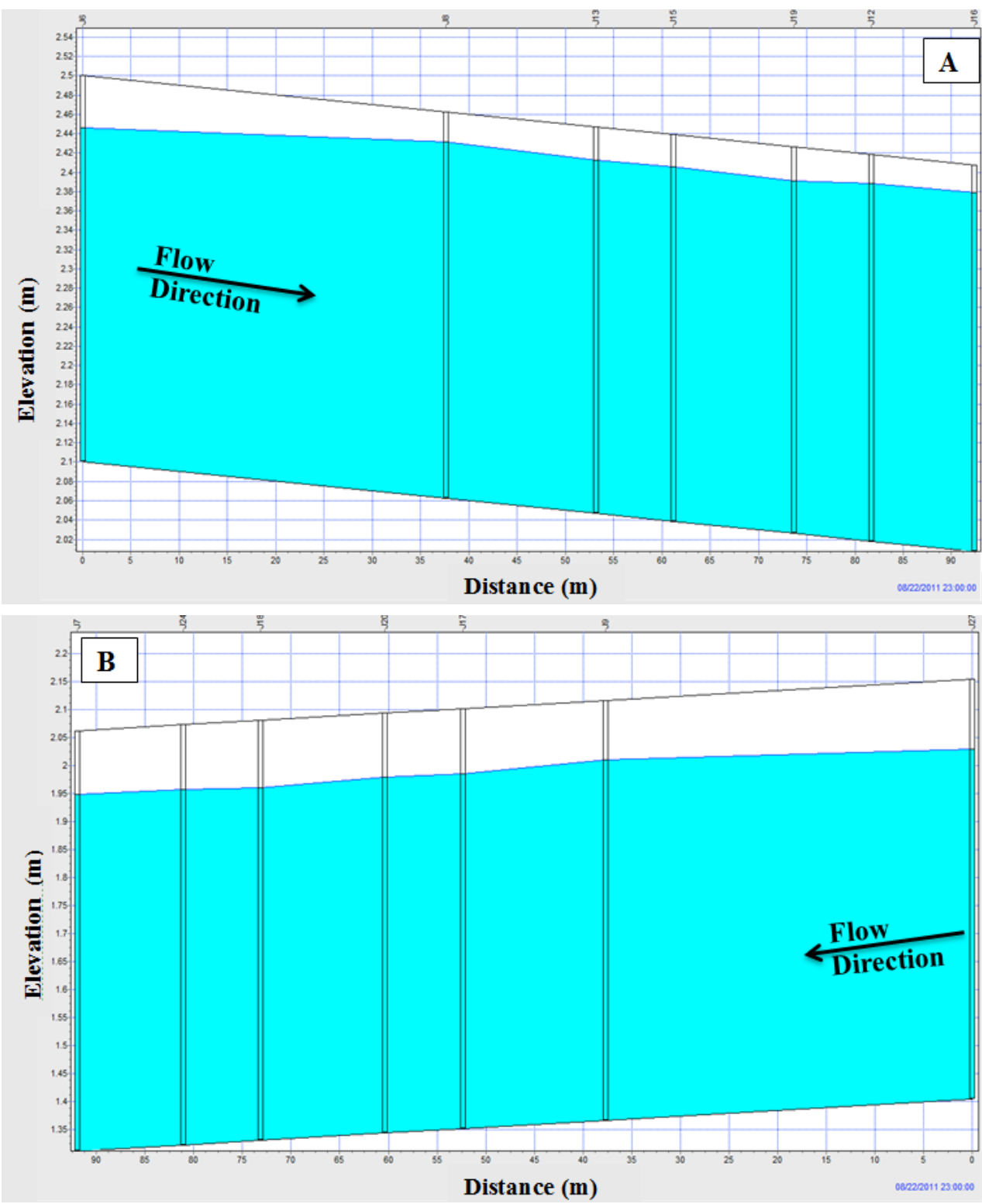


Figure 6.4. Channel profile of the maximum water depth during August 22, 2011 rainfall event. A) West Channel profile. B) East Channel Profile.

Table 6.1. Synthetic rains and historical rains for Sensitivity Analysis

	2yr-3hr	2yr-6hr	2008*	2011**
Accum. Rainfall (mm)	73.34	87.07	204.6	48.3
West Channel flow (m ³ /s)	0.92	1.17	3.86	0.36
East Channel flow (m ³ /s)	4.65	5.83	8.94	1.09

* September 22, 2008 – 24 hr duration

** August 22, 2011 – 24 hr duration

Comparing the synthetic rains with the historic rain, the historic rain offer a better idea of what is occurring in a certain time. Otherwise the synthetic rain is a frequency estimation value which is distributed in a given duration.

In the comparison of the hyetographs, the synthetic rain (see Chapter 9) has symmetric distribution in which the peak of the event can be found at midpoint of the event duration. The historical rain is not symmetric with time. This temporal distribution provides in some cases lapses that let the water infiltrate and sometimes the soil dries depending of the temperature and infiltration capacity of the surface. This scenario can be translated in a lower runoff than the synthetic rain. In synthetic rains the event start to increase until it reaches a peak at 12 hr and then start decreasing.

Additional to the synthetic rain, Table 6.1 shows the historical rains of September 22, 2008, and August 22, 2011. These two events represent the maximum and minimum events used for design analysis. These four events of rainfall are used to set up a sensibility analysis and visualize the design channel operation.

Figure 6.4 shows the operation of the East and West channel during the maximum peak flow (rainfall of September 22, 2008). Figure 6.5, shows the relation between the precipitations, runoff and side weir operation under the design rainfall. The operation of side weirs (SW) from

this profile event are shown in Figure 6.5.C and Figure 6.5.D. The general information of the side weirs can be found in Section 5.7. The design was done considering the rainfall which creates the maximum runoff that could be captured by the channels without overflowing. There is no risk of human hazard on the area and also this AOI belongs to the one of driest zones of Puerto Rico. The design must divert the water and distribute the flow as uniform over the area as possible, in order to be flooding the area. For larger rainfall events, the channel overflows producing an increase in water level, velocity and shear stresses in the channels walls and bed. According to computations, the shear forces produced by the design flow are five to six times smaller than those that the channel can resist. Therefore, the design is capable to resist overflow.

The Figure 6.5.B shows the comparison between the runoff and the design flow for both channels. This runoff conditions belongs to the rainfall of August of 2011. The design flows chosen for this project are the peak runoff caused by this event.

Figure 6.6 is an example of the full water depth in the channels during the peak rainfall event (September 22, 2008). These profiles show that no overflow occurs along the channel during this event. Furthermore it is possible that upstream of the channel can be affected by the runoff accumulation. The Figure 6.7.B shows runoff exceeding the design capacity, producing flooding conditions until the amount of water decreases. The weirs will be overflowing until the runoff reaches the design flow capacity. The modeling of this event was extended during the 5 days to show the channel operation during surcharge conditions.

The Figure 6.7.C and Figure 6.7.D shows the operation of the side weirs during overflowing. The spill flow pattern will continue at the maximum level until the channel flow decreases to the normal design flow. The figures show the increases of spill flow until they reach a maximum point and then the flow decreases reaching the design flow.

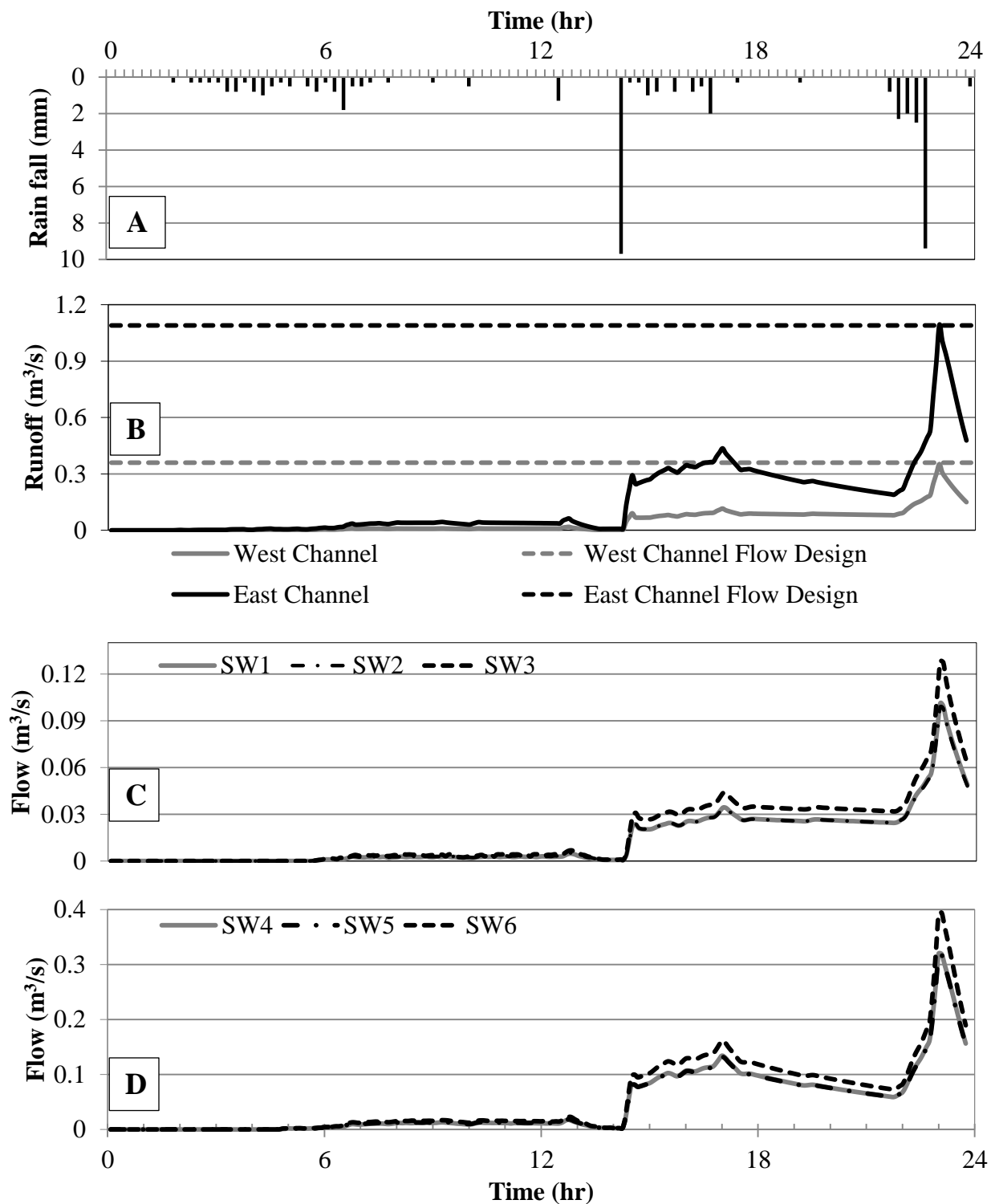


Figure 6.5. A: Historic rainfall from November 22, 2011. B: Amount of runoff that reaches the beginning of both channels C: East Channel. Side weirs operation with the maximum historical rainfall analyzed. D: West Channel. side weirs operation with the maximum historical rainfall analyzed. For location of side weirs (SW) refers to Figure 6.1.

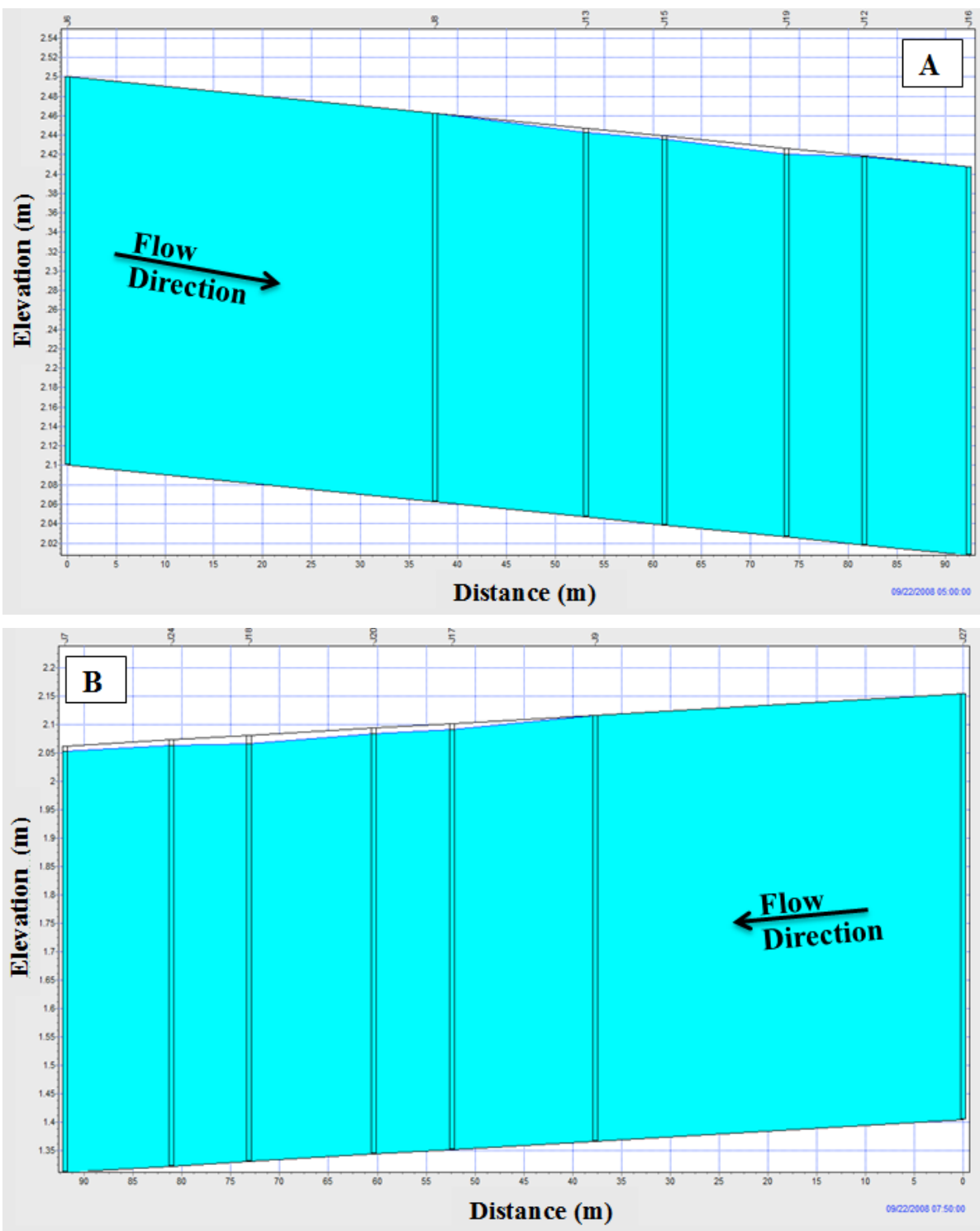


Figure 6.6. Channel profile of the maximum water depth during September 22, 2008 rainfall event. A) West Channel profile. B) East Channel Profile.

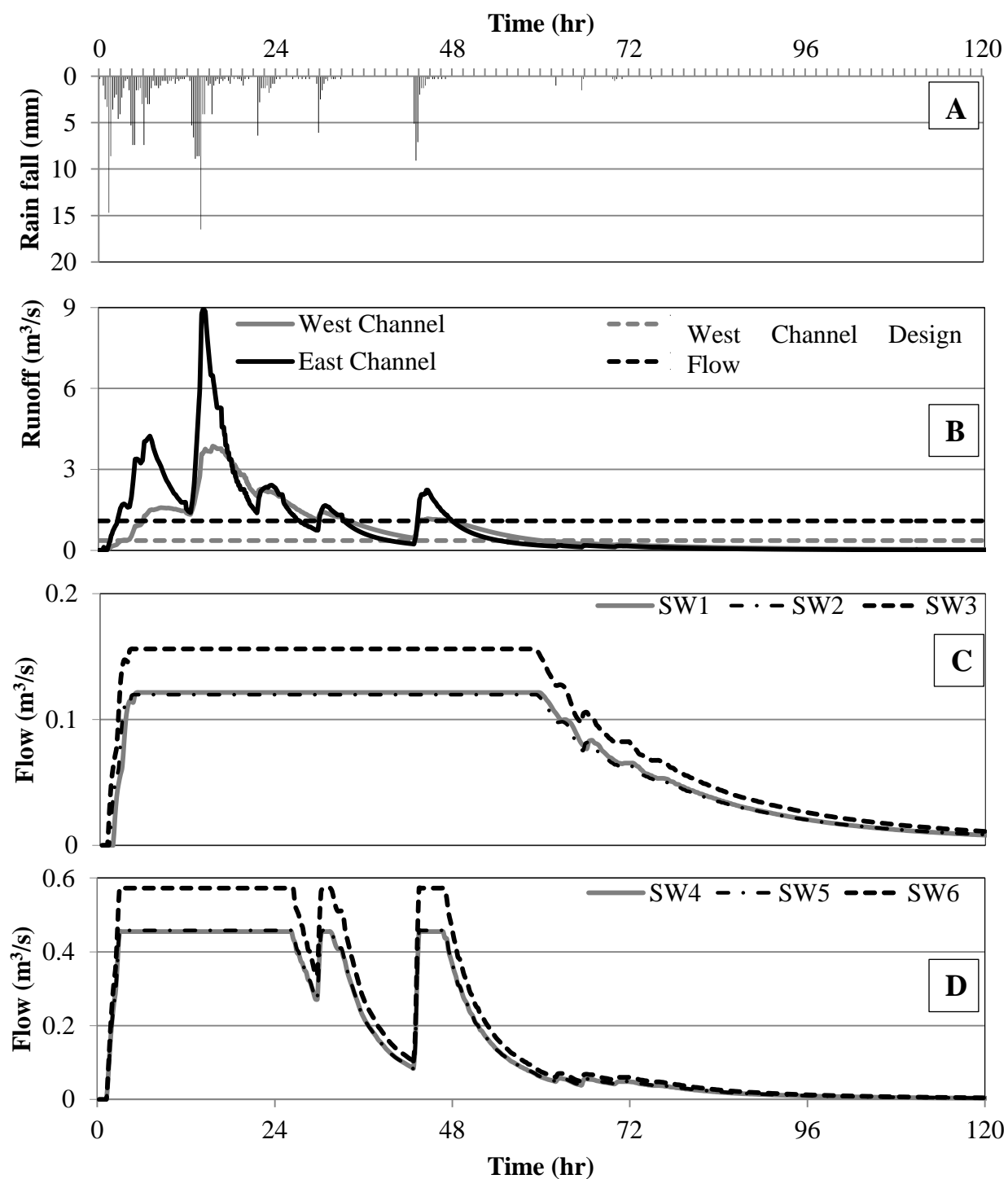


Figure 6.7. A: Historic rainfall from September 22-27, 2008. B: Amount of runoff that reaches the beginning of both channels C: East Channel. side weirs operation with the maximum historical rainfall analyzed. D: West Channel. side weirs operation with the maximum historical rainfall analyzed. For location of side weirs (SW) refers to Figure 6.1.

The spill flows in each weir are until the runoff reaches the maximum. At peak flow, the third weir downstream increases the outflow in about 26% compared with the other two weirs (upstream) in both channels. The flat areas in these figures, represents when the side weir capacity reached maximum operational level and occurred a possible channel overflow.

Figure 6.8 and Figure 6.9 shows the operation of the side weirs with synthetic rains. These synthetic rains can be found between the maximum and minimum rainfall accumulation (see Table 6.1). Also for these events, the behavior of the three side weirs, in each channel, remains the same as the previously discussed in the 2008 event. The two events produce runoff over the design flow. For the event of 2yr-3hr the difference between the first two weirs and the third one is 19% for the East Channel and 31% for the West Channel. For the other synthetic event of 1yr-24hr the difference between the first two weirs and the third one is 30% for the East Channel and 25% for the West Channel. As result, the side weirs reached the maximum flow and operation will be similar to the 2008 event. The difference between this event is the time that will be needed to reach the design flow.

The purpose of the channels design is to manage the water from agricultural irrigation. Unfortunately, data from irrigation is scarce. The only information available is the irrigation amounts by day for corn and sorghum (see Chapter 4).

The following changes were made in the model to simulate the operation of the channels during irrigation:

- The subcatchments were reduced only to the pivot irrigation area.
- Each subcatchment was associated to the corresponding irrigation period. Periods of 22-hour were simulated. As soon one 22 hours period finished, another period started. The simulation was executed during 93 hours.

- The daily irrigation volume was divided into 22 hours/day.
- The irrigation process consist in apply the irrigation in one quarter of the crop circle at a time.
- Irrigation intensity was 0.703 mm/hr (NRCS, 2009).
- Curve numbers and Manning roughness, were transferred from the original subcatchment.

Figure 6.10.A shows the modeling results of the runoff produced by the irrigation which reaches each channel. The maximum runoff produced by the irrigation was around 0.009 m³/s, which is below the design condition for both channels. As a consequence, the spill flow profiles of the weirs have the same pattern as the runoff (see Figure 6.10.B and Figure 6.10.C).

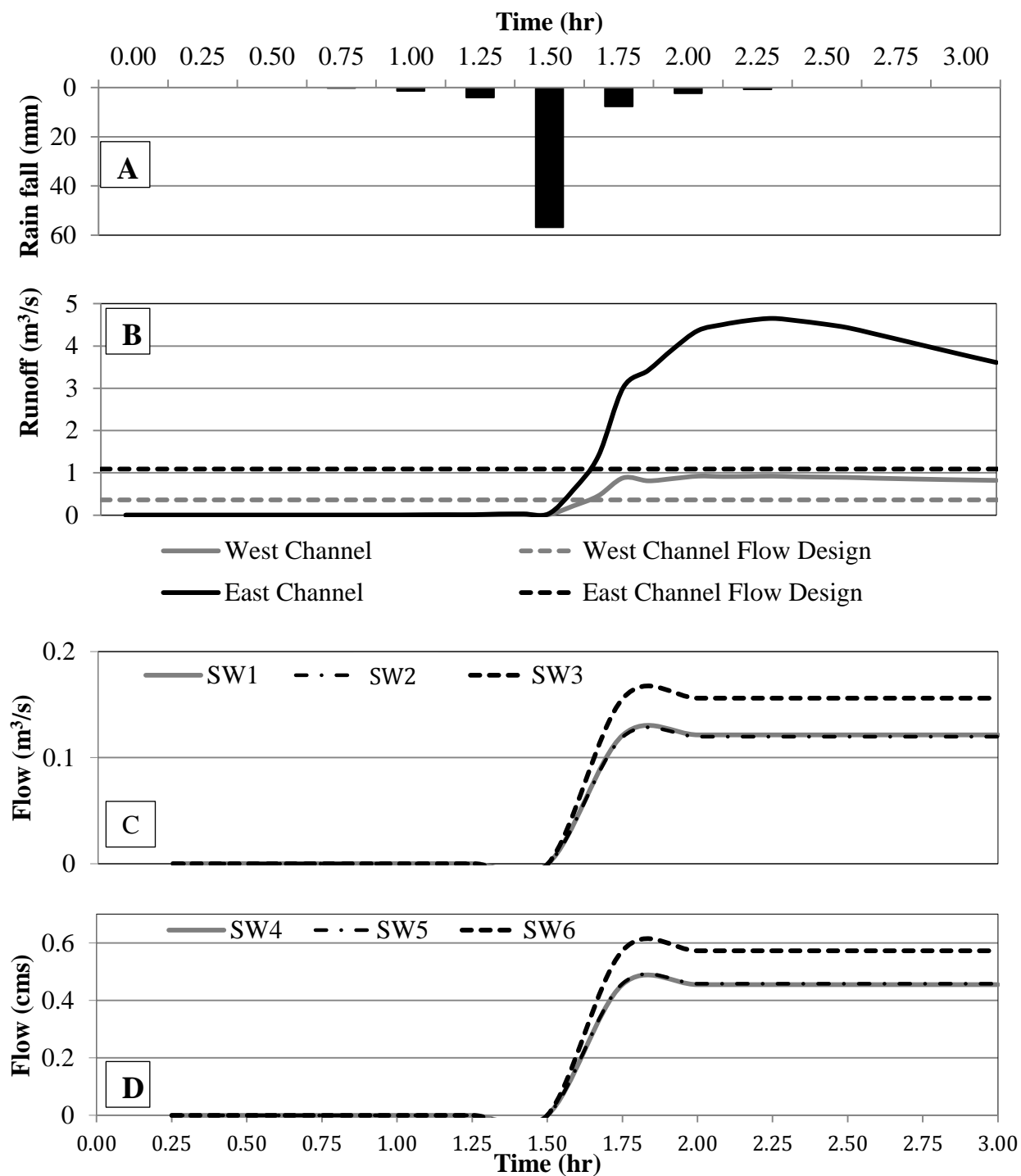


Figure 6.8. A: Synthetic rainfall (2yr-3hr). B: Amount of runoff that reaches the beginning of both channels. C: West Channel. Side Weirs operation with the maximum synthetic rain. D: East Channel. Side Weirs operation with the maximum synthetic rain. For location of side weirs (SW) refers to Figure 6.1.

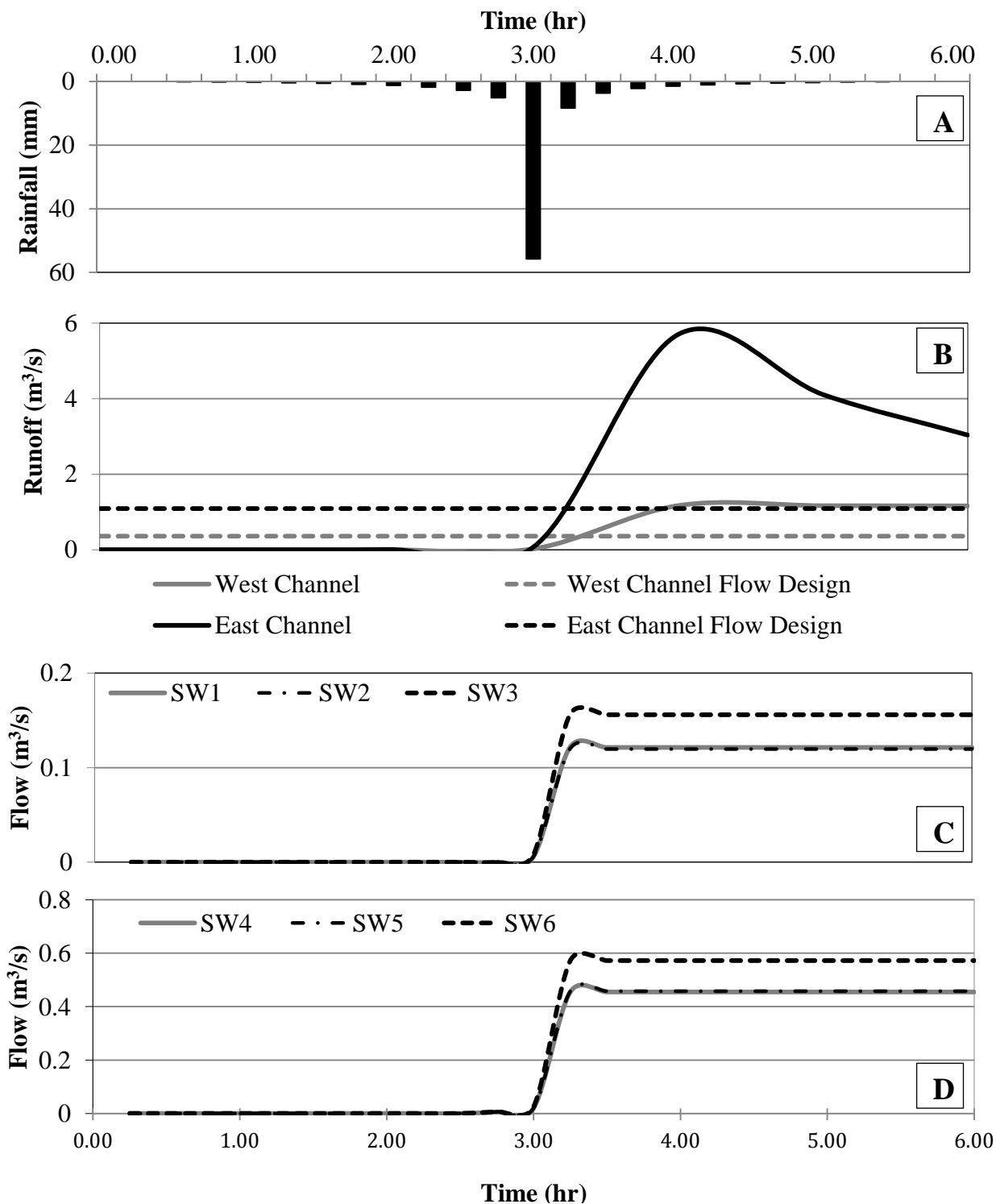


Figure 6.9. A: Synthetic rainfall (2yrs – 6hr) B: Amount of runoff that reaches the beginning of both channels. C: West Channel. Side Weirs operation with the maximum synthetic rain. D: East Channel. Side Weirs operation with the maximum synthetic rain. For location of side weirs (SW) refers to Figure 6.1.

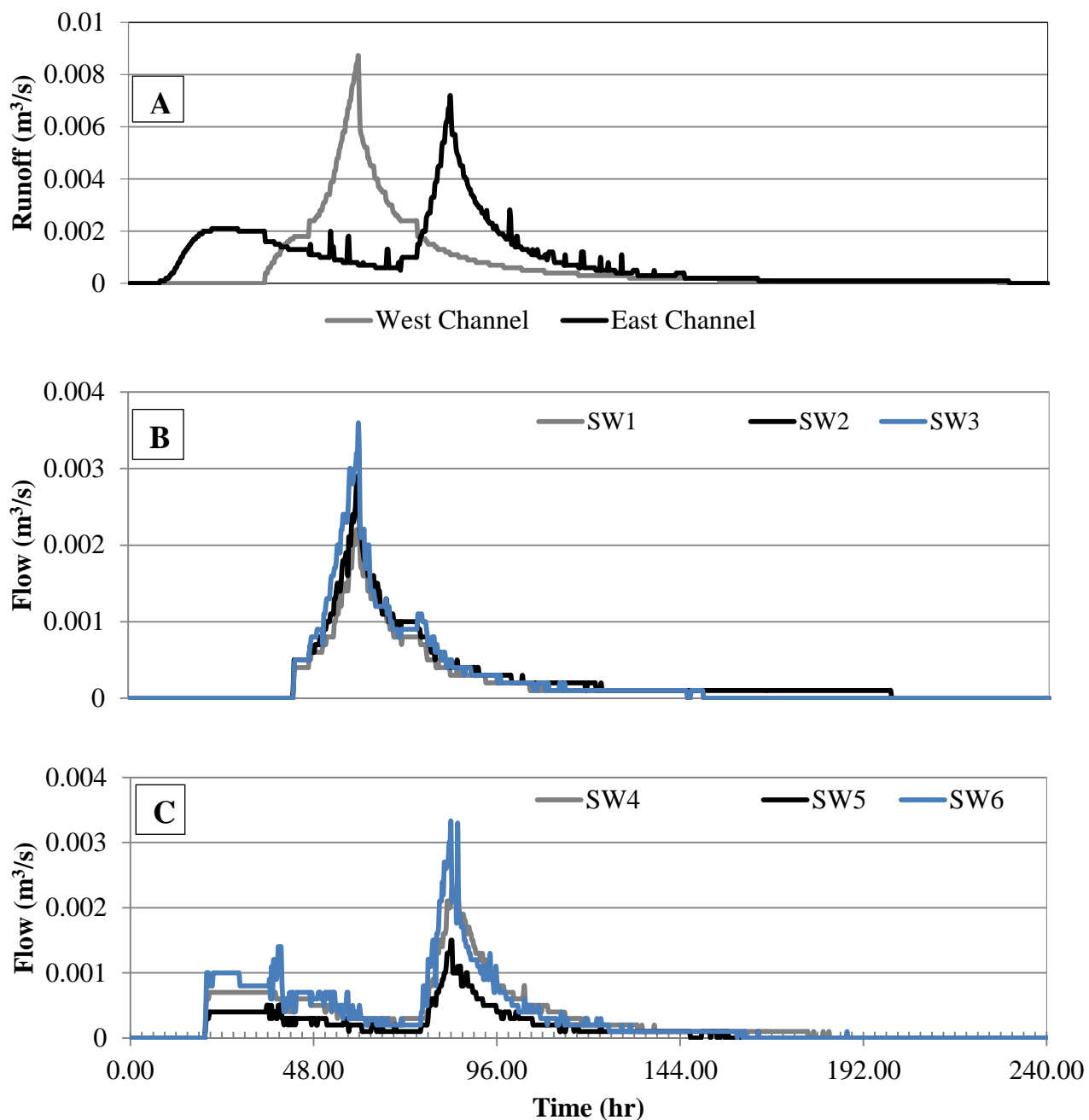


Figure 6.10. A: Amount of runoff that reaches the beginning of both channels (sorghum irrigation data) B: East Channel. Side Weirs operation during irrigation process. C: East Channel. Side Weirs operation during irrigation process. For location of side weirs (SW) refers to Figure 6.1.

CHAPTER 7 DESIGN ALTERNATIVES

For hydraulic design, different channel configurations were analyzed to improve the operation of the channels. All the alternatives and the correspondent description will be discussed in this chapter.

Alternative 1: Single Channel with Positive Slope and Weir Crest Variation

This alternative involves a hydraulic system in which the East and West are transformed into one single channel. The Figure 7.1 shows a profile with a positive slope; from the two inlets towards the culvert at the center. The channel bottom width is 3 meters at the inlet, then decrease to 2.5 meter in the second weir and to 1.5 meter in the third weir. The calculation of depth directly affects the height of the weir crest, but not the depth of the channel. The crest height varies in each side weir.

This alternative was rejected because:

- The west side of the channel has the lowest crest in the center but, the east side has the opposite configuration; the center crest has the highest height. This difference in crest elevation creates an increase in spill flow at the lower weirs. This is produced because it will have higher head of water and as consequence increase the spill flow in the weir. Also, when those higher weirs stop the spill, the lowest weirs will continue having flow until the water depth reaches the level of the crest. This difference of flows does not meet the requirements of the same flow in all weirs. Water will be ponded at the central section, where the culvert is located.

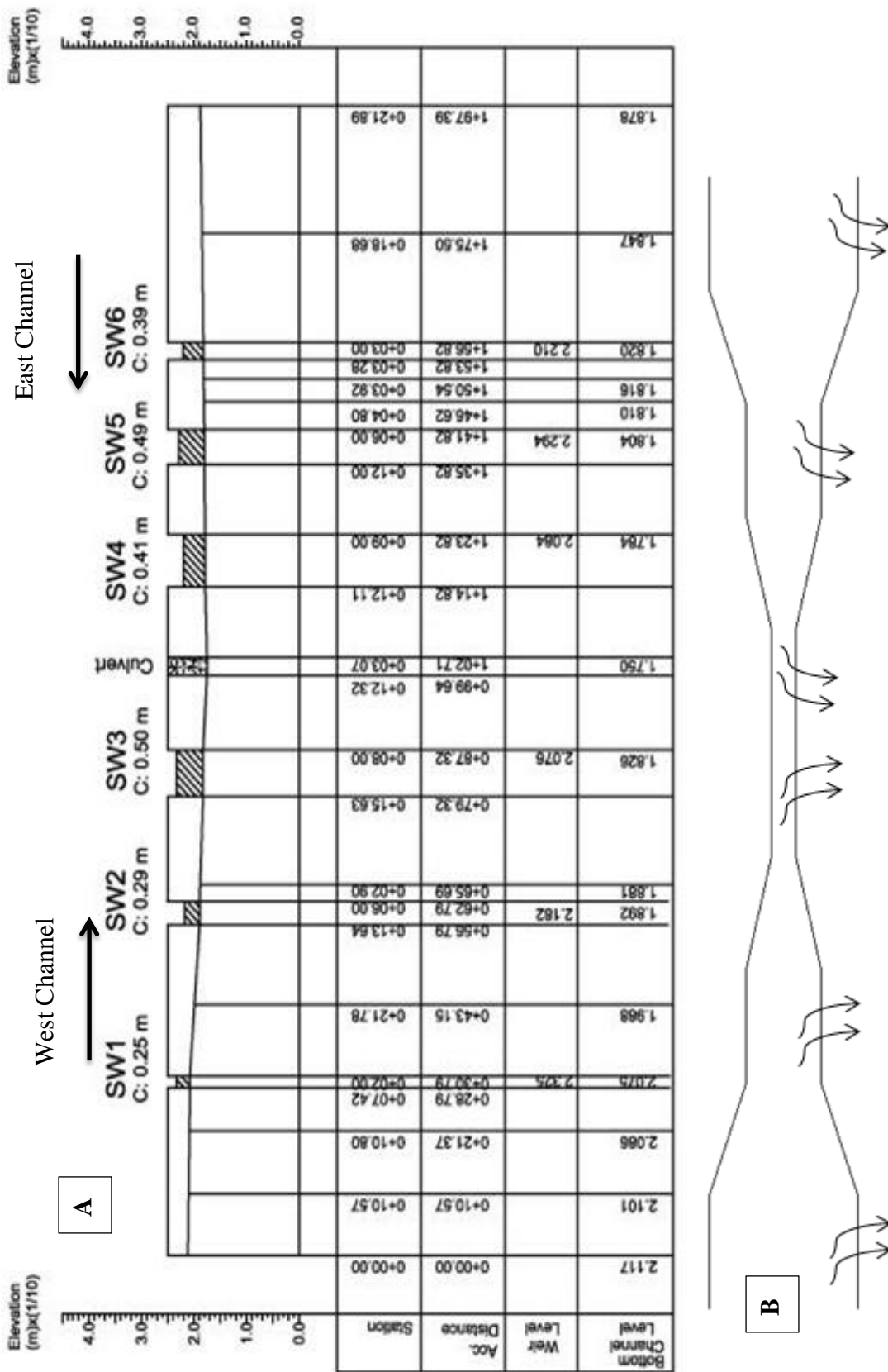


Figure 7.1. A: Single channel with six side weirs and a central culvert. This channel has a positive slope from the inlet to the center; The crest, length of the side weir and width of the channel varies from the inlet in both sides to the center. B: Channel top view geometry, not at scale.

Alternative 2: Two Single Channels with Positive Slope and Three Weirs with Short Length.

The sketch in Figure 7.2 shows two separate channels with three side weir each one. The computation initially started the design with the rainfall event of September 22, 2008. This event produces high run-off, which means that the geometry of the channel can be considered an overdesign for initial purpose. For this reason, the design was recomputed with minimum rainfall event occurred in the last 10 years, which was in November 22, 2011. The length along the channel is around 95 meters. The longitudinal slope is 0.001 and the side slope is 1.5 H: V. This alternative has 3 side weirs and 3 contractions. These contractions reduce the channel bottom width from 3 m to 0.5 m at downstream. The crest height varies depending on the location of the weir. The upstream weirs lengths are between 0.5 m to .093 m (see Chapter Chapter 5) for both Channels. The weirs were designed such that each weir discharge one-third of the total discharge to achieve uniform flow distribution along the channel reach.

This design includes a dead-end at the downstream end of the channel for sediments deposition. Maintenances must be required for this channel to remove sediments.

This alternative was the chosen one for this project. The advantage of this type of alternative is based on individual operation of the channels; the weirs will have similar spill flow operations, which translate in to more uniform water distributions in the flooding area. If higher run-off occurs, the channel will have the capacity to manage it without confronting structural problems. The channel characteristics can be found in Chapter 5.

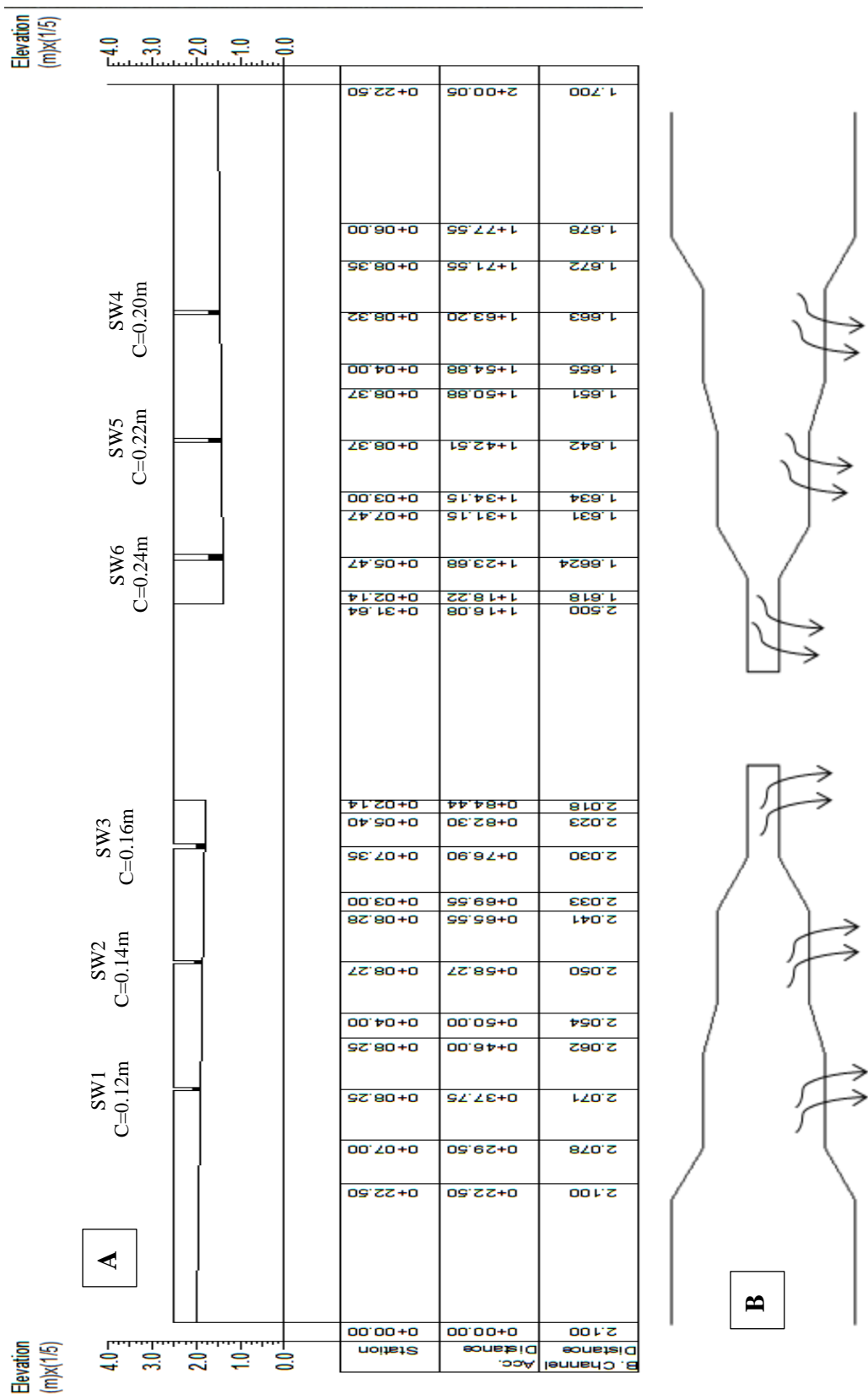


Figure 7.2. A: Two separates channels with 3 side weirs each. Slope is positive and short crest length, side weir length and the channel width. B: Channel top view geometry, not at scale. C= crest elevation.

CHAPTER 8 ANALYSIS AND DISCUSSION

Historically, the north area of the Jobos Reserve has been very active as far as agriculture is concerned. An irrigation pivot system was installed in the area in 1994. The irrigation system increased the amount of runoff flows carrying fertilizers and other chemical compounds used for agriculture, that impacted protected areas. The mangrove area has decreased during the last decade. Hurricane George in 1998 significantly affected the area and caused great damage to the mangrove. The mangrove recovery has not been successful since those events.

Jobos Reserve, specifically the north of Mar Negro, has a geology where the main component is alluvium material. The climatic condition of the area is quite wet during the rainy season, from September to October and the driest month in January.

The hydrological analysis began with the delineation of basins and sub-basins in ArcGIS, using a USGS topographic map, aerial photography (USACE) and field work. The roughness coefficients for overland flow were obtained from the SCS website by entering the watershed as the area of interest. Other variables determined for overland flow computation were the precipitation for design and the abstractions:

- The abstraction method evaluated was the Curve Number method (CN). This method was used to estimate the infiltration from the runoff. The CN values were obtained using high resolution aerial photos, field work and a GIS shapefile of Puerto Rico CN prepared by the SCS.
- The maximum precipitation accumulation during a 24 hr period of historic data was produced in September 22, 2008, which was 204.6 mm. The lowest precipitation in the 10 years analyzed occurred in November 22, 2011 which was 48.7 mm. From the analysis of the current study, the rainfall of 2008 and 2011 produced a total runoff of

12.58 m³/s and 1.35 m³/s, respectively. The 2008 peak runoff produced a 3.86 m³/s reaching the West Channel and 8.94 m³/s reaching the East Channel. The 2011 peak runoff can be divided in 0.36 m³/s reaching the West Channel and 1.09 m³/s for the East Channel inlet.

The rainfall of 2008 and 2011 were equivalent to a frequency event of 10 yr. and 1 yr, respectively. The synthetic event of 1 yr – 24 hr. (see Appendix H) was modeled and compared with the 2011 historical rainfall. This synthetic rain produces a total runoff of 1.73 m³/s which is distributed by the model in 0.75 m³/s for West Channel and 0.98 m³/s for East Channel. The distribution of the synthetic rainfall have a notably effect on the amount of runoff reaching both channel. This synthetic rain doubles the historic rainfall runoff for both West and East Channel.

The 2011 event was chosen as design rain. This project does not represent any risk for human beings and the design is for agricultural irrigations runoff management, which are lower than this event. Irrigation discharge data available is scarce.

- The only irrigation data that was obtained was for sorghum and corn. The sorghum irrigation was modeled in this project to have a general idea of the operation of the channels under this condition. The pivot circle was divided into 4 areas, of the same size. According PRLA, the farmers irrigate a quarter of a circle at a time, for 22 hours per day and at a rate of 0.703 mm/h.
- Flow routing is a computational procedure used to predict the changes in magnitude, speed and shape of a flood wave as a function of time at various points along river channel (Maidment, 1992). Three options of routing methods, steady flow, kinematic

wave, and dynamic wave were introduced on Chapter 4. The method of dynamic wave was chosen due to hydraulics considerations that will be discussed later on this chapter.

The hydraulic analysis started with the channel design modeled in SWMM:

- A topographic survey of the study area for existing conditions was performed. Currently, two trapezoidal channels (at the east and west of the AOI) are operating as runoff collectors and discharging directly to the mangrove area in Jobos bay. The West Channel has a depth of around 0.4 m at the outlet and it increases moving upstream. The East Channel has a depth of 0.8 m and follows the same upstream condition of the West Channel. Both channels have the maximum depth at the boundary of the irrigation pivot circle. This location is the point in which the channels start decreasing in depth upstream until they reach the beginning of the channels.
- The new design involves two separate channels with 90 degrees bend toward the center of the AOI. These channels will have a bottom width of 3 meters as the current channels and they decrease until 0.5 meters at the end of the channel downstream. Each channel distributes the runoff evenly as possible through 3 side weirs. The channel depth is 0.40 m for West Channel and 0.75 m for the East Channel. The side slope is 1.5 and longitudinal slope is 0.001 for both channels.
- The channel lining analysis started with a comparison of different types of lining as earth, cemented, riprap, and grouted riprap linings. The best lining was the riprap, grouted riprap, and reinforced concrete. The reinforce concrete was rejected due the high cost, Section 9.3 presents the cost estimates showing that the cost of concrete is around six times the cost of grouted riprap. The riprap was grouted to eliminate the possibility that an increase of flow can move the layer of rocks and decrease the

- operational efficiency of the channel. Also, in riprap without grout the vegetation can grow between rocks decreasing the flow velocities and increasing the maintenance cost. The grouted riprap is low cost, the grouted layer provides rock stability and decrease the cost of maintenance.
- The lining design was prepared for a riprap size of 90 mm. This size of riprap can produce a roughness of 0.032 but, the grout cement will increase approximately 13% the roughness of the design liner. Other important criterion of design is the shear stress in the channel's wall and bed. The critical shear stress, allowable for the channel bed and walls, are 56.55 MPa and 31.36 MPa, respectively. The maximum shear stress of the West Channel bed and wall exerted by the water flow are 3.38 MPa and 2.70 MPa, respectively. The water flow in the East Channel bottom bed and side wall produced a 5.63 MPa and 4.50 MPa, respectively. The channel liner will support approximately 6% of critical shear stress in the bottom bed and 18% in the side wall.
 - In the channels bends design two main factors were considered: 1) the maximum shear stress produced by the water flow shall not exceed the critical shear stress allowable by the channel liner; and 2) the super elevation to prevent the overflow of the channel due to the increase in water depth in bends. The maximum shear stress produced in walls and bed by the water flow in the bend is 5.02 MPa (9%) and 6.28 MPa (20%), respectively. This maximum shear stress is low compared with the critical shear stress allowable for the riprap design. The super elevation obtained from the design is 0.05 m for the West Channel and 0.10 m for the East Channel.
 - The channels bottom width begins 3 meters upstream and reduces to 0.5 meters downstream. These reductions occur by three inlet transitions in strategic locations.

The transition used was the straight line as recommended by FHWA (2012). All transitions have a flare angle less than 12.5 degrees to keep subcritical flow along the transition. Each transition is located before the weirs. The inlet transitions reduce the width of the channel downstream, increasing the flow velocity and decreasing the water depth.

- The hydraulic design computations used three different equations; mass balance equation, energy equation, and side weir equation. The selection of the weir equation for design purposes required the discharge coefficient for a side weir condition. The most important variables for the discharge coefficient computation are the crest height and the water head. All discharge coefficient equations include these two variables accompanied with other constants which depend on the experimental conditions from which the equation was derived. For Froude numbers less than one the side weir provides the most reliable operation. If the Froude number is higher than one, there is a chance that a hydraulic jump occurs in the weir, decreasing the velocity of the flow and causing a decrease in the operational efficiency. The discharge coefficient proposed by Subramayan, K. and Awasthy, S. C. (Emiroglu, et. al, 2011) was selected based on Chow, (1959), and French, (1987) recommendations. Also this equation produces the higher discharge coefficient and similar values for the three side weirs. The side weir equation requires similar discharge coefficient to adjust the condition of length and crest height, in order of obtain similar spill flow in each one.
- The water profile of the side weirs was computed using the Euler improves method for side weirs (see Appendix G). This method use the equation of gradually varied flow modified for weirs to estimate the water profile. The best side weir operation

- occurs when the channel has a subcritical flow upstream of the weir (May, et al., 2003). This means that the water will increase in depth at the end of side weir at the same time that is losing velocity due to the backwater effect. This transition of water along the side weir produces a backwater effect along of the weir or an M1 profile. On this type of profile the water depth will be equal or greater than normal depth and also greater than critical depth. This event produces an increase of the water depth downstream of the side weir but reduces the velocity as previously mentioned.
- The design prepared in Excel was developed using the steady state method in which the conservation of mass and conservation of energy is computed along each section of the channel. On SWMM, the dynamic routing method was used for the modeling. The model uses the Saint Venant equations to solve the hydraulic computations. This kind of computation method involves the momentum and continuity equations. These equations consider other factors such as friction forces, contraction and expansion, wind shear, and unbalance pressure forces for calculations. The steady state does not consider backwater effect. This backwater analysis by the Saint Venant equation could be one of the reasons of why the last side weir has a higher spill flow (Q_{peak}). After modeling the side weirs using SWMM, the maximum weir discharge obtained fluctuates between 0.100 m³/s to 0.128 m³/s in the West Channel and between 0.32 m³/s to 0.395 m³/s in the East Channel (see Table 8.1). As a pattern, the first two side weirs (from upstream to downstream) have the same amount of flow but the last one has a slightly higher spill flow value. The SWMM model shows a spill flow 15% to 16% lower than the target spill flow for design and approximately 6% to 10% above the design value in the third weir. Percentage error was computed using the steady

state design value versus the values obtained in SWMM. It is believe that these differences in spill flow values were produced by the computational method.

This project introduces the application of side weirs as a mechanism for uniformly water discharge along the channel.

Table 8.1. Comparison between steady state computation and values obtained in PCSWMM.

<i>Steady State - Excel</i>			
	Q_{peak} Per Weir		Q_{peak} Per Weir
West Channel (WC)	0.117	East Channel (EC)	0.373
<i>Unsteady - SWMM</i>			
	$Q_{\text{peak}} / \Delta M\%$		$Q_{\text{peak}} / \Delta M\%$
WC Side Weir 1	0.102 / -14%	EC Side Weir 1	0.32 / -15%
WC Side Weir 2	0.099 / -16%	EC Side Weir 2	0.319 / -15%
WC Side Weir 3	0.128 / 10%	EC Side Weir 3	0.395 / 6%

$\Delta M\%$ = % difference in peak flow between steady state and unsteady condition

CHAPTER 9 DESIGN RECOMMENDATIONS

This Chapter includes all the additional recommendations that can be applied to the design of the channel. Here are included the cross sections profiles with existent geometry, cut and fill profiles and a conceptual cost estimate for design.

9.1 LAND SURVEY

The area of interest (AOI) in Jobos has five north-south trails and other three west-east trails. Two of the north-south trails, contains a battery of five piezometers each trail; the location of these piezometers are shown as red dots in Figure 9.1. Taking advantage of these trails, the cross sections were delineating at the middle trail (C-C'), west trail (A-A') and east trails E-E'. The cross sections B-B` and C-C' are placed following the line of piezometers as shown in Figure 9.1. These cross sections delineate the current conditions of the AOI as maximum elevation, minimum elevations and slope. At north, the line I-I' is a representation of the profile in which the channel location is proposed. The north boundary of the AOI has a maximum elevation of approximately 2.5 meter above mean sea level (a.m.s.l.) and a minimum elevation of about 0.6 meters a.m.s.l. at the south end; with a slope around 0.8%.

The current topography of the area is represented in the cross sections shown from Figure 9.2 to Figure 9.7. The locations of these cross sections in the AOI are shown in Figure 9.1

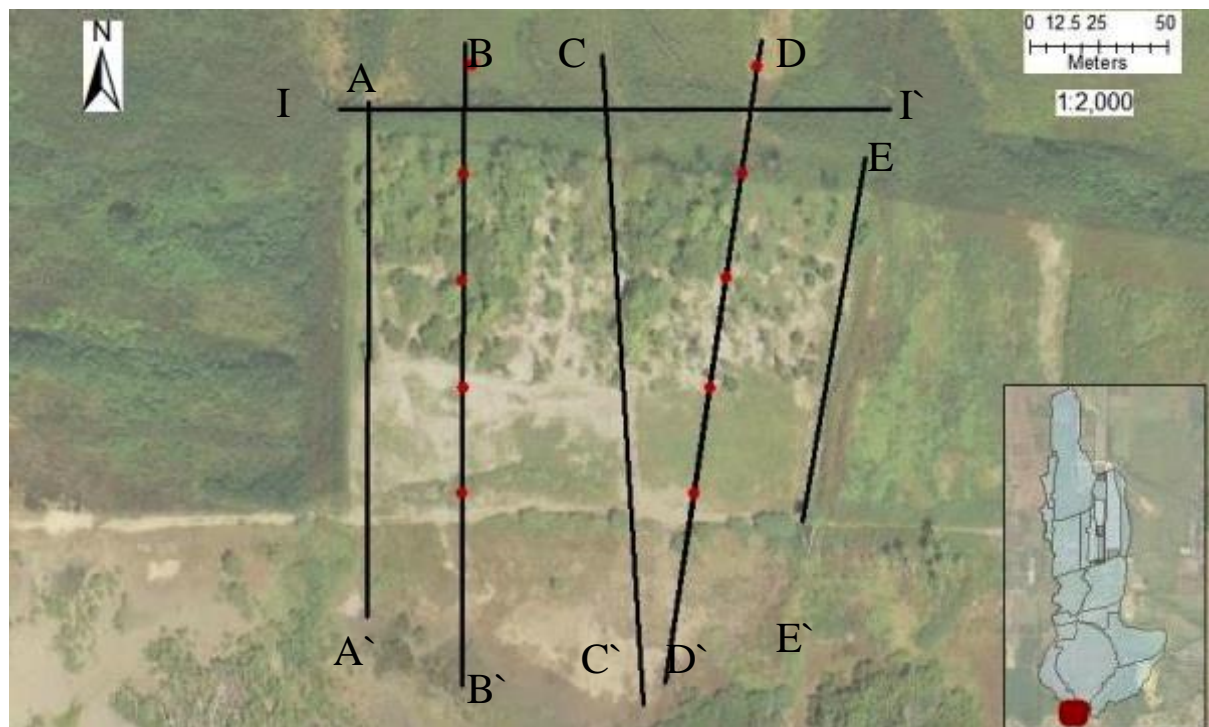


Figure 9.1. Location of the cross sections in the study area. Red dots represent the location of piezometers.

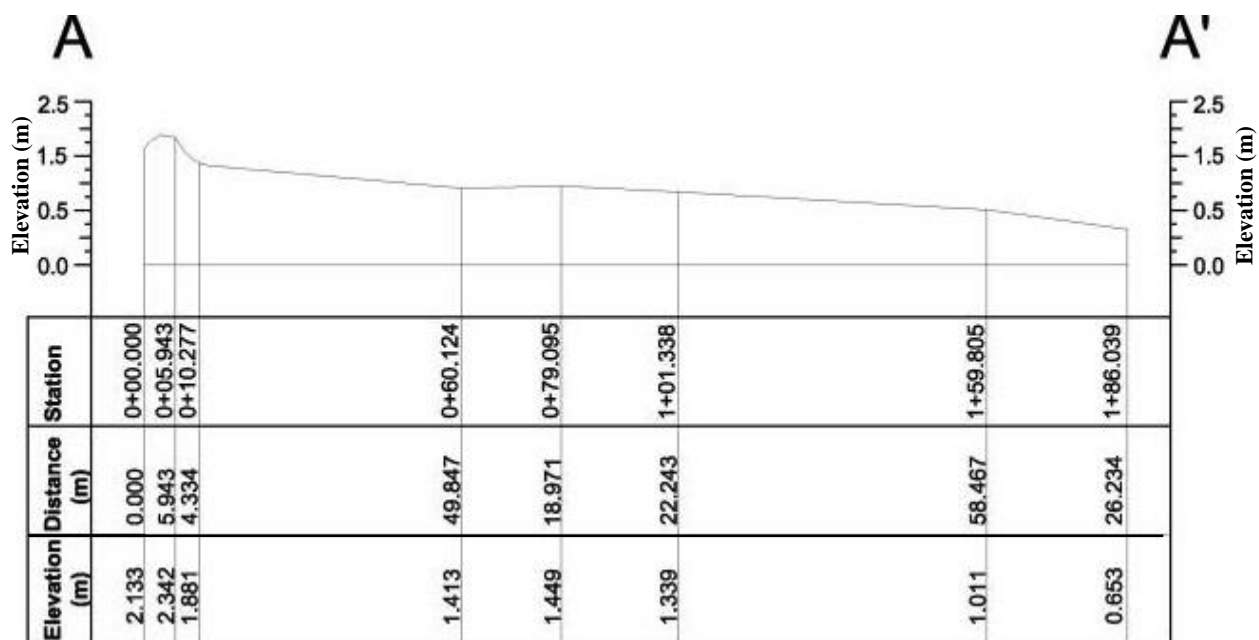


Figure 9.2. Cross Section A – A' with a vertical exaggeration of 10 times. Current Conditions.

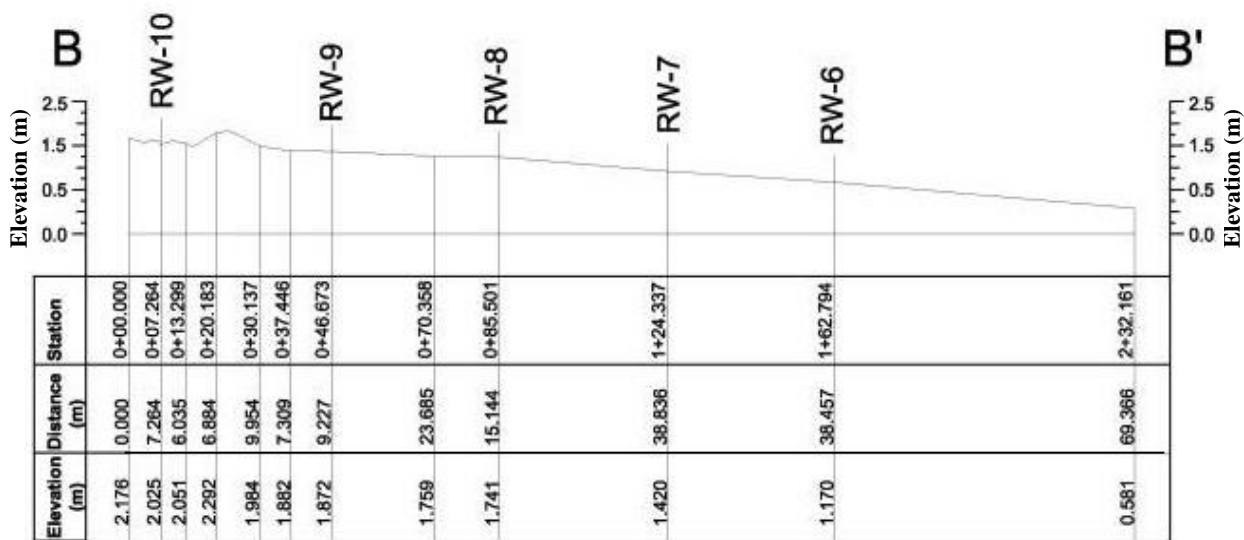


Figure 9.3. Cross Section B – B` with a vertical exaggeration of 10 times. Current Conditions. This profile shows the location of the piezometers along the cross section line.

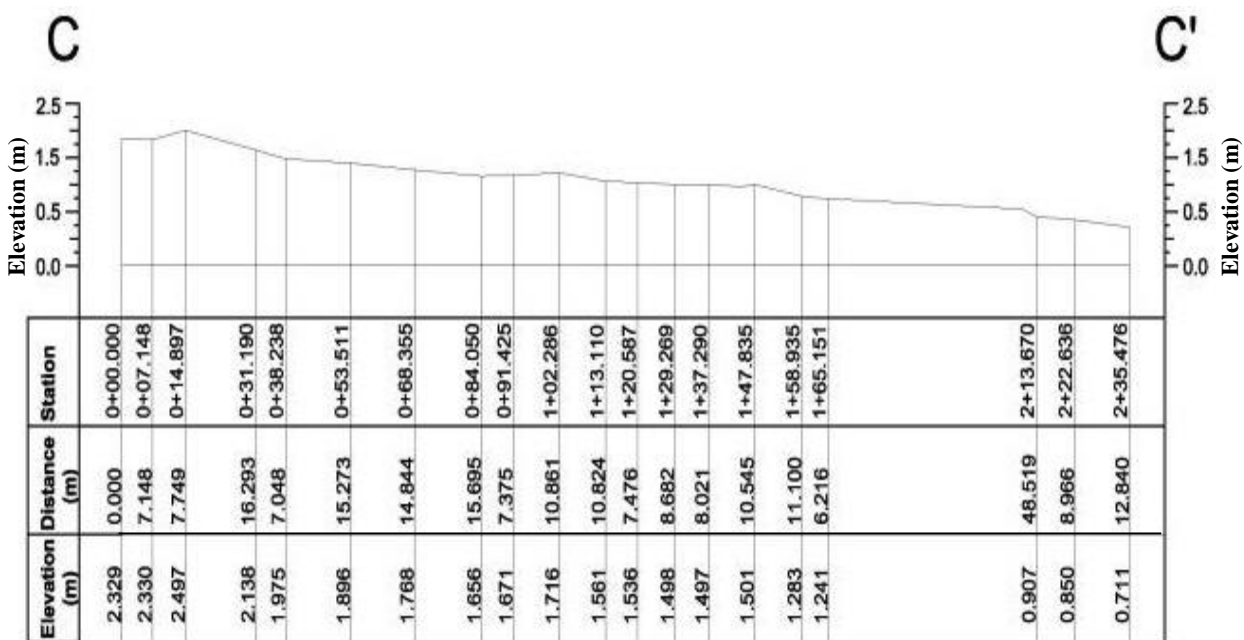


Figure 9.4. Cross Section C – C` with a vertical exaggeration of 10 times. Current Conditions.

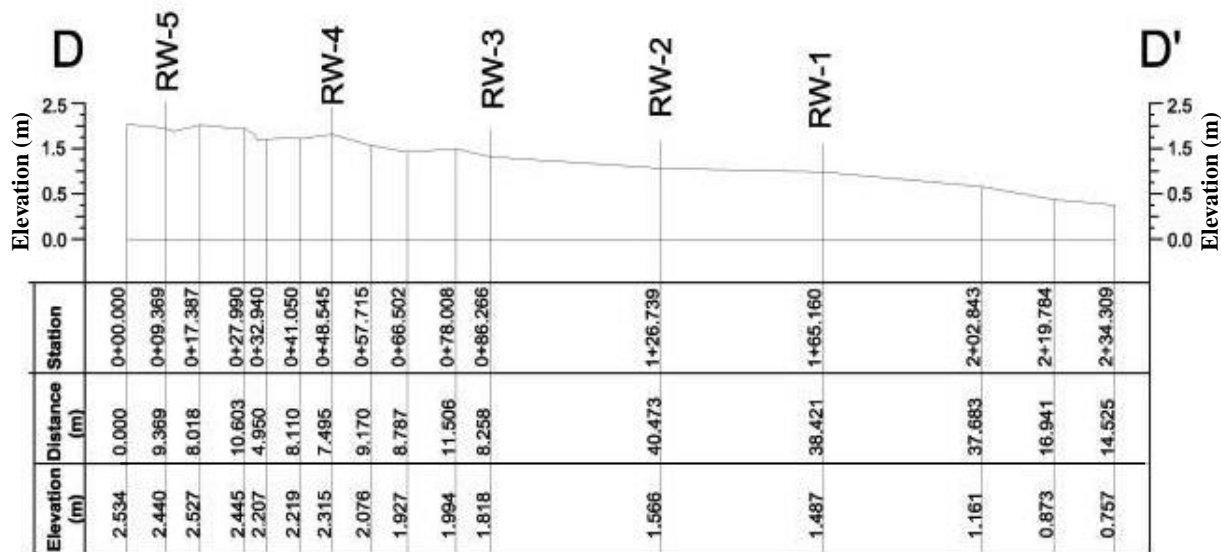


Figure 9.5. Cross Section D – D` with a vertical exaggeration of 10 times. Current Conditions. This profile shows the location of the piezometers along the cross section line..

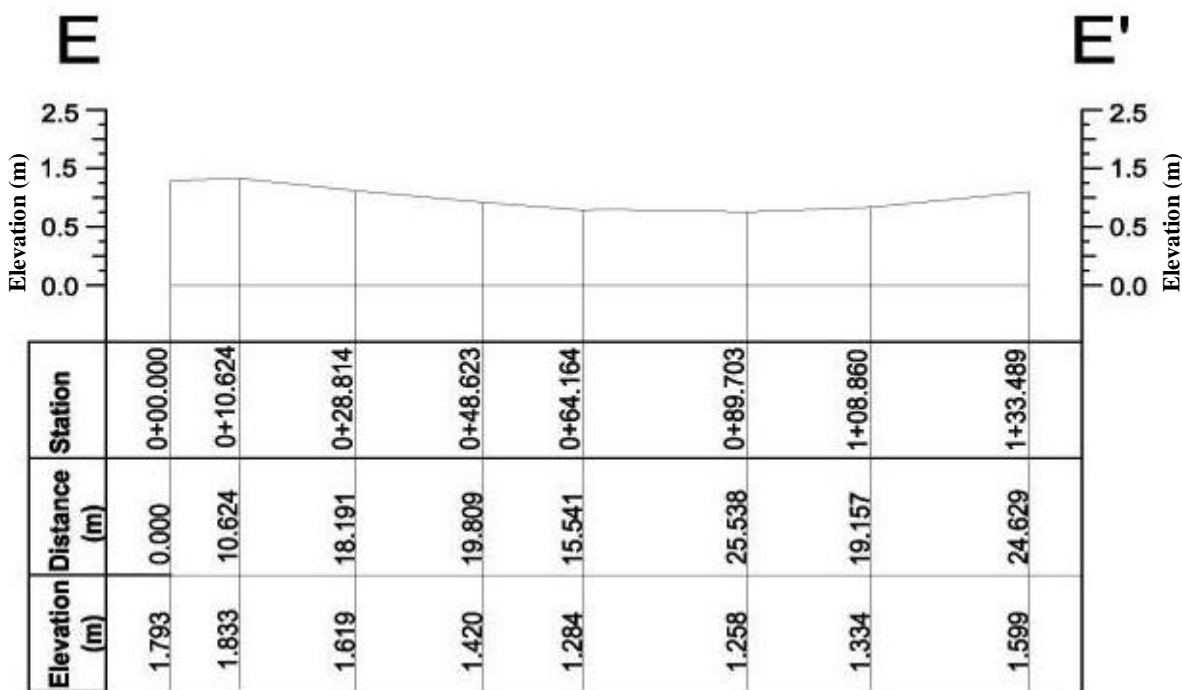


Figure 9.6. Cross Section E – E` with a vertical exaggeration of 10 times. Current Conditions.

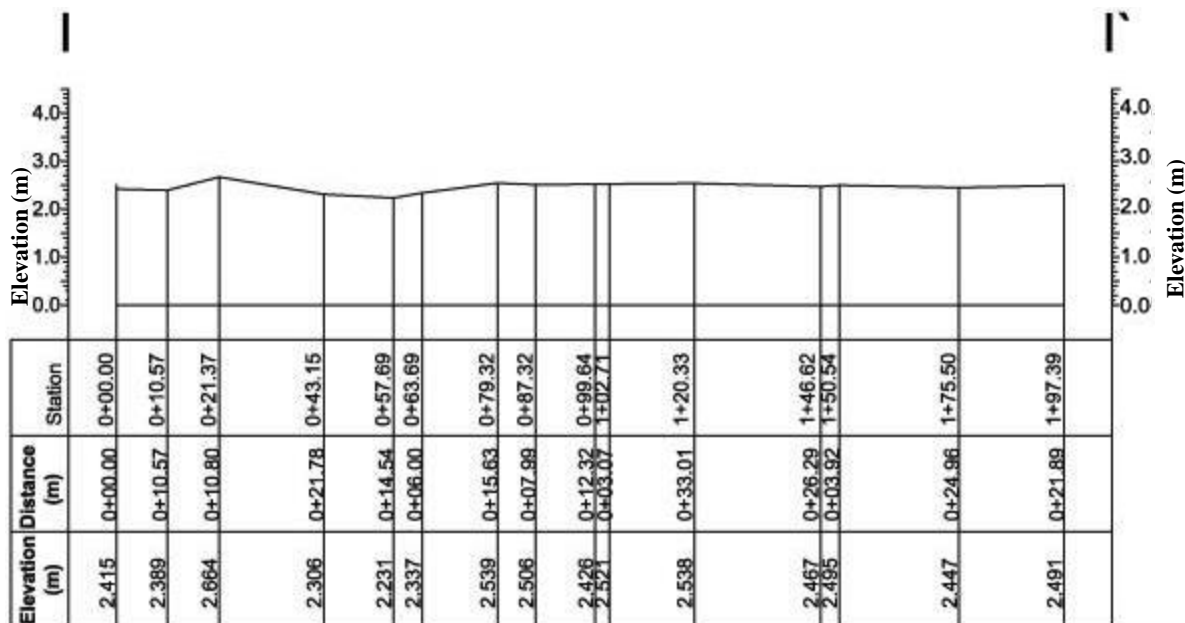


Figure 9.7. Cross Section I – I' with a vertical exaggeration of 10 times. Current Conditions. This cross section represents the area to build the hydraulic design.

9.2 CUT AND FILL

The calculation of cut and fill was prepared using AutoCAD. The area of cut or fill for each cross section was calculated directly by the software and the distance between profiles was measured directly from the cross sections lines (Figure 9.8). The tables of cut and fill results will be shown after each cross-section set.

On the result tables, station values referred to Figure 9.9 which value 0+00 starts in the first line (top) and increases down by 20 meters per line. Each cut and fill analysis will be considering two contiguous profiles.

The cross sections B (Figure 9.10) and D (Figure 9.12), includes the location of the piezometers structures. These piezometers contain a concrete base, which is part of the surface seal of the structure, and serve as datum of the pipe surface elevation. If some excavation is planned on this region, this area has to be protected and possible make a buffer zone to let some room for safety and do not damage these structures.

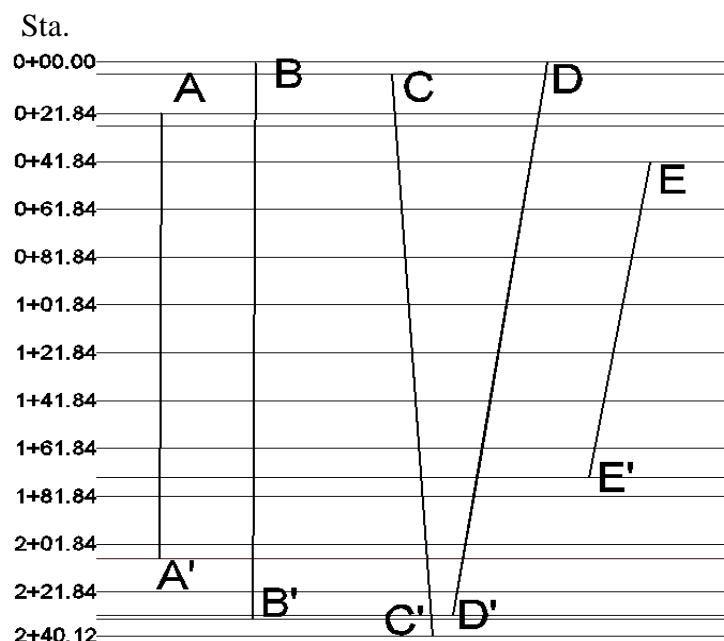


Figure 9.8. Cut and Fill calculation method. Location of stations and the cross sections lines presented in Figure 9.1.

Each of the profiles contains at the top a recommended area of the vegetative strip and a buffer zone. The vegetative filter is located after the channel spill zone and let the runoff move through this zone slowly. This slow movement will make the filter works and absorbed or eliminated most contaminants that bring the water flow. The recommended slope for this zone is 0.5 % and the length to the south of the vegetative filter is around 90 meter. The length is subject to change in the future depending on the type of plants and the substance that want to be removed from the flow. From the center of the study area to the east side, is the higher area elevation section, the slope of 0.5% is not enough to reach the actual slope. Those cross sections indicate that a recommended 0.8% slope until reach the surface slope.

After the vegetative filter, a buffer zone must be placed with other kind of vegetation or may be the same that is used for the filter. This will retard the movement of the water and decreases the amount of water that reaches the mangrove area.

Other recommendation is to use the actual vegetation as a filter instead of cleanup the vegetation. This action will promote the ecosystem that is developed in that area. In this case may clean only those areas where the slope from the proposed channel output is reaching level with the existing surface.

The cross section I-I' in Figure 9.14 is a demonstration of the cut and fill diagram of the channel area. This cross section shows the real elevation and depth of the channel along the surface from west to east.

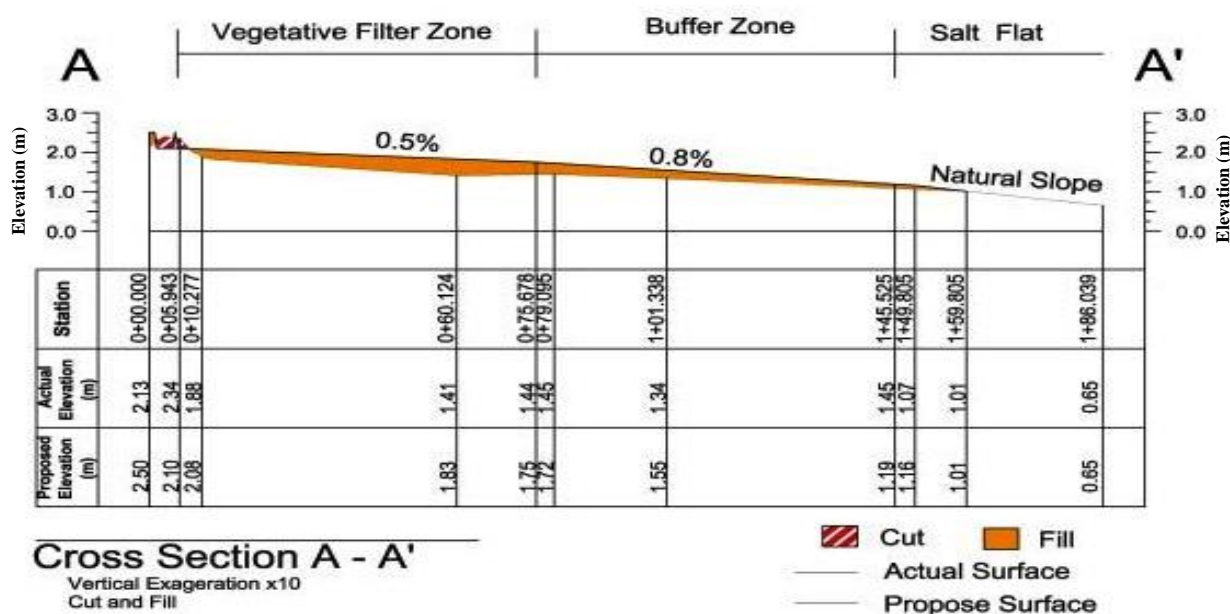


Figure 9.9. Cut and fill Section A-A'.

Table 9.1. Cut and Fill for Area Between Cross Section A-A` and B-B`.

Station	Horizontal Distance	Profile A-A`		Profile B-B`		Volume	
		Fill (m)	Cut (m)	Fill (m)	Cut (m)	Fill (m ³)	Cut (m ³)
0+21.84	34.41	0.37	0.00	0.00	0.03	0.00	0.00
0+26.86	34.38	0.00	0.24	0.00	0.45	0.00	29.62
0+41.84	34.29	0.02	0.00	0.14	0.00	20.56	0.00
0+61.84	34.29	0.09	0.00	0.17	0.00	44.70	0.00
0+81.84	34.34	0.16	0.00	0.21	0.00	63.89	0.00
1+01.84	34.39	0.02	0.00	0.18	0.00	34.57	0.00
1+21.84	34.44	0.00	0.00	0.12	0.00	19.99	0.00
1+41.84	34.48	0.00	0.00	0.08	0.00	13.53	0.00
1+61.84	34.53	0.00	0.00	0.05	0.00	8.37	0.00
1+73.84	34.52	0.00	0.00	0.01	0.00	1.25	0.00
Total Volume (m ³)=						206.85	29.62

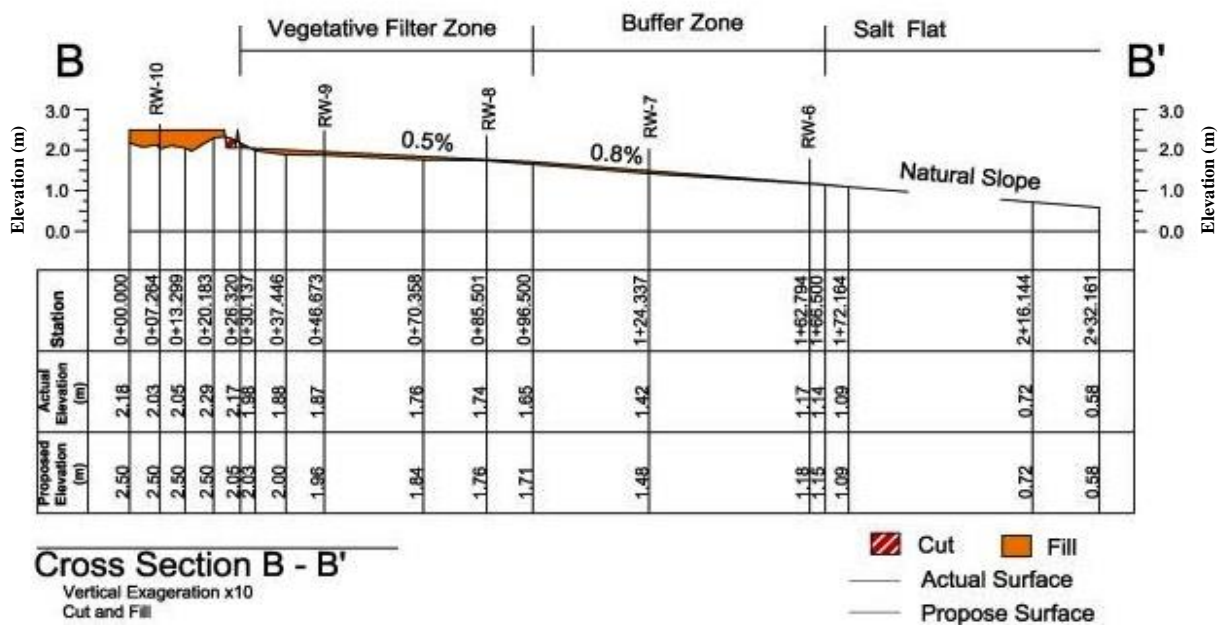


Figure 9.10. Cut and fill Section B-B`.

Table 9.2. Cut and Fill for Area Between Cross Section B-B` and C-C`.

Station	Horizontal Distance	B-B`		C-C`		Volume	
		Fill (m)	Cut (m)	Fill (m)	Cut (m)	Fill (m ³)	Cut (m ³)
0+05.13	50.23	0.07	0.00	0.00	0.08	0.00	0.00
0+21.84	51.45	0.00	0.03	0.00	0.21	0.00	50.51
0+26.86	51.82	0.00	0.45	0.00	0.10	0.00	35.40
0+41.84	52.91	0.14	0.00	0.16	0.00	58.95	0.00
0+61.84	54.26	0.17	0.00	0.20	0.00	99.58	0.00
0+81.84	55.55	0.21	0.00	0.26	0.00	129.24	0.00
1+01.84	56.84	0.18	0.00	0.16	0.00	96.35	0.00
1+21.84	58.14	0.12	0.00	0.15	0.00	75.17	0.00
1+41.84	59.43	0.08	0.00	0.04	0.00	34.01	0.00
1+61.84	60.73	0.05	0.00	0.00	0.00	14.57	0.00
1+73.84	61.54	0.01	0.00	0.00	0.00	2.22	0.00
1+81.84	62.09	0.00	0.00	0.00	0.00	0.00	0.00
2+01.84	63.46	0.00	0.00	0.00	0.00	0.00	0.00
2+07.70	63.68	0.00	0.00	0.00	0.00	0.00	0.00
2+21.84	64.84	0.00	0.00	0.00	0.00	0.00	0.00
2+31.72	65.52	0.00	0.00	0.00	0.00	0.00	0.00
2+33.24	65.62	0.00	0.00	0.00	0.00	0.00	0.00

Total Volume (m³)= 510.08 85.90

Table 9.3. Cut and Fill for Area Between Cross Section C-C` and D-D`

Station	Horizontal Distance	C-C`		D-D`		Volume	
		Fill (m)	Cut (m)	Fill (m)	Cut (m)	Fill (m ³)	Cut (m ³)
0+05.13	56.84	0.00	0.08	0.01	0.00	0.00	0.00
0+21.84	53.34	0.00	0.21	0.02	0.00	0.00	43.63
0+26.86	52.27	0.00	0.10	0.00	0.61	0.00	47.14
0+41.84	49.07	0.16	0.00	0.00	0.46	0.00	55.82
0+61.84	44.78	0.20	0.00	0.00	0.33	0.00	30.31
0+81.84	40.53	0.26	0.00	0.00	0.34	0.00	16.10
1+01.84	36.26	0.16	0.00	0.00	0.26	0.00	18.20
1+21.84	31.99	0.15	0.00	0.00	0.29	0.00	24.98
1+41.84	27.72	0.04	0.00	0.00	0.39	0.00	52.67
1+61.84	23.38	0.00	0.00	0.00	0.51	0.00	65.02
1+73.84	20.81	0.00	0.00	0.00	0.50	0.00	32.89
1+81.84	19.10	0.00	0.00	0.00	0.45	0.00	17.87
2+01.84	14.82	0.00	0.00	0.00	0.33	0.00	27.77
2+07.70	13.53	0.00	0.00	0.00	0.25	0.00	5.16
2+21.84	10.54	0.00	0.00	0.00	0.07	0.00	2.85
2+31.72	8.51	0.00	0.00	0.00	0.01	0.00	0.33

Total Volume (m³)= 0.00 440.74

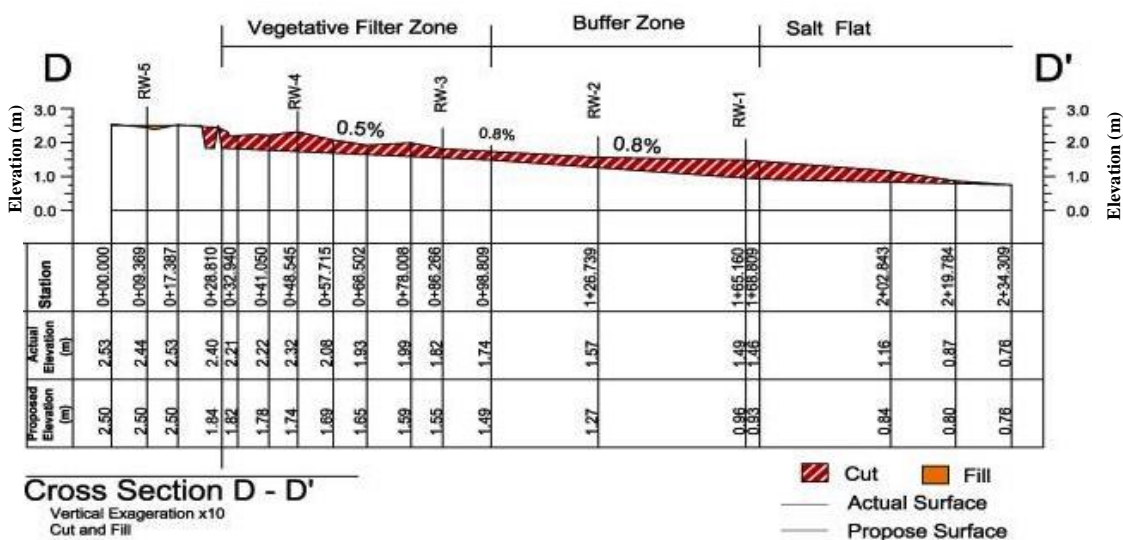


Figure 9.12. Cut and fill Section D-D`.

Table 9.4. Cut and Fill for Area Between Cross Section D-D` and E-E`

Station	Horizontal Distance	D-D'		E-E'		Volume	
		Fill (m)	Cut (m)	Fill (m)	Cut (m)	Fill (m ³)	Cut Volume (m ³)
0+41.84	43.97	0.00	0.46	0.25	0.00	0.00	0.00
0+61.84	43.63	0.00	0.33	0.21	0.00	0.00	26.04
0+81.84	43.18	0.00	0.34	0.33	0.00	0.00	1.82
1+01.84	42.75	0.00	0.26	0.40	0.00	31.26	0.00
1+21.84	42.32	0.00	0.29	0.29	0.00	0.00	0.17
1+41.84	41.89	0.00	0.39	0.11	0.00	0.00	58.86
1+61.84	41.46	0.00	0.51	0.00	0.20	0.00	148.03
1+73.84	41.21	0.00	0.50	0.00	0.47	0.00	119.94

Total Volume (m³)= 31.26 354.86

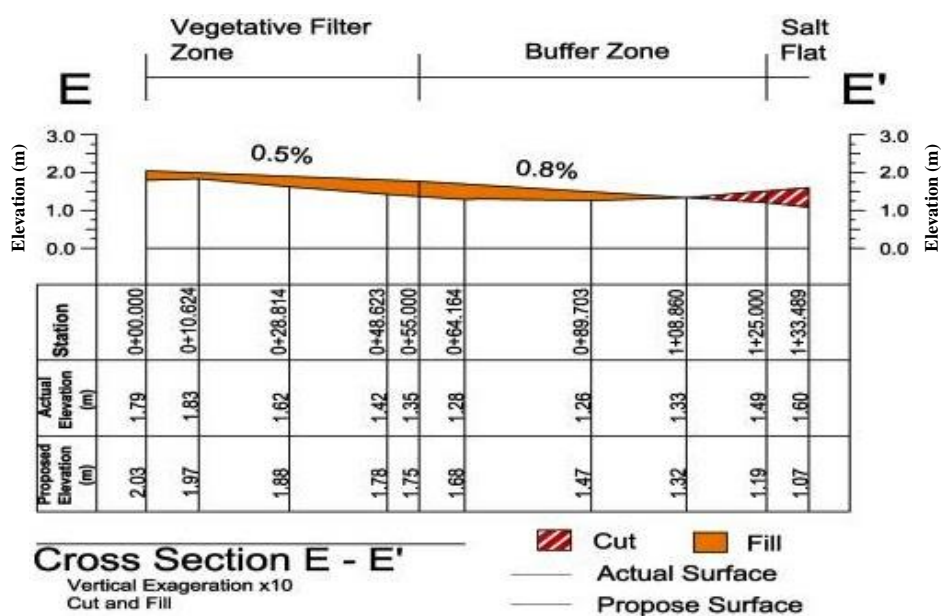


Figure 9.13. Cut and fill Section E-E`.

Table 9.5. Balance cut and fill material volumes.

Sections	Cut (m ³)	Fill (m ³)	Total (m ³)	Description
A-A' to B-B'	29.62	206.85	177.24	Fill
B-B' to C-C'	85.90	510.08	424.18	Fill
C-C' to D-D'	440.74	0.00	440.74	Cut
D-D' to E-E'	354.86	31.26	323.61	Cut

Remaining Volume (m³) = 162.93

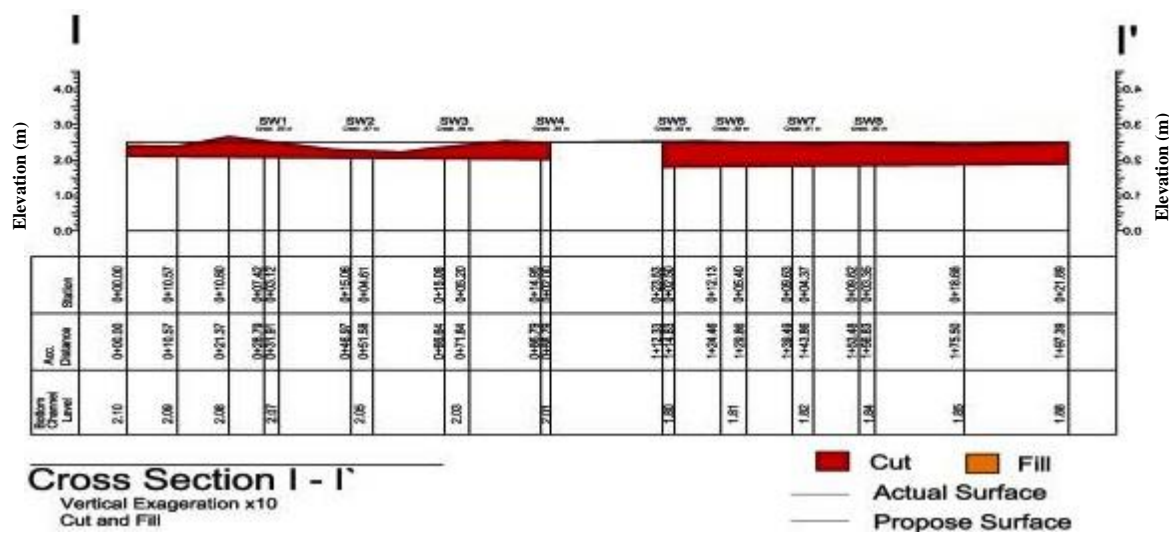


Figure 9.14. Cut and fill Section I-I'.

9.3 COST ESTIMATE

The cost estimate is an approximation of the cost of a project. On this case, the cost estimate is only related to the construction of the designed channel. Table 9.6 shows the cost estimate of the grouted riprap channel. The unit price of the grouted riprap is \$86.00 per cubic yard (Cy) and includes the labor and materials (RS Means, et al., 2004). This cost estimate does not include equipment, machinery or additional labor for the construction of the channel.

The walls cost computation was divided in the two individual channels (West; East) in which the volumes consider the length of the wall (0.72; 1.4m), the width (0.20 m, see Table 5.2) and the length of the channels (92m). The width of the bottom bed varies along the channel and that is why the table shows 4 divisions of the channel. The minimum toe or bed for the channel was 0.30 m (see Table 5.2) and this value was used to compute the area of the lining toe. Table 9.7 shows the same exercise but with reinforced concrete. This option was not used in the project, but for comparison purpose was included in this section. For reinforced concrete, the toe thicknesses as the walls are 0.15m. For volume computation this value was used in the equation.

The unit price for walls is \$650 yd³ and \$550 yd³ cubic for the toe. This value includes materials and labor for construction. The extended price for the reinforcement concrete resulted ten times higher than the riprap. The grouted lining has a cost of around \$19,000 and reinforces concrete \$80,000. Table 9.8 shows the complete conceptual cost estimate of the project. This table includes the operational cost of the machinery leasing (considering the wage of the machine operator and one helper), materials and labor necessary for the excavation process. The total cost of this part is around \$12,000 dollars for one working day. All this information about the machinery cost and labor were taken from the software National Estimator 32 Pro (Craftsman Book Company, 2013).

The total cost of the project is approximately \$45,600 including the material, labor, 35% of overhead and 15% of profit. This cost analysis does not include the transportation of the machinery or materials to the site area. The existing vegetation at the south boundary of the proposed channel, serves as a natural filter for overland flows. This natural filter could help to improve the water quality promoting infiltration before reaching the mangrove area. A new research is recommended to determine which species of plants can promote infiltration and adsorption of pollutants found in previous investigations. If the new project involves the replacement of vegetation, the existing vegetation should be cleared and a new grading should be designed to produce better runoff. To improve the slope of the area is necessary a process of cut and fill, as recommended in the previous section. This process can increase the total project cost to around \$ 60,000 (see Table 9.9).

Table 9.6. Grouted Riprap Lining Estimate Cost.

Description	Units	Unit Price	Quantity	Extended Price
Riprap D50 = 0.09 m Walls Grouted Riprap Lining Depth = 0.18 m				
West Channel Depth: 0.4 m	CY	\$ 86.00	22	\$ 1,892.00
East Channel Depth: 0.8 m	CY	\$ 86.00	40	\$ 3,440.00
Bed Grouted Riprap* Lining Depth = 0.30 m Bottom Width Sections:				
3 m	CY	\$ 86.00	106	\$ 9,116.00
1.5 m	CY	\$ 86.00	26	\$ 2,236.00
1.0 m	CY	\$ 86.00	16	\$ 1,376.00
0.5 m	CY	\$ 86.00	6	\$ 516.00
Side Weir Metal Plate and Accessories**		\$ 400.00	1	\$ 400.00

* Both channels considered

CY = Cubic Yards

Unit price includes labor and materials

**Accessories include anchorage, bolts and nuts.

Total \$ 18,976.00

Table 9.7. Reinforced Concrete Lining Cost Estimate. Channel wall and bed width is 0.15 m.

Description	Units	Unit Price	Quantity	Extended Price
Walls				
West Channel Depth: 0.4 m	CY	\$ 650.00	20	\$ 13,000.00
East Channel Depth: 0.8 m	CY	\$ 650.00	34	\$ 22,100.00
Bed * Bottom Width Sections:				
3 m	CY	\$ 550.00	54	\$ 29,700.00
1.5 m	CY	\$ 550.00	14	\$ 7,700.00
1.0 m	CY	\$ 550.00	8	\$ 4,400.00
0.5 m	CY	\$ 550.00	4	\$ 2,200.00
Side Weir Metal Plate and Accessories**		\$ 400.00	1	\$ 400.00

* Both channels considered

CY = Cubic Yards

Unit price includes labor and materials

**Accessories include anchorage, bolts and nuts.

Total \$ 79,500.00

BIBLIOGRAPHY

- 3001, Inc. (2007). *Islans, Orthophoto Production in Puerto Rico and Adjacent*. Peachtree City, GA: U.S. Army Corps Of Engineers.
- Akan, A. O. (2006). *Open Channel Hydraulics*. Burlington, MA: Butterworth-Hainemann.
- Anderson, A. G., Paintal, A. S., & Davenport, J. T. (1970). *Tentative Design Procedure For RipRap-Lined Channels*. National Cooperative Highway Research Program, Federal Highway Administration. Washington, D.C.: Federal Highway Administration.
- Bagchi, A. (2004). *Design of Landfills and Integrated Solid Waste Management*. Hoboken, NJ: John Wiley and Sons, Inc.
- Bedient, P. B., Huber, W. C., & Vieux, B. E. (2008). *Hydrology and Floodplain Analysis* (fourth Edition ed.). Upper Saddle River: Pearson, Prentice Hall.
- Blanckaert, K., & De Vriend, H. J. (2004). Secondary flow in sharp open-channel bends. *Journal of Fluid Mechanics*, 498, 353-380.
- Chaudry, H. M. (2008). *Open-Channel Flow* (Second Edition ed.). New York, NY: Springer Science+Business Media, LLC.
- Cherry, G. S. (2001). Simulation of Flow in the Upper North Coast Limestone Aquifer, Manatí-Vega Baja Area, Puerto Rico. San Juan, PR: USGS.
- CHI. (2011). *PCSWWM*. Retrieved 2011, from CHI: <http://www.chiwater.com/Software/PCSWMM.NET/index.asp>
- Chow, V. T. (1959). *Open-Channel Hydraulics*. Caldwell, NJ: McGraw Hill Book Company, Inc.
- City of EL Paso, Engineering Department. (2008). *Drainage Design Manual*. El Paso, TX: The City of el Paso.
- Craftsman Book Company. (2013, November 5). *2014 National Construction Estimator*. Retrieved Novermer 5, 2013, from Craftsman Book Company: <http://craftsman-book.com/>
- Demopoulos, A. W. (2004). Black Mangrove Benthic Community Structure , Seedling Groth and Survival, and Sediment Characteristics in Anthropogenically Disturbed and Pristine Habitats. Jobos Bay National Estuarine Research Reserve. Jobos Bay National Estuarine Research Reserve.
- Dieppa, A., Field, R., Laboy, E. N., Capella, J., Robles, P. O., & González, C. O. (2008). *Jobos Bay Estuarine Profile, A National Estuarine Research Reserve*. Aguirre: Jobos Bay NER.

- Eftekharzadeh, S. (1985). *Canal Side Weirs for Water Delivery to Irrigation Furrows*. Sierra Vista, Az.: The University of Arizona.
- Eijkelkamp Agrisearch Equipment. (1999). *Operating Instructions 09-04 Double Ring Infiltrometer Set*. Giesbeek, NL: Eijkelkamp Agrisearch Equipment.
- Emiroglu, M., Agaccioglu, H., & Kayaa, N. (2011, August). *Discharging capacity of rectangular side weirs in straight open channels* (Vol. 22). ELSEVIER.
- Engman, E. T. (1986). Roughness Coefficients for Routing Surface Runoff. *Journal of Irrigation and Drainage Engineering.*, 112, 39-53.
- Environmental Protection Agency. (2013, February 1). Storm Water Management Model (SWMM). Retrieved from <http://www.epa.gov/nrmrl/wswrd/wq/models/swmm/>
- Federal Highway Administration. (1988). *Open Channel Hydraulics*. Federal Highway Administration.
- Federal Highway Administration. (2012, 8 29). *Hydraulics Engineering*. (V. Ghelardi, Editor, & U.S. Department of Transportation) Retrieved 2 12, 2013, from Introduction to Highway Hydraulics - Chapter 4 - Open-Channel Flow: <http://www.fhwa.dot.gov/engineering/hydraulics/pubs/08090/04.cfm>
- French, R. H. (1987). *Open-Channel Hydraulics*. (J. Z. Margolies, Ed.) New York: MacGraw-Hill Book Co.
- Garber, N. J., & Hoel, L. A. (2002). *Traffic and Highway Engineering* (Third Edition ed.). Pacific Grove, CA: Brooks Cole.
- Garcia, M. H. (2007). *Sedimentation engineering: processes, measurements, modeling, and practice*. Reston, VA: American Society of Civil Engineers.
- Ghere, D. (2011). Design of Roadside Channels with Flexible Linings. In F. H. Administration, *Hydraulic Engineering Circular Number 15, Third Edition*. Federal Highway Administration.
- Glover, L. (1961). *Preliminary Geologic Map of the Salinas Quadrangle*. U.S. Geological Survey. U.S. Geological Survey.
- Gonzalez, C. M. (2010). *Jobos Bay National Estuarine Research Reserve Management Plan Final 2010-2015*. Puerto Rico Department of Natural and Environmental Resource. Aguirre, PR: Puerto Rico Department of Natural and Environmental Resource.
- Graves, R. P. (1992). *Geohydrology of the Aguirre and Pozo Hondo Areas, Southern Puerto Rico*. US Geological Survey. San Juan, P.R.: US Geological Survey.
- Gregory L. Morris & Associates. (2000). *Hydrologic-Hydraulic and Biological Analysis of Jobos Estuary Mangrove Mortality Jobos, Puerto Rico*. Santurce, P.R.: Puerto Rico Land Authority.

- Hager, W. H., & ASCE, M. (1986). Lateral Outflow Over Side Weirs. *113*. Journal of Hydraulic Engineering.
- Henderson, F. M. (1966). *Open Channel Flow*. New York, NY: Macmillan Publishing Comp., Inc.
- Ippen, A. T., & Drinker, P. A. (1961). *Boundary Shear Stresses in Curved Trapezoidal Channels*. Cambridge, MA: Massachusetts Institute of Technology.
- James, R., James, W., Finney, K., & Lee, M. (2012, January 12). Urban Drainage Modeling Workbook. *CHI Press R231*. Guelph, Ontario, Canada: Computational Hydraulics International.
- James, W., & James, R. C. (2000). Water System Models Hydrology, A guide to the Rain, Temperature and Runoff Models of the USEPA Swmm4. Canada: Computational Hydraulics International.
- James, W., Rossman, L. E., & James, W. C. (2011). *Water System Models, User`Guise to SWMM5* (13th Edition ed.). Ontario, Canada: Computational Hydraulics International.
- Ka-Leung, L., & Holley, E. (2002). *Physical Modeling For Side Channel Weirs*. The University of Texas at Austin, Harris Flood Control District, TX. Austin, TX.: Center for Research in Water Resources.
- Kuniansky, E. L., & Rodríguez, J. M. (2010). Effects of Changes in Irrigation Practices and Aquifer Development on Groundwater Discharge to the Jobos Bay National Estuarine Research Reserve near Salinas, Puerto Rico. U.S. Geological Survey.
- Maidment, D. R. (1992). *Handbook of Hydrology*. New York: McGraw-Hill Inc.
- May, R., Bromwich, B., Gasowski, Y., & Rickard, C. (2003). *Hydraulic Design of Side Wiers*. Reston, VA: Thomas Telford Publishing.
- Mays, L. W. (2005). *Water Resources Engineering* (2005 Edition ed.). Hoboken, NJ, NJ: Hamilton Printing Company.
- Miller, J. F. (1965). *Two- to Ten-Day Rainfall for Return Periods of 2 to 100 Years in Puerto Rico and Virgin Islands*. Weather Bureau, Department of Commerce. Washington D.C.: U.S. Government Printing Office.
- Mockus, V. (2004). Hydrologic Soil over Complexes. In N. R. Service, *Part 630, National Engineering Handbook*. Beltsville, MA: U. S. Departemn of Agriculture.
- Mohan Das, M., & Das Saikia, M. (2009). *Hydrology*. Connaught Circus, New Dejlhi: Asoke K. Ghosh, PHI Learning Limited.
- National Climatic Data Center (NCDC). (2010). *NOAA Satellite and Information Service*. Retrieved February 12, 2012, from www.ncdc.noaa.gov/oa/climate/stationlocator.html

National Estuarine Research Reserve System. (2012). 0.1. Retrieved January 7, 2012, from Centralize Data Management Office: <http://cdmo.baruch.sc.edu/get/gisapp.cfm?fileType=Shapefile>

National Oceanic and Atmospheric Administration (NOAA). (2010). *National Climate Data Center*. Retrieved January 2011, from Climate Data Online: <http://www.ncdc.noaa.gov/cdo-web/search>

National Weather Service Weather Forecast Office. (2009, April 29). *San Juan*. Retrieved January 17, 2012, from Puerto Rico Mean Annual Precipitation 1971-2000 : http://www.srh.noaa.gov/sju/?n=mean_annual_precipitation

Natural Resources Conservation Service. (2011, 11 20). *Custom Soil Resource Report for Humacao Area, Puerto Rico Eastern*. Retrieved from <http://websoilsurvey.nrcs.usda.gov/app/websoilsurvey.aspx>

Natural Resources Conservation Service Caribbean Area. (2012, August 7). Saltflat Vegetation for Soil and Wildlife Conservation Associated with Coastal Tidal Flats. (*Cooperative Agreement # 68-F352-09-02*). NRCS Fact Sheet.

NOAA, Atlas 14. (2012, 12 3). *Point Precipitation Frequency Estimates*, Volume 3, Version 4 . (N. N. Services, Producer) Retrieved 03 26, 2013, from Hydrometeorological Design Study Center: http://hdsc.nws.noaa.gov/hdsc/pfds/pfds_printpage.html?lat=17.9529&lon=-66.2461&data=depth&units=english&series=pds

NRCS. (1986). *Urban Hydrology for Small watersheds (TR-55)*. Natural Resources Conservation Service, U. S. Department of Agriculture. NRCS.

NRCS. (2009). Salinas Forage Farm Location; Puerto Rico, USA. (p. 41). Natural Resources Conservation Service.

Ormsby, T., Napoleon, E., Burke, R., Groessl, C., & Bowden, L. (2009). *Getting to Know ArcGIS Desktop*. New York: ESRI Press.

Quiñones-Aponte, V., Gómez-Gómez, F., & Renken, R. A. (1996). *Geohydrology and Simulation of Ground_Water Flow in the Salinas to Patillas Area, Puerto Rico*. U.S. Geological Survey, NOAA Technical Memorandum NOSNCCOS 76. San Juan, P.R.: U.S. Geological Survey.

Rawis, W. J., Ahuja, L. R., Brakensiek, D. L., & Shirmohammadi, A. (1992). Infiltration and Soil Water Movement. In D. R. Maidment, *Handbook of Hydrology* (pp. 5.0-5.46). New York, New York, U.S.: MacGraw-Hill, Inc.

Renken, R. A., Ward, W., Gill, I., Gómez-Gómez, F., & Rodríguez-Martínez, J. (2002). *Geology and Hydrogeology of the Caribbean Islands Aquifer System of the Commonwealth of Puerto Rico and the U.S. Virgin Islands*. Reston, Virginia: U.S. Department of the Interior, U.S. Geological Survey.

- Rodríguez, J. M. (2006). Evaluation of Hydrologic Conditions and Nitrate Concentrations in the Río Nigua de Salinas Alluvial Fan Aquifer, Salinas, Puerto Rico, 2002-03. U.S. Geological Survey. Reston, VA: U.S. Geological Survey.
- Roman Guzman, I. M. (2010). Estudio Comparativo Entre el Perfil Bacteriano de Sedimento de Mangle en la Ciénaga Cucharillas y Bahía de Jobos por Medio de la Técnica "Terminal Restriction Fragment Length Polymorphism" (T-RFLP). San Juan: Universidad Metropolitana.
- Rosier, B. (2007). *Interaction of Side Weir Overflow With Bed-load Transport and Bed Morphology in a Channel*. Karlsruhe University, Civil Engineering. Switzerland: Ecole Polytechnique, Federale de Lausanne.
- Rosier, B., Boillat, J.-L., & J. Schleiss, A. (2008). Outflow angle for side weirs in a channel. (pp. 199-208). INTERPRAEVENT 2008 – Conference Proceedings, Vol. 1.
- Rossman, L. A. (2010, July). Storm Water Management Model User's Manual version 5.0. Cincinnati, Ohio, U.S.: Water Supply and Water Resources Division.
- Rowlings, D. S. (2010). *An Experimental and Theoretical Investigation of Side Weirs*. University of Southern Queensland.
- RS Means, Barbara Balboni, Robert A. Bastoni. (2004). *Building Construction Cost Data 2005* (63 ed.). Portland, OR: RS Means.
- Soil Conservation Service. (2013, 2 15). *Web Soil Survey*. Retrieved 10 25, 2013, from USDA, Natural Resources Conservation Service: <http://websoilsurvey.nrcs.usda.gov/app/WebSoilSurvey.aspx>
- Sturm, T. W. (2011). *Open Channel Hydraulics* (Second ed.). New York, New York, U.S.: McGraw-Hill Companies Inc.
- Thompson, P. L., & Kilgore, R. T. (2006). *Hydraulic Design of Energy Dissipators for Culverts and Channels*. Federal Highway Administration, U.S. Department of Transportation. Federal Highway Administration.
- Thornton, C. I., & Ursic, M. E. (2011). Quantification of Shear Stress in a Meandering Native Topographic Channel Using a Physical Hydraulic Model. Fort Collins, Colorado: Colorado State University.
- Torres-Gonzales, S., Planert, M., & Rodriguez, J. M. (1996). Hydrogeology and Simulation of Ground-Water Flow in the Upper Aquifer of the Rio Camuy to Rio Grande de Manati Area, Puerto Rico . San Juan, PR: USGS.
- U.S. Army Corps of Engineers (USACE). (1994). Hydraulic Design of Flood Control Channels," Engineering and Design Manual.
- U.S. Department of Agriculture (USDA). (2004). *Orthophoto Mosaic for Puerto Rico*. Fort Worth, TX: USDA, Natural Resources Conservation Service.

U.S. Geological Survey (USGS). (2006). *National Elevation Dataset*. Retrieved December 2011, from EROS data Center: <http://gisdata.usgs.net/ned/>

Veve, T. D., & Taggart, B. E. (1996). *Atlas of Ground Water Resources in Puerto Rico and the U. S. Virgin Islands*. U.S. Geological Survey. San Juan, P.R.: U.S. Geological Survey.

Vidiani.com Maps of the World. (2011). *Large detailed relief map of Puerto Rico*. Retrieved February 15, 2012, from <http://www.vidiani.com/?p=6290>

WEF and ASCE. (1992). *Design and construction of Urban Stormwater Management System*. Water Environment Federation (WEF) and American Society of Civil Engineers (ASCE).

Whitall, D. R., Costa, B. M., Bauer, L. J., Dieppa, A., & Hile, S. D. (2011). *A Baseline Assessment of the Ecological Resources of Jobos Bay, Puerto Rico*. National Oceanic and Atmospheric Administration, U.S. Department of Commerce. Silver Spring, MD: National Oceanic and Atmospheric Administration.

Williams, C. O., Lowrance, R., Bosch, D. D., Williams, J. R., Benham, E., Dieppa, A., et al. (2012, September 28). Hydrology and Water Quality of a Field and Riparian Buffer Adjacent to a Mangrove Wetland in Jobos Bay Watershed, Puerto Rico. *Ecological Engineering*(ECOENG-2313;), 9.

Zitello, A. G., Whitall, D. R., Dieppa, A., Christensen, J. D., Monaco, M. E., & Rohman, S. O. (2008). *Characterizing Jobos Bay, Puerto Rico: A Watershed Modeling Analysis and Monitoring Plan*. National Oceanic and Atmospheric Administration, U.S. Department of Agriculture. Silver Spring, MD: National Oceanic and Atmospheric Administration.

APPENDIX

Appendix A Curve Number Tables

Table A.1. Curve Number For hydrologic soil groups (NRCS, 1986).

Cover description			Curve numbers for hydrologic soil group			
Cover type	Treatment ^{2/}	Hydrologic condition ^{3/}	A	B	C	D
Fallow	Bare soil	—	77	86	91	94
	Crop residue cover (CR)	Poor	76	85	90	93
		Good	74	83	88	90
Row crops	Straight row (SR)	Poor	72	81	88	91
		Good	67	78	85	89
	SR + CR	Poor	71	80	87	90
		Good	64	75	82	85
	Contoured (C)	Poor	70	79	84	88
		Good	65	75	82	86
	C + CR	Poor	69	78	83	87
		Good	64	74	81	85
	Contoured & terraced (C&T)	Poor	66	74	80	82
		Good	62	71	78	81
C&T+ CR	Poor	65	73	79	81	
	Good	61	70	77	80	
Small grain	SR	Poor	65	76	84	88
		Good	63	75	83	87
	SR + CR	Poor	64	75	83	86
		Good	60	72	80	84
	C	Poor	63	74	82	85
		Good	61	73	81	84
	C + CR	Poor	62	73	81	84
		Good	60	72	80	83
	C&T	Poor	61	72	79	82
		Good	59	70	78	81
C&T+ CR	Poor	60	71	78	81	
	Good	58	69	77	80	
Close-seeded or broadcast legumes or rotation meadow	SR	Poor	66	77	85	89
		Good	58	72	81	85
	C	Poor	64	75	83	85
		Good	55	69	78	83
	C&T	Poor	63	73	80	83
Good	51	67	76	80		

¹ Average runoff condition, and $I_a=0.2S$

² Crop residue cover applies only if residue is on at least 5% of the surface throughout the year.

³ Hydraulic condition is based on combination factors that affect infiltration and runoff, including (a) density and canopy of vegetative areas, (b) amount of year-round cover, (c) amount of grass or close-seeded legumes, (d) percent of residue cover on the land surface (good $\geq 20\%$), and (e) degree of surface roughness.

Appendix B Maximum 24-hr Rainfall for each year of analysis period.

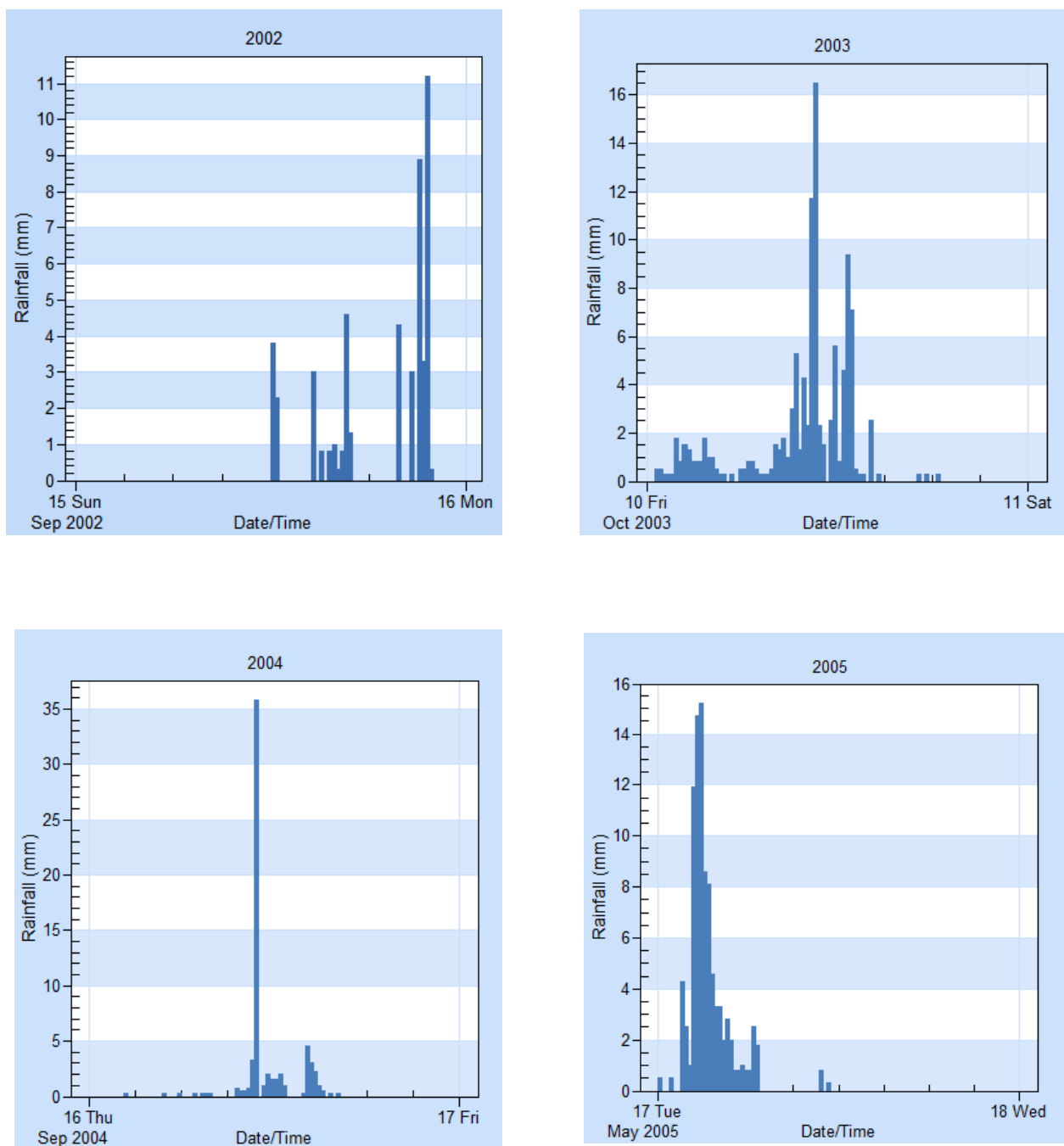


Figure B.1. Historical Rainfall Events (Hyetographs) from 2002 to 2005.

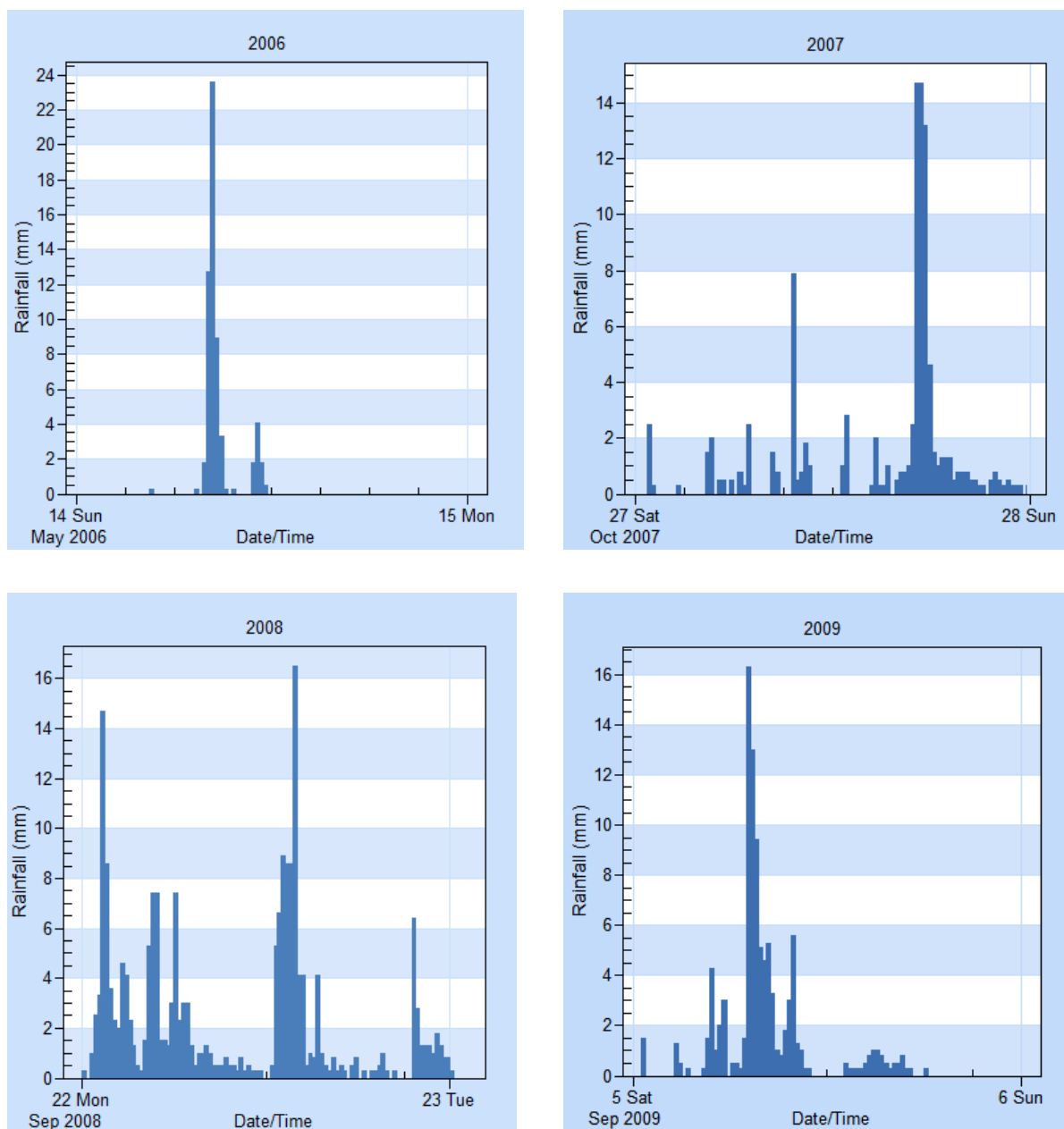


Figure B.2. Historical Rainfall Events (Hyetographs) from 2006 to 2009.

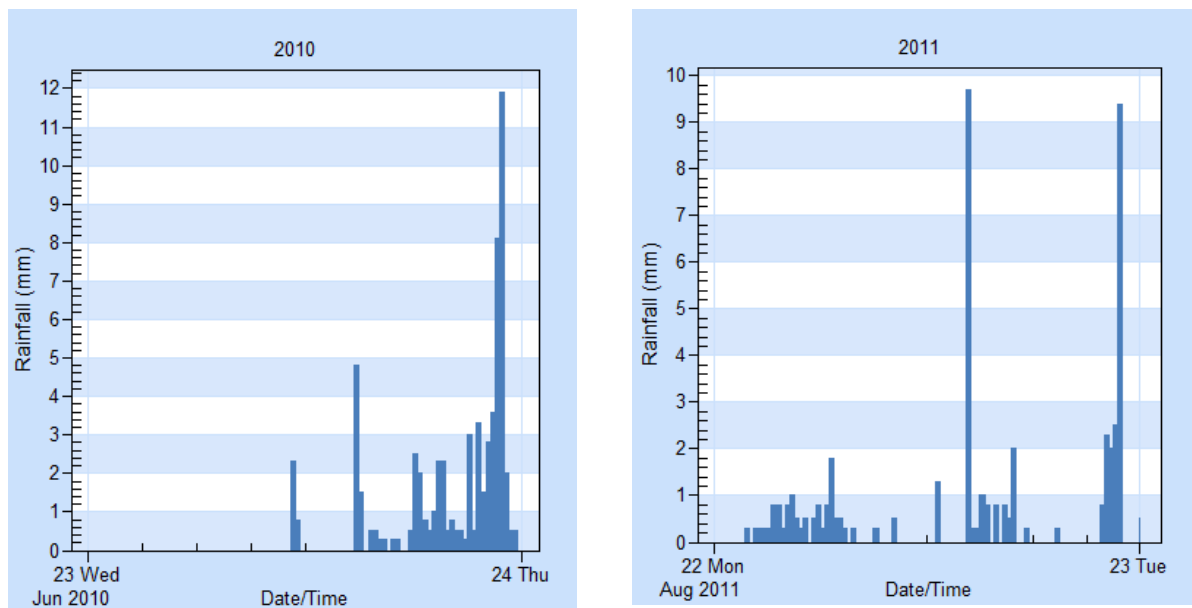


Figure B.3. Historical Rainfall Events (Hyetographs) from 2006 to 2009.

Appendix C Complete Storm Events Hyetographs

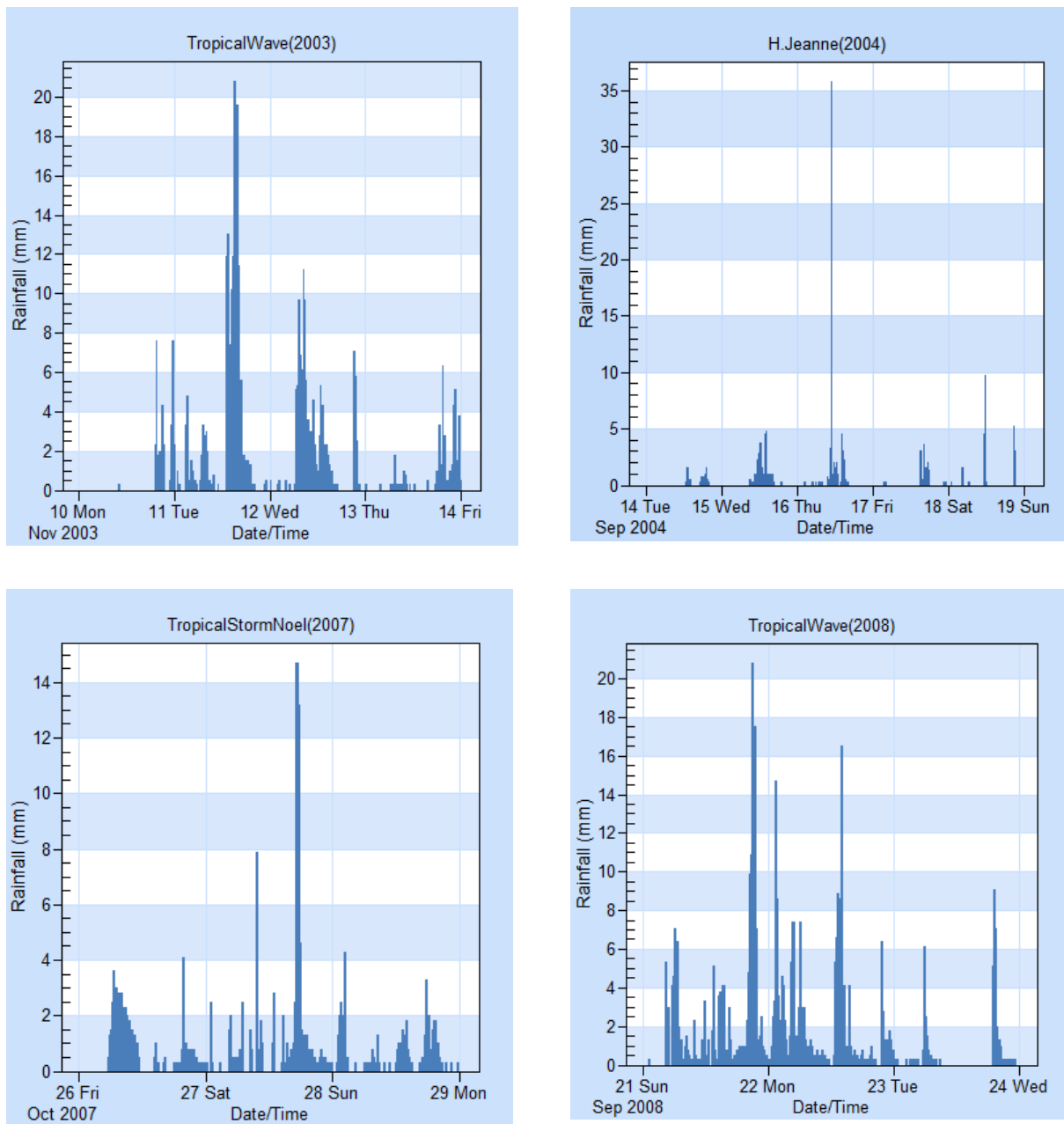


Figure C.1. Complete Storm Events (Hyetographs) from 2002 to 2004 and 2007 to 2008.

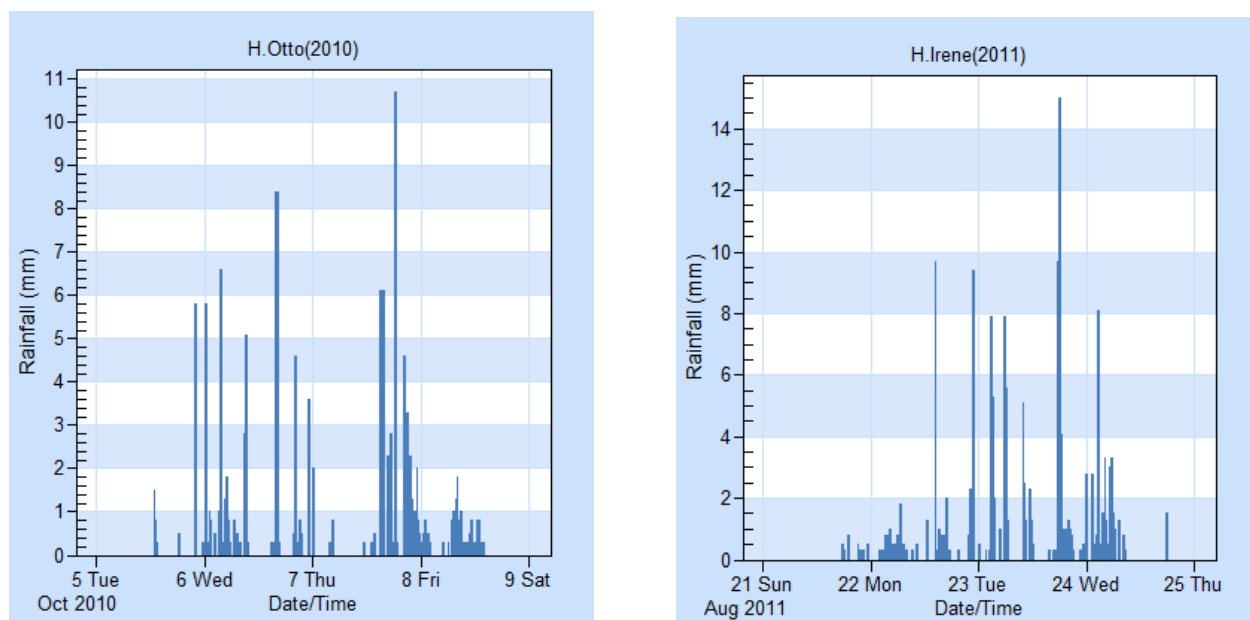


Figure C.2. Complete Storm Events (Hyetographs) from 2010 to 2011.

Appendix D Depth-Duration–Frequency Curves for Guayama, Puerto Rico

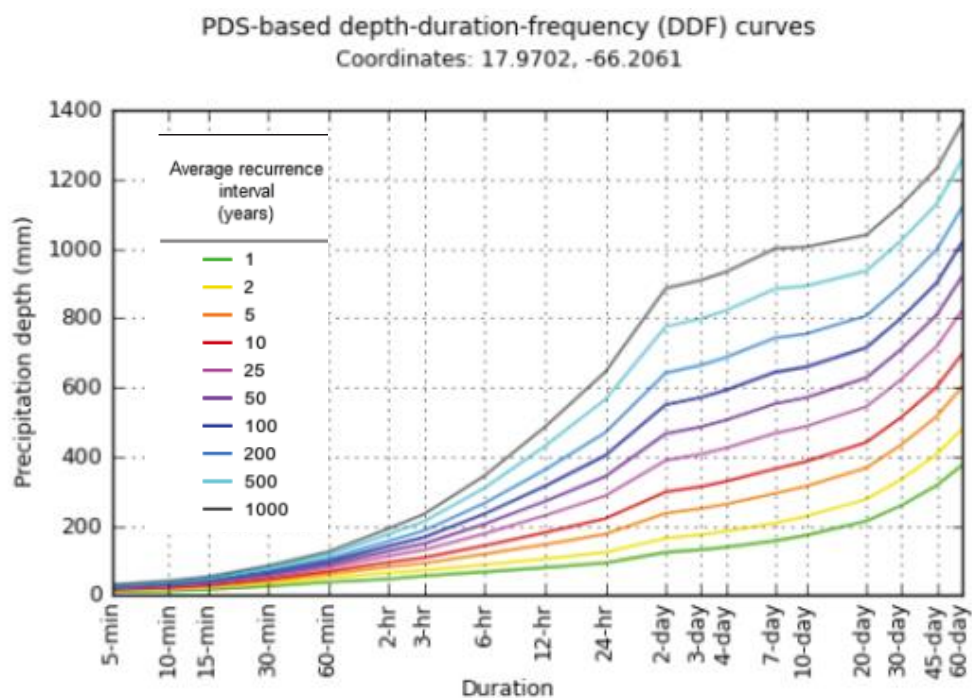


Figure D.1. PDS- Depth-duration-frequencies for Guayama’s Area (NOAA, Atlas 14, 2012).

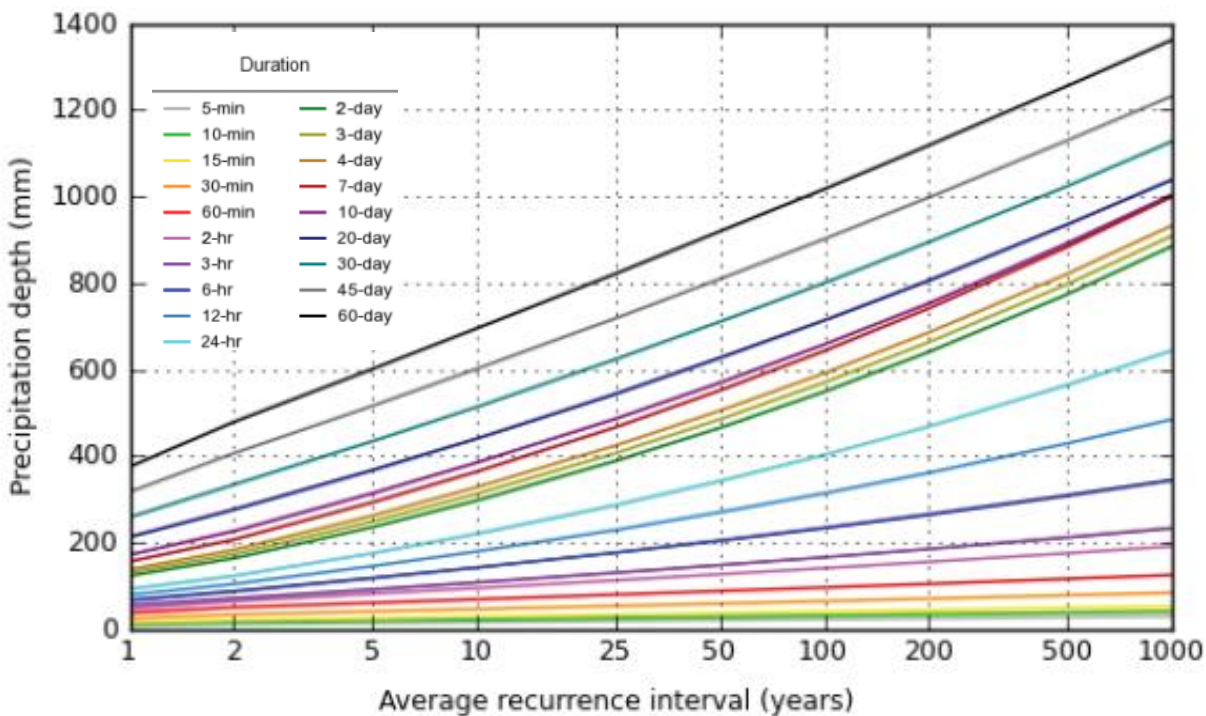


Figure D.2. PDS-Precipitation depth - Recurrence Curve (NOAA, Atlas 14, 2012).

Appendix E Riprap freeboard chart

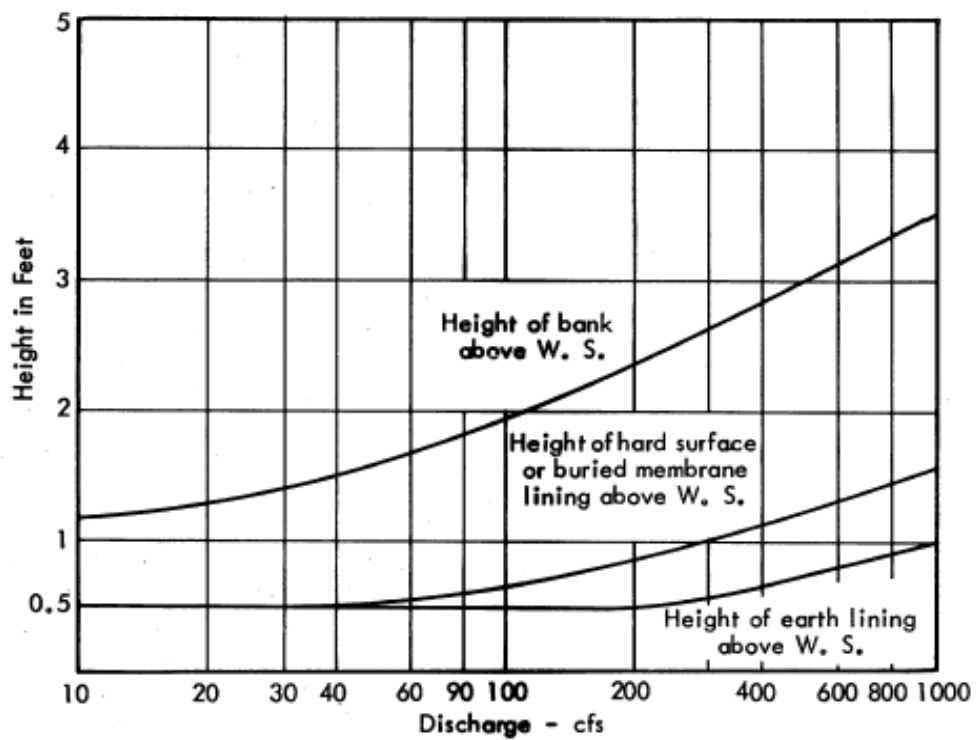


Figure E.1. Freeboard chart. Height of bank above water surface (Anderson, Paintal, & Davenport, 1970).

Appendix F Spillflow Coefficient Charts for side weirs

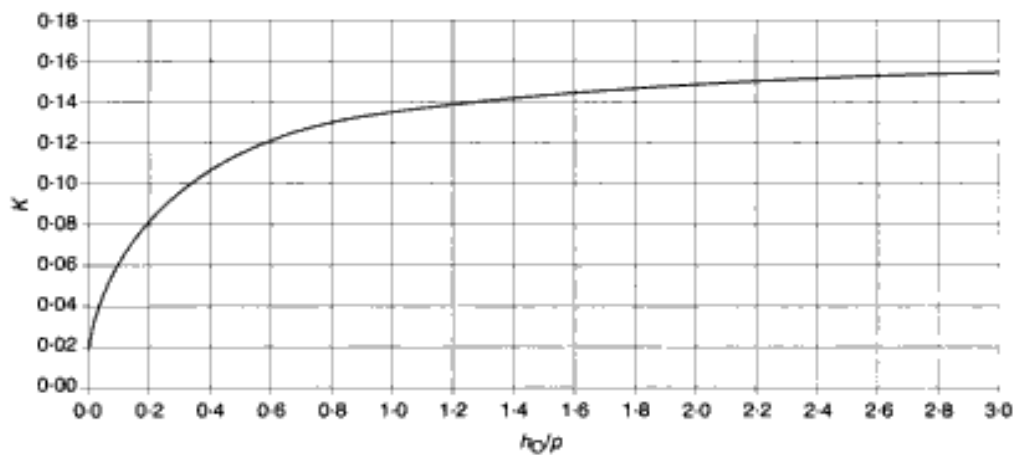


Figure F.1. Chart of J coefficient. Source (May, Bromwich, Gasowski and Rickard, 2003)

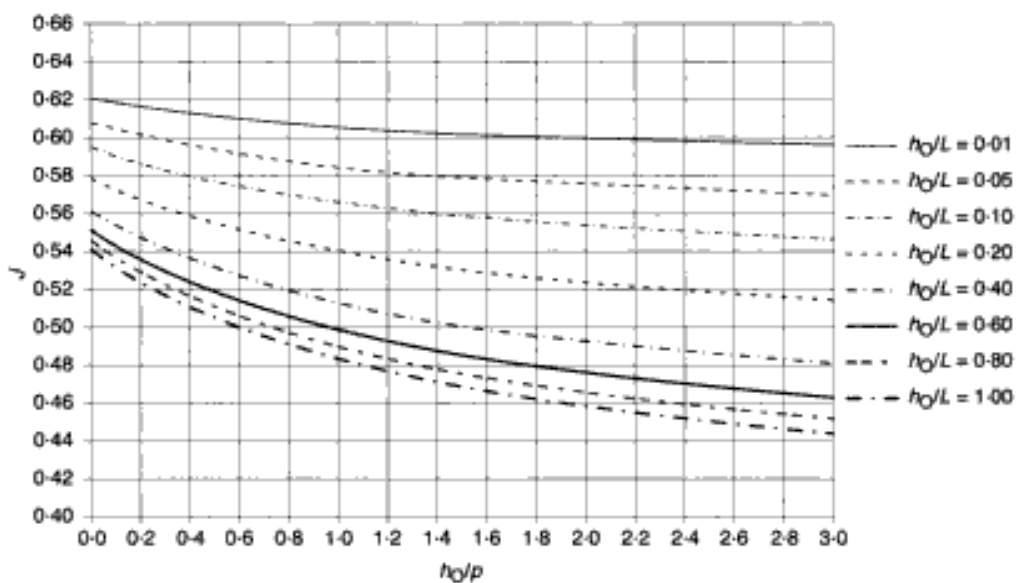


Figure F.2. Chart of K coefficient. Source (May, Bromwich, Gasowski and Rickard, 2003)

Appendix G Euler improved method for side weir water profile – Excel VBA

Option Explicit
Sub ImprovedEuler2()

'Other variables:

,

'B = Channel Bottom Widht

'S= Channel Lateral Slope

'S0 = Channel Longitudina Slope

'MN = Channel Mannings Coef

'Q = Main Channel Discharge

'YD = Downstream Depht

'qweir = Weir Disch. per unit length

'N = Number of reaches for compilation

'L = Weir Length:

'G = Accel of Gravity

'Alpha = Kinetic Energy Coef

'A = Area

'R = Hydraulic radius

'Sf = Friction slope

Dim X(100) As Single, YY(100) As Single, Y As Single, B0 As Single, S As Single

Dim SO As Single, MN As Single, Q As Single, YD As Single, qweir As Single, N As Integer

Dim L As Single, G As Single, Alpha As Single, Cman As Single, DX As Single

Dim A As Single, P As Single, R As Single, I As Integer, SF1 As Single, Sf2 As Single

Dim B As Single, Num1 As Single, Num2 As Single, Den1 As Single, Den2 As Single

Dim DY1 As Single, DY2 As Single, Y2 As Single

With Worksheets("WDesign").Range("J30")

Range(.Offset(1, 0), .End(xlDown).End(xlToRight)).ClearContents

End With

`Variable calls from excel

B0 = Range("I17")

S = Range("I18")

SO = Range("I19")

MN = Range("I20")

Q = Range("I21")

YD = Range("I22")

qweir = Range("I23")

N = Range("I24")

L = Range("I25")

G = Range("I26")

```

'Computations
Alpha = Range("I27")
Cman = 1
Worksheets("WDesign").Range("H31") = "Problem in International Units"
If G > 12 Then
Cman = 1.49
Worksheets("WDesign").Range("H31") = "Problem in English Units"
End If
Y = YD
DX = -L / N
For I = 1 To N
A = Y * (B0 + S * Y)
P = B0 + 2 * Y * Sqr(1 + S * S)
R = A / P
If I = 1 Then
Worksheets("WDesign").Range("I31").Offset(0, 1) = 0 'offset produce un movimiento hacia la
izquierda en cada iteracion
Worksheets("WDesign").Range("I31").Offset(0, 2) = Y
Worksheets("WDesign").Range("I31").Offset(0, 3) = Q
Worksheets("WDesign").Range("I31").Offset(0, 4) = qweir * Abs(X(I))
Worksheets("WDesign").Range("I31").Offset(0, 5) = Y * (B0 + S * Y)
Worksheets("WDesign").Range("I31").Offset(0, 6) = B0 + 2 * Y * Sqr(1 + S * S)
Worksheets("WDesign").Range("I31").Offset(0, 7) = (Y * (B0 + S * Y)) / (B0 + 2 * Y * Sqr(1 +
S * S))
End If
' Downstream
SF1 = (MN * Q) ^ 2 / (A * A * R ^ (4 / 3) * Cman ^ 2) ' Friction loss downstream
B = B0 + 2 * S * Y
Num1 = SO - SF1 - (Alpha * qweir * Q) / (G * A ^ 2) ' numerator of the Gradually Varied flow
equation
Den1 = 1 - ((B * Q * Q * Alpha) / (G * A ^ 3)) ' denominator of the Gradually Varied flow
equation
DY1 = Num1 / Den1 ' Gradually Varied Flow equation

'upstream
Y2 = Y + DY1 * DX ' Change in Depth - moving upstream
A = Y2 * (B0 + S * Y2) ' Area Upstream
P = B0 + 2 * Y2 * Sqr(1 + S * S)
R = A / P
Q = Q + qweir * Abs(DX) ' qweir is negative because is the substration of water (weir) from the
system
Sf2 = (MN * Q) ^ 2 / (A * A * R ^ (4 / 3) * Cman ^ 2) ' Friction loss upstream
B = B0 + 2 * S * Y2
Num2 = SO - Sf2 - (Alpha * qweir * Q) / (G * A ^ 2) 'dividend of the Gradually Varied Flow
equation
Den2 = 1 - (B * Q * Q * Alpha) / (G * A ^ 3) ' dividend of the Gradually Varied Flow equation

```

$$DY2 = \text{Num2} / \text{Den2}$$

$$Y = Y + 0.5 * (DY1 + DY2) * DX$$

$$X(I) = I * DX$$

$$YY(I) = Y$$

Worksheets("WDesign").Range("I31").Offset(I, 1) = X(I)

Worksheets("WDesign").Range("I31").Offset(I, 2) = YY(I)

Worksheets("WDesign").Range("I31").Offset(I, 3) = Q

Worksheets("WDesign").Range("I31").Offset(I, 4) = qweir * Abs(X(I))

Worksheets("WDesign").Range("I31").Offset(I, 5) = YY(I) * (B0 + S * YY(I))

Worksheets("WDesign").Range("I31").Offset(I, 6) = B0 + 2 * YY(I) * Sqr(1 + S * S)

Worksheets("WDesign").Range("I31").Offset(I, 7) = (YY(I) * (B0 + S * YY(I))) / (B0 + 2 * YY(I) * Sqr(1 + S * S))

Next I

End Sub

Appendix H Synthetic rain 1yr-24hr

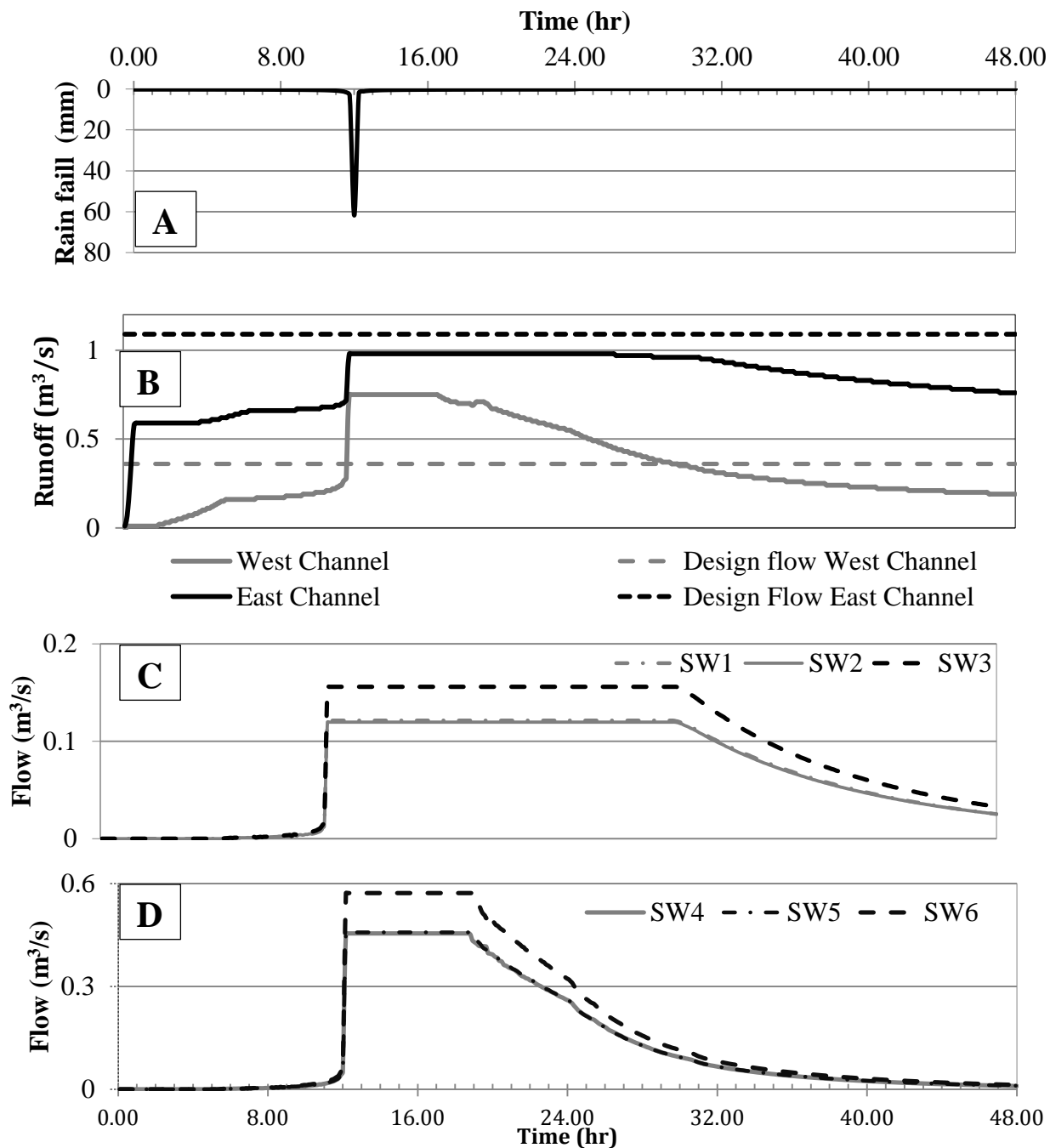


Figure H.1. A: Synthetic rainfall. 1yr-24hr. B: Amount of runoff that reaches the beginning of both channels C: East Channel. side weirs operation. D: West Channel side weirs operation.

Appendix I Synthetic rains

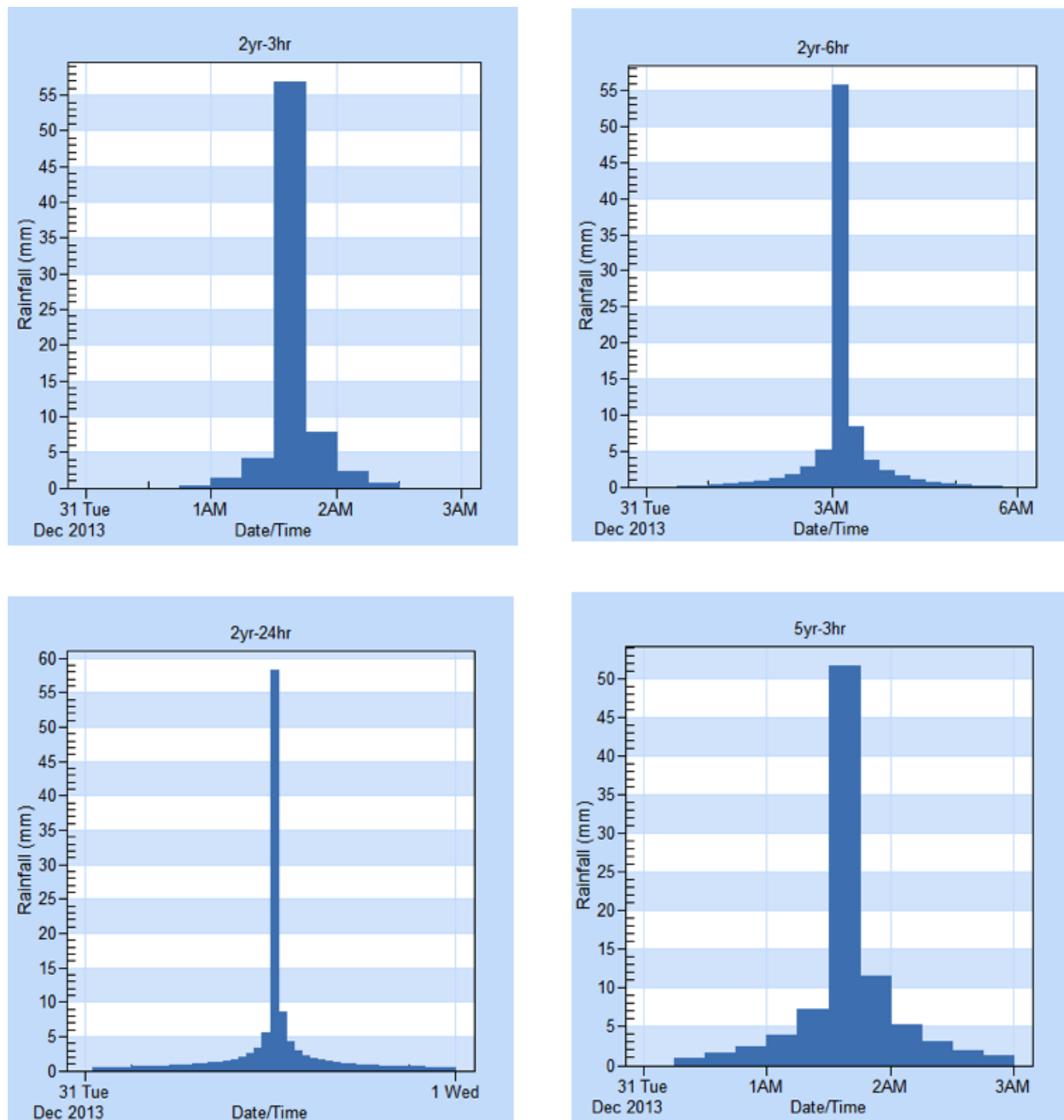


Figure I.1. Synthetic Storms (Hyetographs).

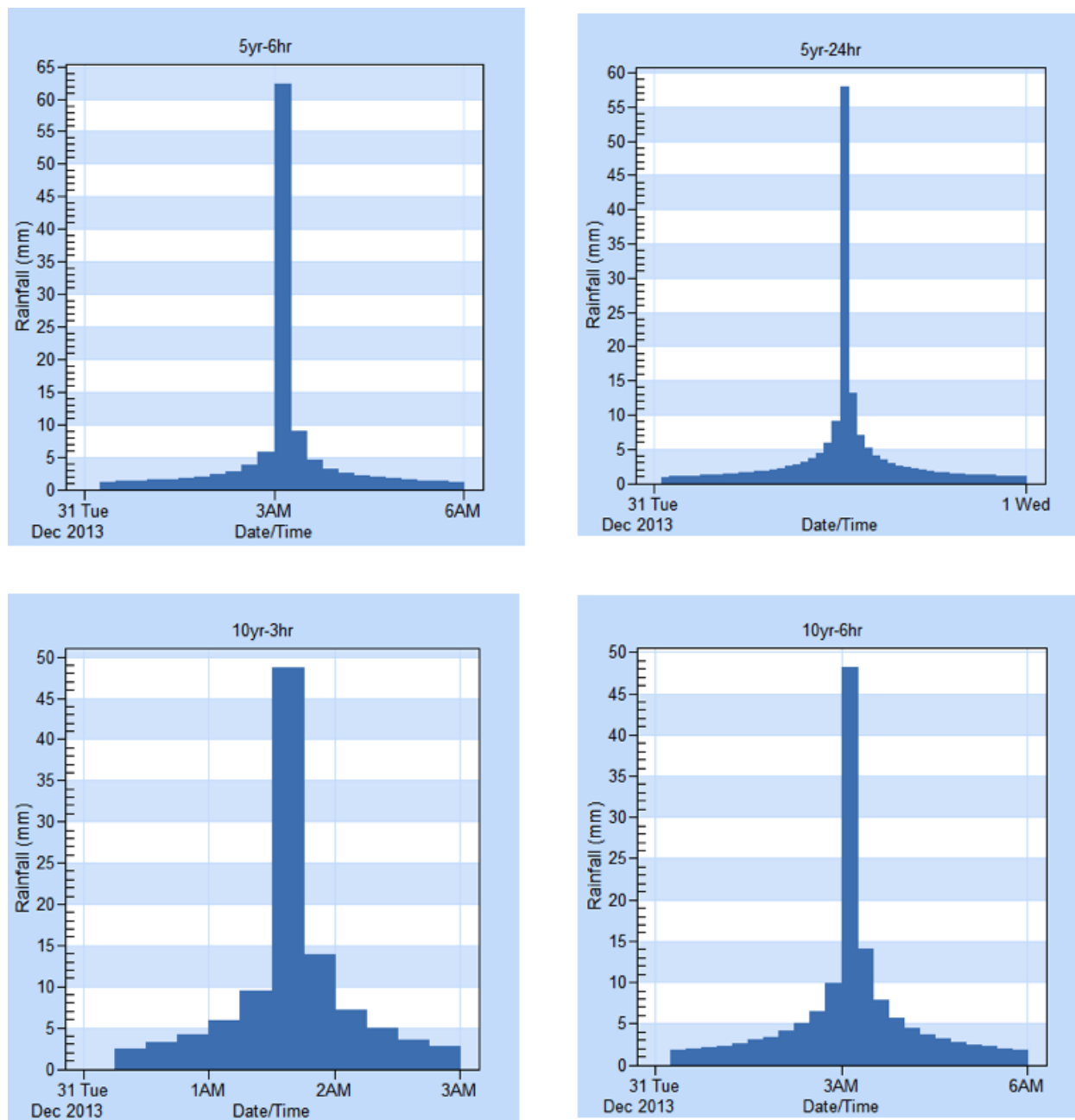


Figure I.2. Synthetic Storms (Hyetographs).

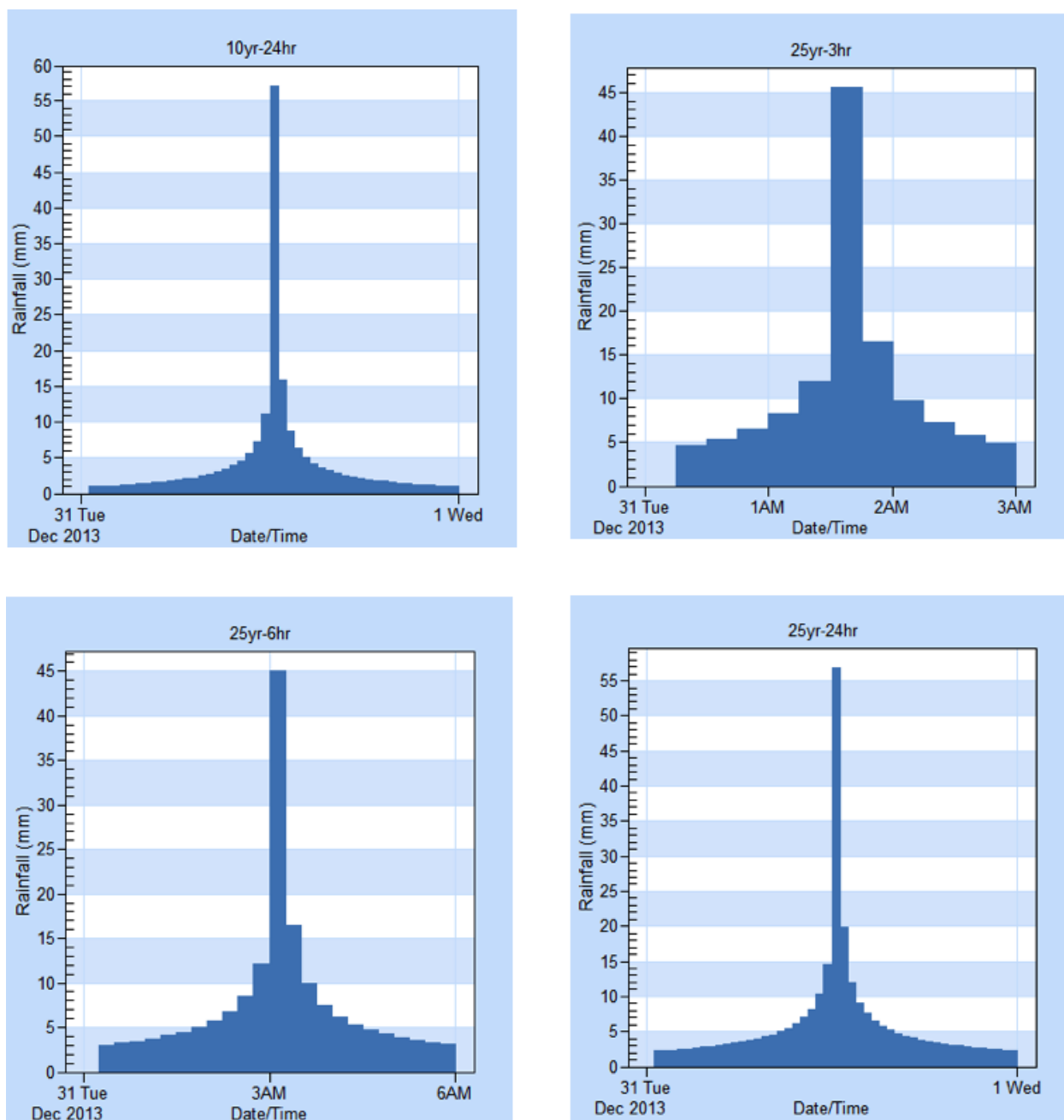


Figure I.3. Synthetic Storm (Hyetographs).

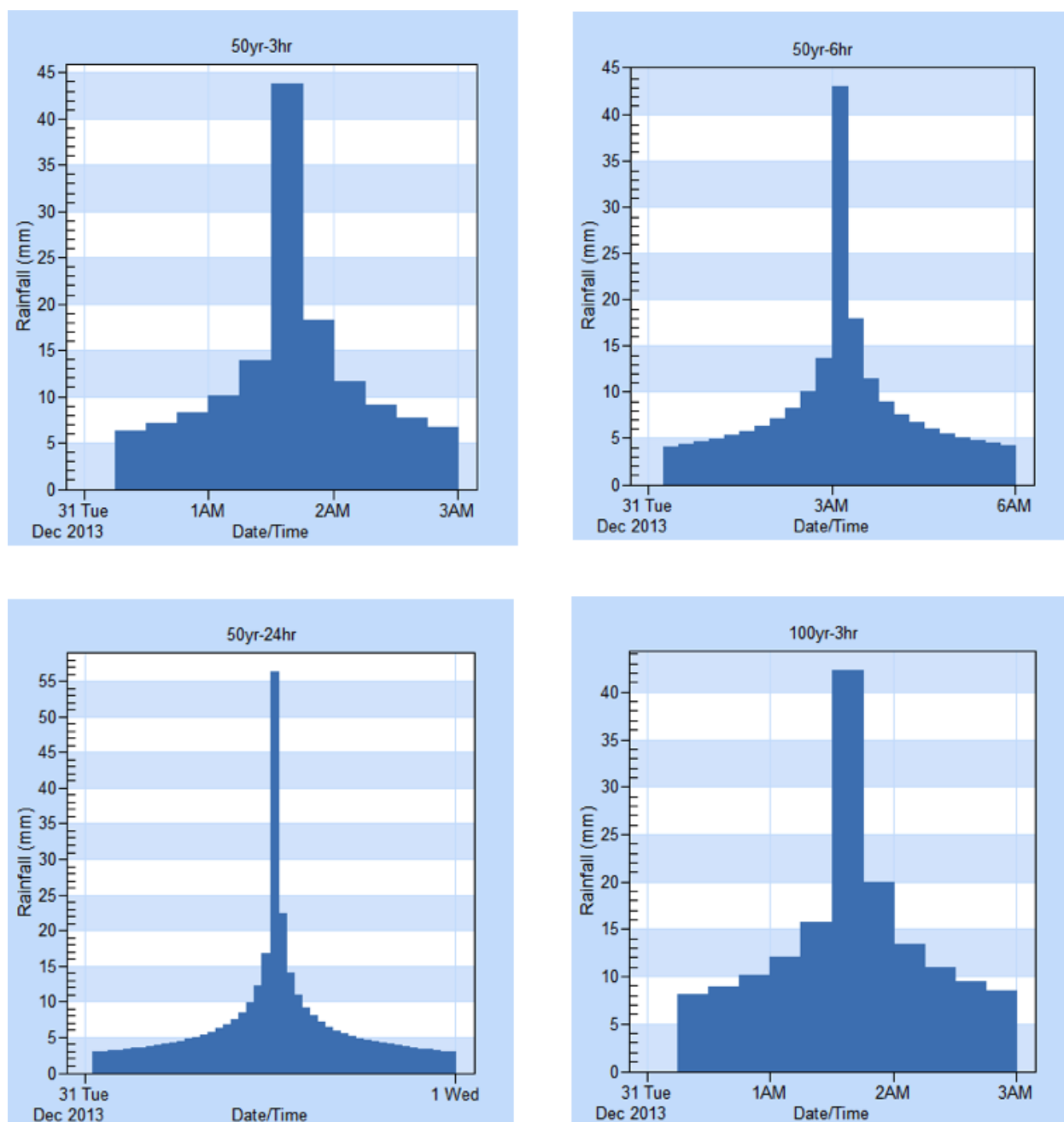


Figure I.4. Synthetic Storm (Hyetographs).

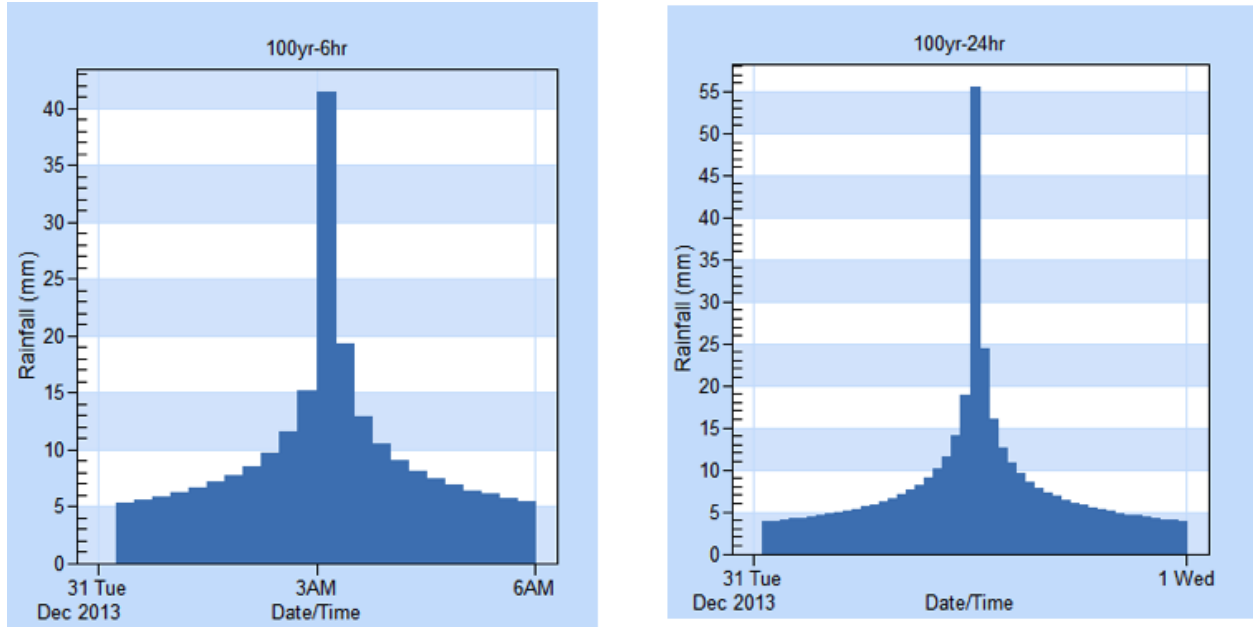


Figure I.5. Synthetic Storm (Hyetographs).

Appendix J Miscellaneous

VBA Hydraulic scripts

Variables

<i>Y</i>	=	<i>Water depth</i>
<i>Ac</i>	=	<i>Area</i>
<i>R</i>	=	<i>Hydraulic radius</i>
<i>N</i>	=	<i>Roughness coefficient</i>
<i>Q</i>	=	<i>Flow</i>
<i>S0</i>	=	<i>Longitudinal slope</i>
<i>m</i>	=	<i>Channel side slope</i>
<i>P</i>	=	<i>Wetted perimeter</i>
<i>fc</i>	=	<i>Function of Manning equation</i>
<i>ffc</i>	=	<i>First derivative of Manning Equation</i>
<i>Bc</i>	=	<i>Top width</i>
<i>frc</i>	=	<i>Function of Froude equation</i>
<i>ffrc</i>	=	<i>First derivative of Froude Equation</i>
<i>G</i>	=	<i>Aceleration by gravity</i>
<i>B</i>	=	<i>Bottom width</i>
<i>dyc</i>	=	<i>Counter limits precision</i>
<i>Range(" ")</i>	=	<i>Location in excel where to call or save the value</i>

Computation of Normal Depth

$B = \text{Range}("C235").\text{Value}$

$Y = 0.0001$

$dyc = 0.0001$

While $\text{Abs}(dyc) > 0.000001$

$Ac = B * Y + m * Y ^ 2$

$Bc = B + 2 * m * Y$

$P = B + 2 * Y * (m ^ 2 + 1) ^ 0.5$

$R = Ac / P$

$fc = S0 ^ 0.5 * Ac * R ^ (2 / 3) / N - Q1$

```

ffc = (S0 ^ 0.5 / N) * (R ^ (2 / 3) * Bc + Bc / P - (2 * Y * R / P))
Y = Y - fc / ffc
dyc = -fc / ffc

```

Wend

```
Range("C329").Value = Y
```

Computation of Critical Depth

```

ycd = 0.0001
dyc = 0.0001

```

```
While Abs(dyc) > 0.000001
```

```
  Ac = B * ycd + m * ycd ^ 2
```

```
  Bc = B + 2 * m * ycd
```

```
  frc = Ac ^ (3 / 2) / (Bc ^ (1 / 2)) - Q1 / (G) ^ 0.5
```

```
  fffc = Ac ^ (3 / 2) * (-1 / 2) * Bc ^ (-3 / 2) * 2 * m + Bc ^ (-1 / 2) * (3 / 2) * Ac ^ (1 / 2) * Bc
```

```
  ycd = ycd - fc / ffc
```

```
  dyc = -frc / fffc
```

Wend

```
Range("C328").Value = ycd
```

Appendix K Conversion Factors

Multiply	By	To obtain:
cubic meter (m ³)	1.30796	cubic yard
cubic meter (m ³)	35.31073	cubic foot (ft ³)
cubic meter per second (m ³ /s)	35.31073	cubic foot per second (ft ³ /s)
cubic meter per second (m ³ /s)	22.82584	million gallons per day (Mgal/d)
hectare (ha)	0.00386	square mile (mi ²)
Kilometer (km)	0.62150	mile (mi)
meter (m)	3.28084	foot (ft)
meter per day (m/d)	3.28084	foot per day (ft/d)
meter squared per day (m ² /d)	10.76426	foot squared per day (ft ² /d)
millimeter (mm)	0.03937	inch (in.)
million liters per day (ML/d)	35.31073	million gallons per day (Mgal/d)
Pascal (Pa)	0.000145	pounds per square inch (psi)
square kilometer (km ²)	0.38610	square mile (mi ²)

Temperature in degrees Celsius (°C) may be converted to degrees Fahrenheit (°F) as follows:

$$^{\circ}\text{F} = (^{\circ}\text{C} \times 9/5) + 32$$